Danish Meteorological Institute
Ministry of Transport

Scientific Report 06-08

EUCOS space/terrestrial OSE study using the DMI-HIRLAM 3D-Var data assimilation system. Part II: A summer period

Bjarne Amstrup

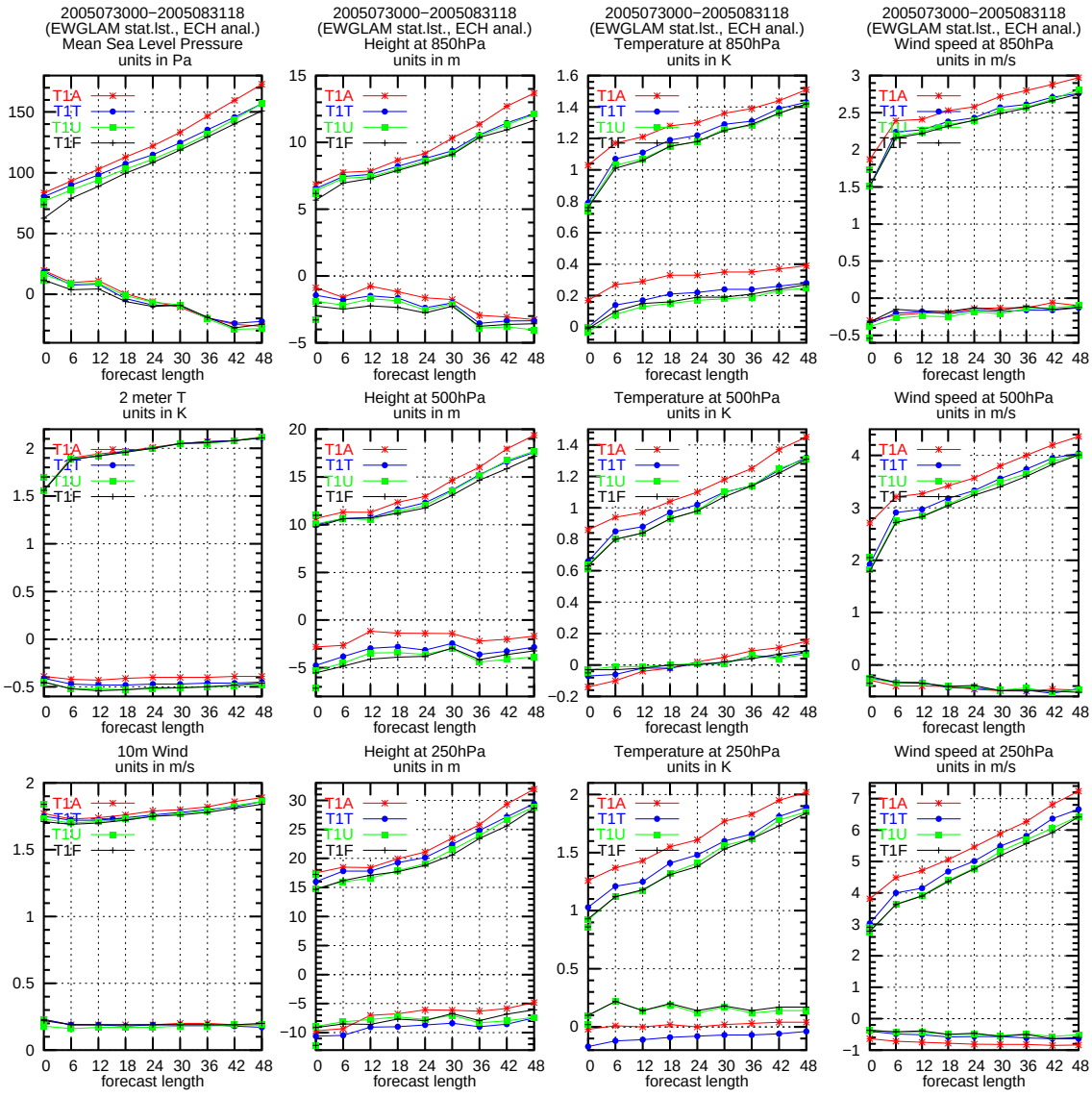

Colophone Serial title:
Scientific Report 06-08

Title:
EUCOS space/terrestrial OSE study using the DMI-HIRLAM 3D-Var data assimilation system. Part II: A summer period

Subtitle:

Authors:
Bjarne Amstrup

Other Contributers:

Responsible Institution:
Danish Meteorological Institute

Language:
English

Keywords:
HIRLAM, Observing System Experiments, EUCOS

Url:
www.dmi.dk/dmi/sr06-08

ISSN:
1399-1949

Version:

Link til hjemmeside:
www.dmi.dk

Contents

Abstract

EUCOS has decided to make an assessment of the impact on NWP forecasts of different components of the current observing systems in various combinations. As part of this a number of OSEs (Observing System Experiments) has to be executed by NWP centres. Both some running global models and by centres running limited area models. The Danish Meteorological Institute is one of the centres to make OSEs with a limited area model (HIRLAM). The lateral boundaries for these OSEs are provided by runs made by ECMWF (one of the centres to make OSEs with global models). Since the OSEs are to be made by the then operational HIRLAM model at DMI it is quite computer intensive. The following runs have been made by DMI (two periods one month each): 1) Baseline system (BL); 2) BL + all aircraft; 3) BL + non-GUAN wind; 4) BL + non-GUAN temp and wind; 5) BL + wind-profiler; 6) as (4) + aircraft; 7i) as (4) + non-GUAN humidity; 8) as BL + all in-situ data (full combined system); and 9) BL + E-AMDAR.

The results from the summer period run are presented in this report and they confirm to a large extent the findings in the winter period. The main conclusions are that the radiosonde data are the most important data, closely followed by the aircraft data; and that aircraft data and radiosonde data are complementary and not redundant data. Furthermore the results show that it is important to have both wind and temperature data – wind data alone give much poorer impact.

Resumé

I dette projekt, iværksat af EUCOS (EUMETNET (European Meteorological Network) Composite Observing System), undersøges indflydelsen af forskellige typer in situ (“terrestrial”) vind- og temperaturmålinger på prognosemodellernes analyser og, via det, indflydelsen på prognosernes kvalitet. Denne undersøgelse, sammen med tilsvarende undersøgelser ved andre institutter, er iværksat med henblik på den fremtidige strategi for observationsnetværket.

I modsætning til normalt, hvor man bruger det fulde sæt af observationer som udgangspunkt, tager man her udgangspunkt i det fulde sæt af satellitobservationer som bruges i analyserne, samt et minimalt sæt af radiosonde- (GUAN (GCOS (Global Climate Observing System) Upper-Air Network) netværket) og SYNOP-målinger (GSN (GCOS Surface Network) netværket) samt alle overfladebøjemålinger. Der laves test i en vinterperiode (medio december 2004 til medio januar 2005) og i en sommermåned (august 2005). Indflydelsen af følgende observationer i forhold til det ovennævnte grundsæt undersøges: 1) Alle flyobservationer (vind og temperatur), 2) vindmålinger fra de øvrige (d.v.s. "non-GUAN") radiosonder, 3) vind- og temperaturmålinger fra de øvrige radiosonder, 4) vindmålinger fra windprofilers, 5) vind- og temperaturmålinger fra de øvrige radiosonder og fra fly, 6) vind-, temperatur- og fugtighedsmålinger fra de øvrige radiosonder, 7) vind- og temperaturmålinger fra EUCOS AMDAR (Aircraft Meteorological Data Relay), og 8) alle tidligere ekskluderede in situ data (dvs. det fulde observationssystem). Denne rapport indeholder resultaterne fra sommerperioden og de giver i høj grad anledning til de samme konklusioner som fundet i vinterperioden. De væsentligste konklusioner er, at radiosondedata stadig er de vigtigste in situ data til brug i prognosemodellernes analyser skarp forfulgt af data fra fly; og at data fra fly komplementerer radiosondedata og er således ikke redundante. Desuden viser resultaterne at det er vigtigt med både vind- og temperaturobservationer. Vindobservationer alene er ikke tilstrækkeligt for at få en effektiv virkning.

1 Introduction

Normally Observing System Experiments (OSEs) at DMI are made by either adding a new data type to, or denying a data type from, the very large set of other observations used already in operations (see, e.g. Amstrup, 2000; Amstrup and Mogensen, 2000; Amstrup, 2001; Amstrup and Mogensen, 2004; Amstrup, 2004; Vedel and Huang, 2004; Guerrero and Amstrup, 2005. See also Vignes *et al.*, 2005). This large set of "basic" observations makes it difficult to identify a (significant) impact in an OSE from a particular type of observations and it is becoming more difficult as the number of used observations is steadily increasing. That DMI operational analyses are further improved by reanalyses twice (now four times) a day, in which 4D-Var ECMWF[1] analyses are blended (see next section) into the HIRLAM[2] analysis, makes it even more difficult. The same is to some extent the case for the European area for centres running global forecasting models (see, e.g., Graham *et al.*, 1998; Lacroix *et al.*, 1998; Gérard and Saunders, 1999; Deblonde, 1999; English *et al.*, 2000; Tomassini *et al.*, 1999; Bouttier and Kelly, 2001; Bormann *et al.*, 2003; Cardinali *et al.*, 2003; Köpken *et al.*, 2003; Marécal and Mahfouf, 2003; Isaksen and Janssen, 2004; Bormann and Thépaut, 2004; Langland and Baker, 2004; Fourrié *et al.*, 2006; Healy and Thépaut, 2006; McNally *et al.*, 2006; Andersson *et al.*, 2006; Okamoto and Derber, 2006; Bauer *et al.*, 2006a; Bauer *et al.*, 2006b).

In this study, initiated by EUCOS[3] and EUMETSAT[4], the impact of different terrestrial (in situ) observing systems is investigated by adding selected terrestrial datasets to the full set of satellite data used in operations and a very limited basic set of terrestrial observations. In this report the results for a summer period from July 29 to August 31, 2005 are given. The results for a winter period (December 13, 2004 to January 15, 2005) are given in Amstrup, 2006a.

The forecasting and analysis system used in these OSEs is based on the HIRLAM reference system including a 3D-Var analysis scheme (Gustafsson *et al.*, 2001; Lindskog *et al.*, 2001) and a forecast model (Undén *et al.*, 2002), both with some local DMI modifications.

The set of OSEs is briefly described in Table 1 including the model names used in the figures and tables in this report.

The summer period experiments differ in a few ways from the experiments made for the winter period. The three most important ones are: 1) usage of data as in operations (except for NOAA18 AMSU-A data), 2) usage of the corresponding ECMWF experiment for lateral boundary conditions, and 3) use of the newer structure functions made for DMI-HIRLAM-T15 that went into the operational DMI-HIRLAM in November 2005. 1) means that data from the operational short cut off runs have been archived and subsequently been used for these experiments. Accordingly, the number of data used is the same as for the operational runs in August 2005; an exception being NOAA18 AMSU-A data since they were not operational at that time. NOAA18 data from local receiving stations were available from August 8 and additional data from EARS were available the last two days of August.

The report is organized in the following way: Section 2 describes the setup used for these OSEs, section 3 give the results obtained in terms of verification measures and other statistics, and finally the conclusions are given in section 4.

[1] European Centre for Medium-Range Weather Forecasts
[2] High Resolution Limited Area Model
[3] EUMETNET Composite Observing System
[4] European Organisation for the Exploitation of Meteorological Satellites

Table 1: OSE description with experiment names and (internal) EUCOS number in the column named model. See section 2.4 for further details and comments.

model	Description
1-T1A	Control/baseline run (with GUAN radiosondes)
2-T1B	as T1A plus addition of all aircraft data
3-T1W	as T1A plus addition of all wind data from non-GUAN radiosondes
4-T1T	as T1A plus addition of all wind and temperature data from non-GUAN radiosondes
5-T1V	as T1A plus addition of wind profiler data
6-T1U	as T1T plus addition of all aircraft data
7-T1D	as T1A plus addition of data from non-GUAN radiosondes
8-T1F	'all' observations and use of similar ECMWF run for lateral boundaries
9-T1X	as T1A plus addition of E-AMDAR data

2 Experimental setup

The experimental set-up is based on the operational DMI-HIRLAM set-up in the summer 2005 (Yang *et al.*, 2005b) with some updates to the 3D-Var system also applied operational in November 2005. The model version DMI-HIRLAM-T15 (T15) was run in all the experiments. The model versions DMI-HIRLAM-S05 and DMI-HIRLAM-Q05 were not run in these experiments as it was considered much too (computationally) costly and, furthermore, they do not make their own analysis.

2.1 Domain(s)

The operational DMI-HIRLAM model domains from late summer 2005 are shown in Figure 1. All domains are defined on a rotated grid. The polar coordinates $(P_{\mathrm{lat}}, P_{\mathrm{lon}})$, the starting coordinates (southwest corner) in the rotated coordinate system and model resolutions for the domains are given in Table 2.

2.2 Forecast model and lateral boundary files

The model grid is a rotated, regular lat.-lon. Arakawa C grid with 40 levels in the atmosphere and the model top at 10 hPa. The forecast system is based on HIRLAM reference version 6.2.3 (see Undén *et al.*, 2002, for a more detailed description of the reference system) with a number of modifications. The following options and specifications apply to the system:

- ▷ HIRLAM 6.2.3 physics with recent extensions (of which some are mentioned below).
- ▷ Semi-Lagrangian dynamics option (SETTLS option is true, see Lindberg, 2005).
- ▷ Incremental digital filter initialization.
- ▷ Implicit 6th order horizontal diffusion.
- ▷ The HIRLAM 6.2.5 experimental version of the CBR scheme is used. The parameterization of turbulence is based upon turbulent kinetic energy (TKE).

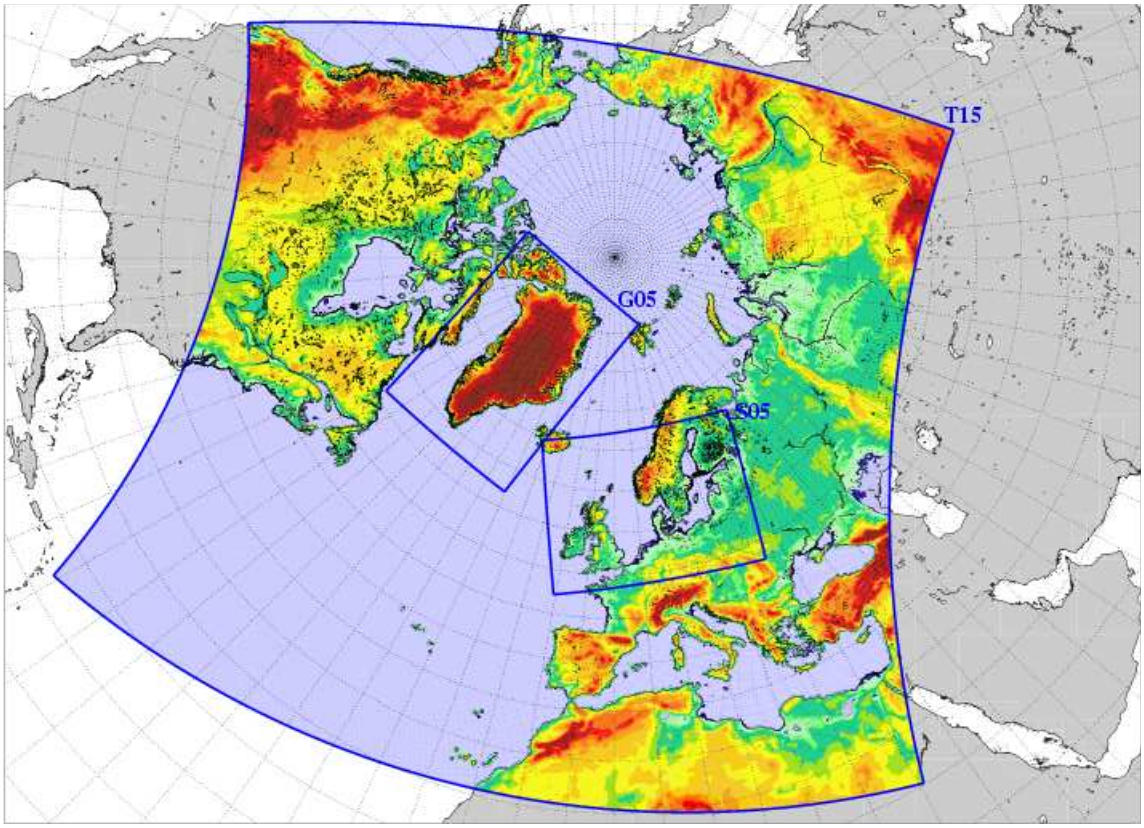

Figure 1: Operational DMI-HIRLAM areas from late August 2005. DMI-HIRLAM-T15 (large area), DMI-HIRLAM-Q05 (G05) and DMI-HIRLAM-S05 all have 40 vertical levels. The horizontal resolution of DMI-HIRLAM-T15 is $0.15^\circ \times 0.15^\circ$ and the horizontal resolution of DMI-HIRLAM-S05 and DMI-HIRLAM-Q05 is $0.05^\circ \times 0.05^\circ$.

- ISBA[5] surface scheme and surface analysis is used. However, upgrades to the SST- and ice-analysis have been made. ECMWF disseminated SST-data and ice-data are used more efficiently to update sea surface temperature and for diagnosing fraction of ice. This is of particular importance close to coastal areas. In addition SSTs from the Ocean & Sea Ice SAF[6] are used.

- The STRACO convection scheme is used (Sass, 2002).

- Schedule: 3-hourly data assimilation cycles for T15. For S05 and G05 6-hourly updates are made and no reassimilation. Long forecasts for 00 UTC, 06 UTC, 12 UTC and 18 UTC for T15, S05 and G05. DMI-HIRLAM-T15 is restarted via blending from ECMWF 3D-Var analysis (here the ECMWF 4D-Var analysis) (0.45° resolution) twice a day before the long 00 UTC and 12 UTC runs (see Yang *et al.*, 2005a, for further details on the blending scheme). Normal HIRLAM cycles then follow (03 UTC, 06 UTC, 09 UTC) in the morning for T15 to produce an 'up-to-date' status of the atmosphere. In the evening the subsequent analyses are valid at 15 UTC, 18 UTC and 21 UTC respectively. Table 3 show the operational schedule as of June 2005 for T15 and S05. As an example 'T06+5 h' denote a T15 analysis valid at 06 UTC followed by a 5 h forecast.

- Adjustment of diagnostics for V10m, T2m and RH2m (see Geleyn, 1998) and an improved algorithm for calculation of the reduction from surface pressure to msl pressure (Feddersen, 2004).

- The "vegetation" roughness and "thermal" roughness over land have been modified.

[5] Integrated Soil Biosphere Atmosphere
[6] Satellite Application Facility

Table 2: Model variables for DMI operational runs. The geographical coordinates $(P_{\rm lon}, P_{\rm lat})$ of the rotated south pole and the coordinates, $(x_{\rm lon,1}, y_{\rm lat,1})$ of the south-west corner in the rotated grid are given as well. See text for changes to this in the present setup.

Model Identification	T15	S05	G05
grid points (mlon)	610	496	550
grid points (mlat)	568	372	378
no. of vertical levels	40	40	40
horizontal resolution	0.15°	0.05°	0.05°
hor. res. (assimilation)	0.15°	—	—
$(P_{\rm lon}, P_{\rm lat})$	$(80°, 0°)$	$(10°, -40°)$	$(50°, 0°)$
$x_{\rm lon,1}$	$-64.325°$	$-13.675°$	$-32.200°$
$y_{\rm lat,1}$	$-37.527°$	$-1.027°$	$-8.000°$
time step (dynamics)	360 s	120 s	120 s
time step (physics)	360 s	120 s	120 s
boundary age (in forec.)	6 h	0 h	0 h
boundary age (in ass.)	0 h–6 h	0 h	0 h
host model	ECMWF	T15	T15
boundary frequency	1/(3 h)	1/(1 h)	1/(1 h)
data assimilation cycle	3 h	6 h	6 h
forecast length (long)	60	54	36
long forecasts per day	4	4	4

▷ Adaption of the analysis increment method for the high resolution models DMI-HIRLAM-Q05 and DMI-HIRLAM-S05 using analyses from DMI-HIRLAM-T15.

The basic model applied in the present OSE study is DMI-HIRLAM-T15 with the forecast model version operational June 2005. The resolution of the (disseminated) ECMWF sst- and ice-fields used is 0.5°. As listed in Table 2, the horizontal resolution of DMI-HIRLAM-T15 is $0.15°$, the number of vertical levels 40, the number of grid points is 610×568, the dynamics as well as the physics time step is 360 s and the lateral boundary values are updated every 3 hours from ECMWF (the so called "frames" boundaries), with 0.45° horizontal resolution, 00 UTC or 12 UTC forecasts. The lateral boundaries for the operational T15 runs are also 3 hourly 'frames' (with 0.45° horizontal resolution) disseminated from ECMWF and are 6 h older than the forecasts for the long runs. However, in the present setup the ECMWF baseline runs do not include 06 UTC and 18 UTC forecasts, and accordingly 12 h old lateral boundaries are used for the long 00 UTC and 12 UTC runs in these tests. The number of passive boundary points is 12. Long (48 hour) forecasts are made at the four major synoptic times (00, 06, 12 and 18 UTC).

As mentioned, a reassimilation is made before the long 00 UTC and 12 UTC runs. This is done in order to take advantage of both the extra observations that arrive after the relative short cut off for the long runs, and also to take advantage of the ECMWF analyses. The ECMWF system is expected to produce somewhat better 'large scale' analyses, since they use much more (in particular satellite) observations than are used at DMI, and due

Table 3: Operational time schedule for T15 and S05 used in June 2005. The times in the left column indicate the start of the preprocessing of boundary data and ISBA. The 3D-Var analysis (for DMI-HIRLAM-T15) begins ca. 5-7 min later. T_E denotes restart from ECMWF analysis.

UTC	T	S
1:37	T00+60 h	
2:29		S00+54 h
ECMWF 00 UTC		
7:37	T06+60 h	
8:29		S06+54 h
ECMWF 06 UTC		
11:45	T_E00+05 h T03+05 h T06+05 h T09+05 h	
12:43		S00+03 h S03+03 h S06+03 h S09+03 h
13:37	T12+60 h	
14:29		S12+54 h
ECMWF 12 UTC		
19:37	T18+60 h	
20:29		S18+54 h
ECMWF 18 UTC		
23:50	T_E12+05 h T15+05 h T18+05 h T21+05 h	
24:48		S12+03 h S15+03 h S18+03 h S21+03 h

also to their use of 4D-Var within a global forecasting system. Therefore, a new analysis is made, and based on this analysis and large scale blending of the ECMWF analysis a short forecast is made. Subsequently, further analyses and short forecasts are made to make up-to-date first guess fields for the following long forecast run at 12 UTC or 00 UTC.

2.3 3D-Var and observation types used

The analysis version used here is the HIRLAM 3D-Var 6.3.6 MPI version modified to use RTTOV8[7] developed in the Numerical Weather Prediction SAF[8] project setup by EUMETSAT (see Schyberg *et al.*, 2003, for further details on the use of ATOVS data in the HIRLAM 3D-Var system). The observation window covers a 6 h span around the analysis times 06 UTC and 18 UTC before the long forecasts starting from these. For the other runs the observation window covers a 3 h span around the analysis time (00, 03, 06, 09, 12, 15, 18, 21 UTC).

The background error statistics are based on non-separable structure functions estimated using “the NMC method” (See Berre, 2000; Gustafsson *et al.*, 2001 and references therein for further details) from differences

[7] Radiative Transfer model for TOVS, release 8
[8] Satellite Application Facility

Table 4: Observation error standard deviations for AMV wind.

Pressure (hPa)	1000	850	700	500	400	300	250	200
u/v (m/s)	2.00	2.00	2.00	2.45	3.10	3.60	3.80	3.80
Pressure (hPa)		150	100	70	50	30	20	10
u/v (m/s)		5.00	5.00	5.00	5.00	5.00	5.00	5.70

Table 5: Diagonal elements of observation covariance matrix for NOAA15, NOAA16 and NOAA18 AMSU-A. Values (σ^2) are in kelvin squared.

Channel #:	1-3	4	5	6	7	8	9	10
open sea:	900	1.40	0.35	0.35	0.35	0.35	0.70	1.40
sea ice:	9×10^6	9×10^6	9×10^6	1.40	0.35	0.35	0.70	1.40

between $+12$ h and $+36$ h forecasts, valid at the same time, from the operational DMI-HIRLAM-T15 forecast. They were implemented operationally in November 2005 and also used in these summer runs. For the winter runs an old set based on rather old data were used. It is also being investigated how the relation between background errors and observation errors can be tuned (see Navascués *et al.*, 2006) since they are not optimal anymore.

Since November 2005 the following observation types have been used operationally in the DMI-HIRLAM system: SYNOP (surface pressure), SHIP (surface pressure), DRIBU (surface pressure), PILOT (wind at all levels), TEMP (wind, temperature and humidity at all levels), AIREP (wind and temperature; includes AMDAR[9] and ACARS[10]), NOAA15 and NOAA16 AMSU-A brightness temperature data from channels 1-10 (effectively only channels 4-10 over open sea and channels 6-10 over sea ice) are included (from local receiving stations and via EARS[11]), Meteosat-8 AMV[12] winds and QuikScat winds (near surface wind data from the SeaWinds scatterometer; see Portabella and Stoffelen, 2004, and references therein). The AMSU-A data are thinned to 0.9° for NOAA15 and NOAA16 (and for NOAA18 data in the setup used here) data separately.

The Meteosat-8 AMV data are used over open sea and over land south of 30°N. Furthermore, the distributed data includes two quality indices. Based on these two quality indices the data are rejected if the indices are below 20 or 30, respectively. The observation error standard deviations used in the analyses are given in Table 4. The first guess check of Meteosat-8 AMV data and other single level wind data is traditional and includes an "asymmetry check" (see Guerrero and Amstrup, 2005). In the present setup available NOAA18 data have been used as well.

For bias-correction of AMSU-A brightness temperatures a Harris-Kelly (Harris and Kelly, 2001) scheme with 7 predictors from the background model (model first guess) is used. The initial examination that was done for NOAA16 data (Schyberg *et al.*, 2003) showed that the scatter of the difference between observed and modeled brightness temperature varied significantly with latitude. It was therefore decided to have separate bias correction coefficients for three latitude bands: 1) up to 50°N, 2) between 50°N and 65°N, and 3) north of 65°N. The AMSU-A bias correction for the 3D-Var version used here is based on a 5 month period from January 2005 through May 2005 using archived operational 3 h T15 forecast data as first guess files. The bias correction coefficients are calculated independently for data over sea ice and for data over open sea. See also Amstrup, 2006b, for a study of the predictors used in DMI-HIRLAM and the difference they make.

[9] Aircraft Meteorological Data Relay
[10] Aircraft Communication Addressing and Reporting System
[11] EUMETSAT ATOVS/Advanced Retransmission Service
[12] Atmospheric Motion Vectors

At present a diagonal observation error covariance matrix is used for AMSU-A data. Based on the experience from the initial tests with RTTOV8 (Amstrup, 2005) the observation error for channel 4 data over open sea has been reduced compared to when using RTTOV7, so that these channel 4 data have more weight than previously. The values for NOAA15, NOAA16 and NOAA18 are listed in Table 5. Some of the channels that 'see' the surface are given a large observation error so that they are effectively not used, that is in particular true for data over sea ice. Since the model surface temperature over sea ice can differ considerable from the real surface temperature and due to uncertainties in the emissivity over sea ice, an extra screening is done for these data. The data are discarded if the difference between the modelled and observed brightness temperatures for channels 4 and 5 disagree by more than 1.0 K and 0.8 K, respectively.

The FGAT (First-Guess at the Appropriate Time) option is used (see Huang *et al.*, 2002, for further details).

The DMI summer baseline run consists of the following satellite data: i) NOAA15, NOAA16 and NOAA18 AMSU-A data over open sea and over sea ice, ii) QuikScat surface winds, iii) Meteosat-8 AMV winds. In addition to the satellite data, the baseline setup consists of the following conventional data: i) the GUAN[13] radiosonde network, ii) the GSN[14] surface network and iii) buoy data. See Appendix A in Amstrup, 2006a, for a list of the WMO[15] station identification numbers in the GUAN and GSN networks.

An example (the cycle with most baseline radiosonde stations included) of the coverage of the baseline radiosonde data and surface data is shown in Figure 2. The distribution for 00 UTC as shown here is reasonable except for a rather low number of radiosonde data in the Atlantic. The distance between stations are also much higher than in a normal 00 UTC analysis. The figure also shows the difference between the similar data set shown in Amstrup, 2006a. In average the 12 UTC runs in the summer period had data from a little more than 2 additional GUAN radiosonde stations available compared to the 12 UTC runs in the winter period (40.0 stations versus 37.9 stations). For the 00 UTC analyses the summer and winter period runs had in average data from almost the same number of GUAN radiosonde stations (39.64 stations versus 39.47 stations). Similarly, the distribution of surface pressure data in the baseline setup via buoys and SYNOPs are shown in the lower part of the figure. Figure 3 shows the available data for the T1F experiment (full observing system) and includes PILOTs and ship data as well for the same analysis time. Note that PILOTs are considered redundant if a TEMP is available from the same station position. For this analysis, T1F had data from 207 more radiosonde stations than the baseline experiment. The figure also demonstrate the number of radiosonde stations from which DMI received data after the short cut off analysis run for this specific cycle. For this specific cycle it was 42 (17 %) out of 250 active stations. Beside data from these stations, additional data from a number of the other stations were received after the short cut off time.

2.4 Short description and comments on different experiments

T1A Baseline run. This includes a fairly small amount of radiosonde and SYNOP data (an example of the data coverage is shown in Figure 2), and in addition buoy data are included to 'anchor' the satellite data (studies at ECMWF have shown that AMSU-A data in their data assimilation system do not perform well in the absence of sea surface pressure data (Jean-Noël Thépaut, in a presentation at the "Alpbach workshop", `http://www.wmo.int/web/www/GOS/Alpbach2004/Agenda-index.html`)). No aircraft data, no ship data, and no PILOT data are included.

T1B Baseline and all aircraft (AMDAR, ACARS and standard AIREP) data included.

T1X Baseline and E-AMDAR data included (AMDAR observations with station id starting with 'EU').

[13] GCOS (Global Climate Observing System) Upper-Air Network
[14] GCOS Surface Network
[15] World Meteorological Organization

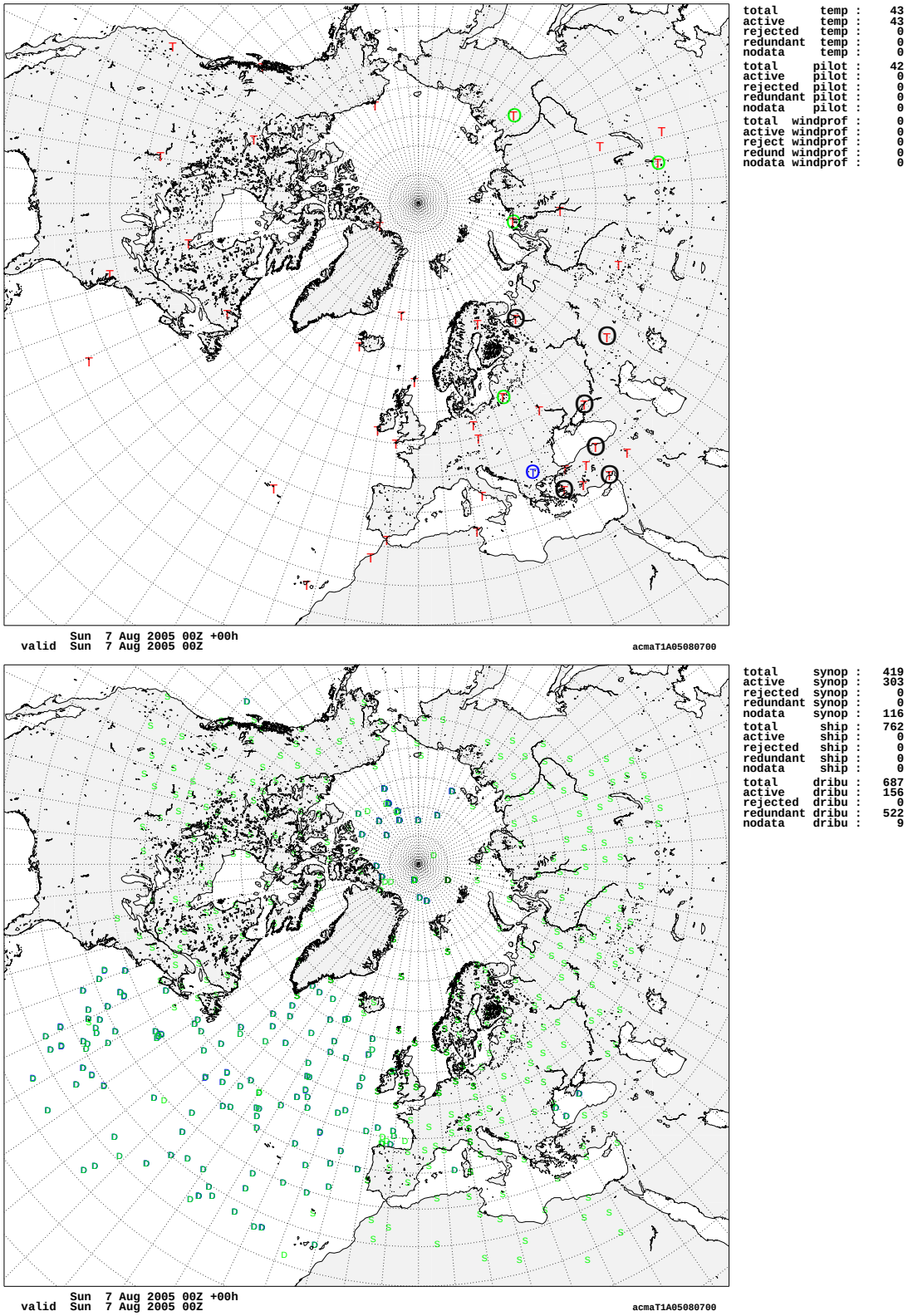

Figure 2: An example of the coverage of the baseline radiosondes (upper, red 'T's) and surface (lower, green 'S's for SYNOP, 'D's for buoys) data available for the long cut off run on 00 UTC August 7, 2005. The radiosonde stations are GUAN stations and the SYNOP stations are GSN stations. The 4 green circled T's are new compared to the plot from 12 UTC December 18, 2004 shown in Amstrup, 2006a, and the blue circled T was available then, but not now. The 6 black circled T's were not available for the short cut off analysis.

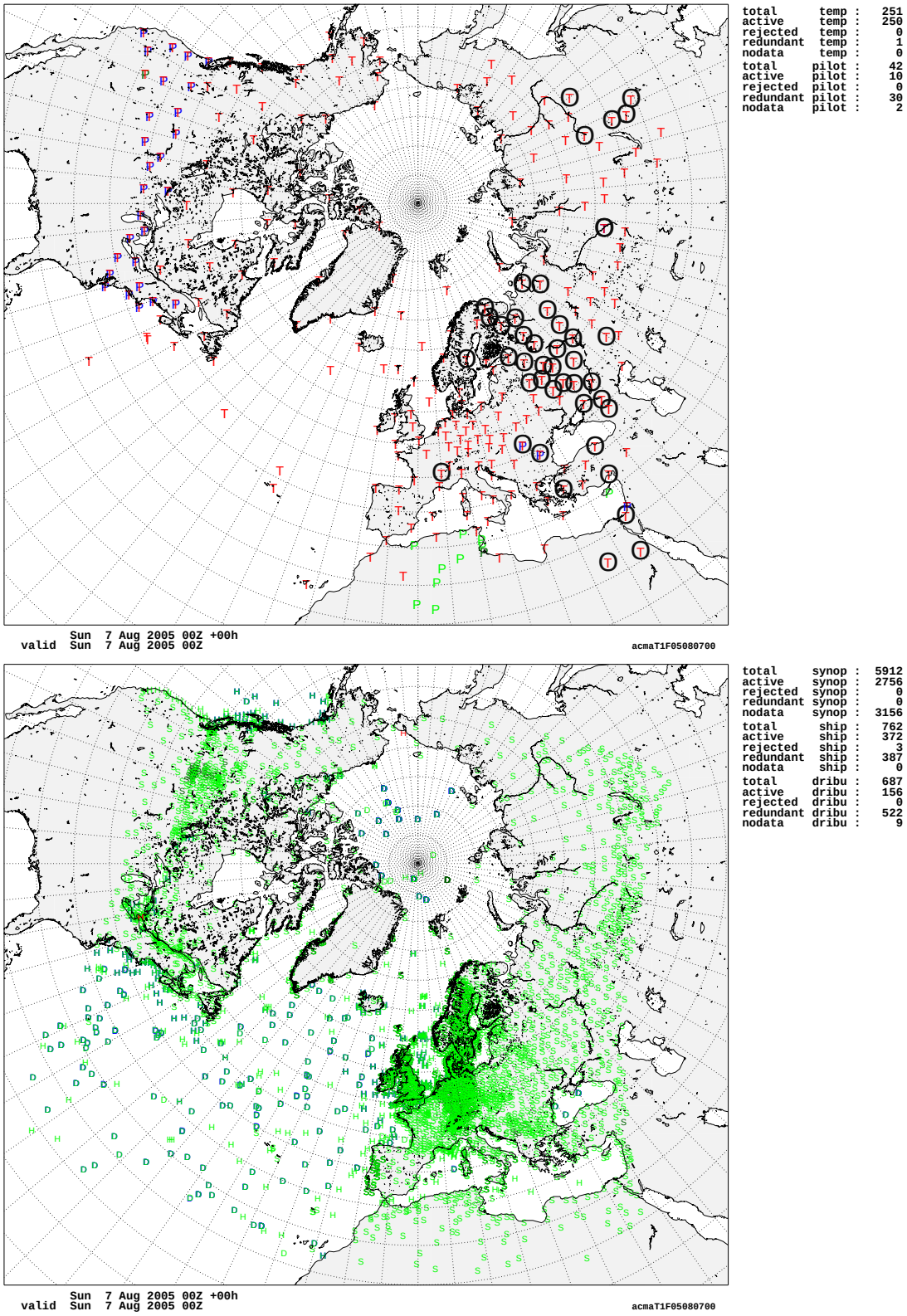

Figure 3: An example of the coverage of the radiosondes (upper, red 'T's) and PILOTs (upper, blue 'P's for redundant, green 'P's for active) and surface (lower, green 'S's for SYNOP, 'D's for buoys and 'H's for ships) data available for the long cut off run on 00 UTC August 7, 2005. The (42) black circled T's were not available for the short cut off run.

T1W Baseline and wind from the non-GUAN radiosondes added.

T1T Baseline and wind and temperature from the non-GUAN radiosonde added.

T1D Baseline and all data (wind, temperature, humidity) from the non-GUAN radiosondes added.

T1U Baseline and wind and temperature from the non-GUAN radiosonde and from all aircraft are added.

T1V Baseline and wind profiler data extracted from the ECMWF mars archive. The ECMWF white list has been used to specify which wind profilers are used. These data are not used operationally at DMI and, accordingly, they have been used with the analysis system as is. Some data may therefore not have been used as they were supposed to be and some may not have been used at all even if they were supposed to. In this experiment data from 13 stations have been used. Wind profiler data are not included in the real time DMI bufr-database and have therefore not been monitored at all at DMI for a long time.

T1F The control run including all observations.

Figures 4-7 show the number of observation reports used in the main (short cut off) analyses and the reassimilation analyses at 00 UTC, 06 UTC, 12 UTC and 18 UTC for the baseline experiment (T1A) and the control (T1F, 'all observations included') experiment. With respect to aircraft data, the number of reports used for the 'E-AMDAR' (T1X) experiment are shown as well. Note the relative few AMSU-A data for the 00 UTC analyses and in particular for the short cut off analyses – sometimes even none were available. It should also be noted that normally data from quite a few radiosonde stations arrive at DMI after the short cut off analyses at 00 UTC and 12 UTC. An example of this is illustrated in Figure 3.

3 Results

The results are compared in different ways. A standard observation verification, where forecast results are compared to standard SYNOP and radiosonde observations using an EWGLAM[16] station list is done, and the results are shown and commented upon in section 3.1. Furthermore, significance tests by use of students t-test, with 90 % two sided significance interval, are shown (Mike Fisher, memorandum ECMWF research department, May 2001). Results of forecasted 12 h precipitation amounts against observations from SYNOP stations at 06 UTC and 18 UTC are given in terms of standard contingency tables and as equitable threat scores in section 3.2. Some results from field verification, where forecasts are compared to the control experiment (T1F) verifying analyses, are given in section 3.3. Section 3.4 has some case studies. Finally, in section 3.5 the statistics of wind speed data observations from Meteosat-8 AMV, aircrafts and radiosonde, as well as temperature data from radiosondes and aircrafts, are compared with similar model data.

3.1 Observation verification

The experiments are verified by calculation of bias (forecast value minus observed value) and root mean square (rms) for the surface variables 10 m wind speed, mslp (mean sea level pressure) and 2 m temperature; for the upper level variables temperature, wind speed and geopotential height at 850 hPa, 500 hPa and 250 hPa; and for relative humidity at 850 hPa, 700 hPa and 500 hPa as function of forecast length in one type of figures (Figures 8-12). In a second type of figures (Figures 13-21), the vertical structure of temperature and geopotential height offsets is illustrated by plotting the rms scores for a test experiment on the left hand side and differences in rms scores between the experiment and the baseline experiment on the right hand side. Also some inter comparisons between experiments are made. The scores are shown at analysis time and for the 12, 24, 36 and 48 hour forecasts as a function of pressure. Figure 22 shows bias and rms scores for the full combined system to

[16] European Working Group on Limited Area Model

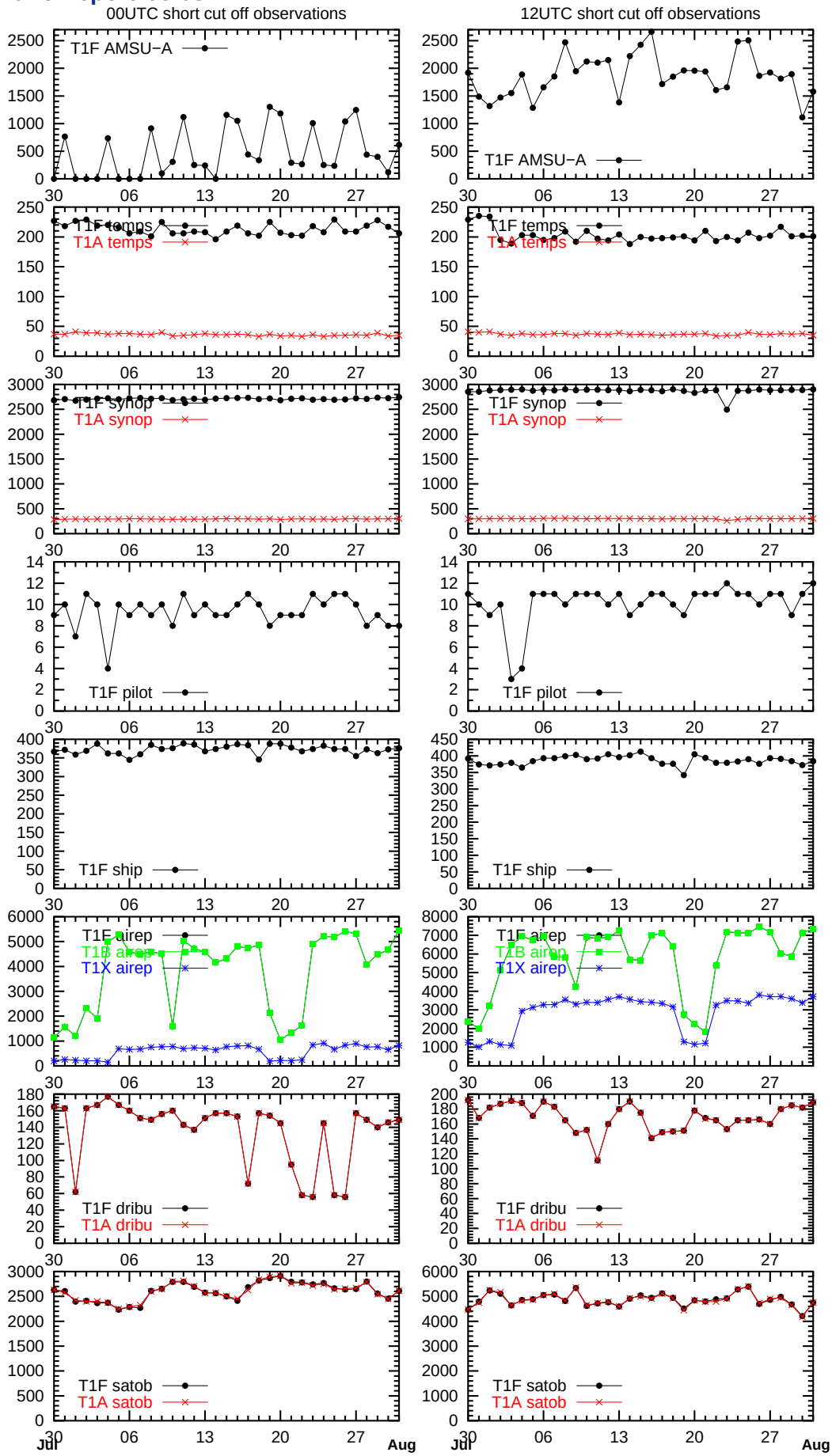

Figure 4: Observation usage for 00 UTC analyses (left) and 12 UTC analyses (right) with short cut off (before the long forecast runs). Note that PILOT and SHIP data are used in the T1F experiment only.

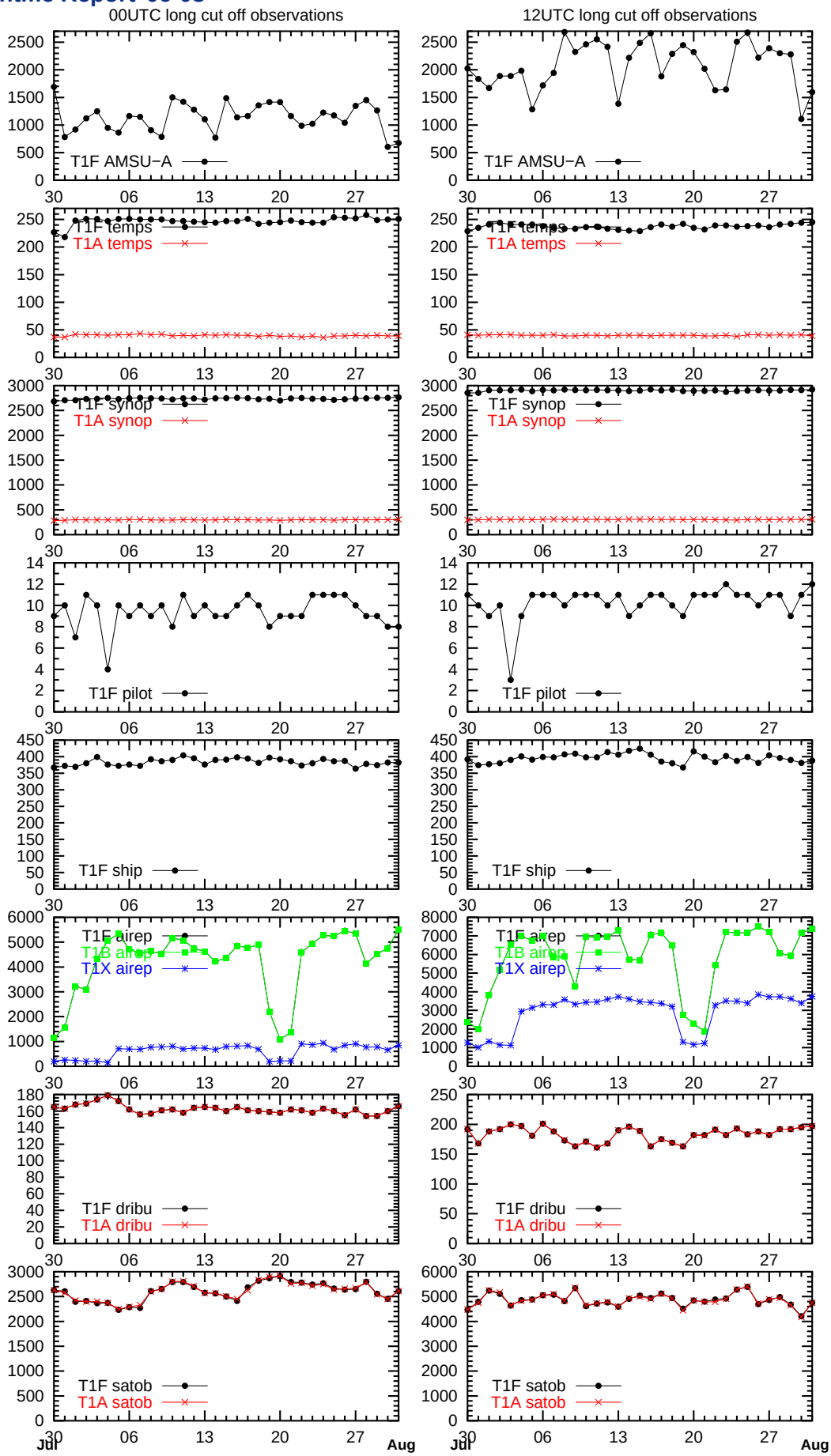

Figure 5: Observation usage for 00 UTC analyses (left) and 12 UTC analyses (right) with long cut off (used in the reassimilation cycles). Note that PILOT and SHIP data are used in the T1F experiment only.

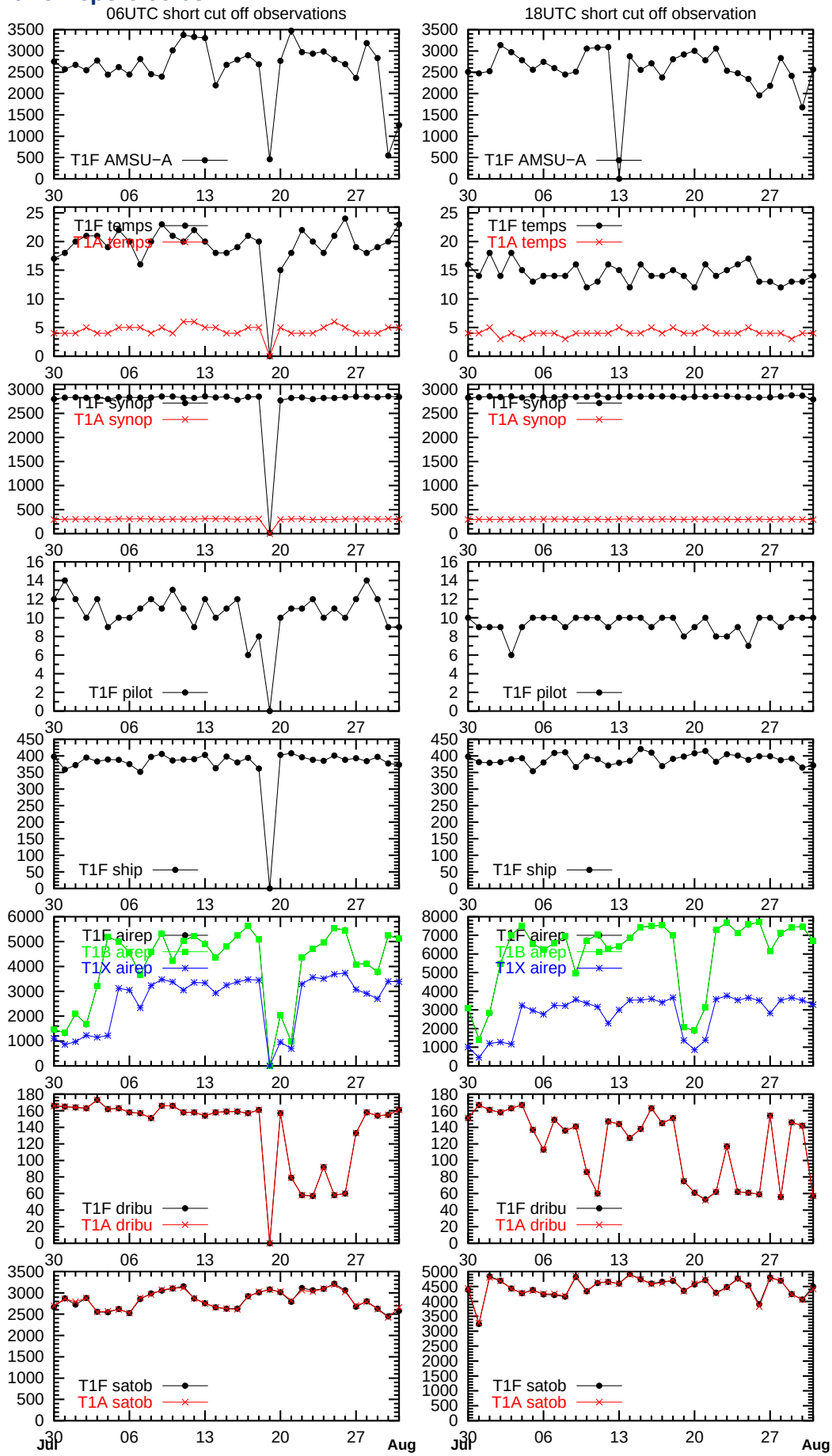

Figure 6: Observation usage for 06 UTC analyses (left) and 18 UTC analyses (right) with short cut off (before the long forecast runs). Note that PILOT and SHIP data are used in the T1F experiment only.

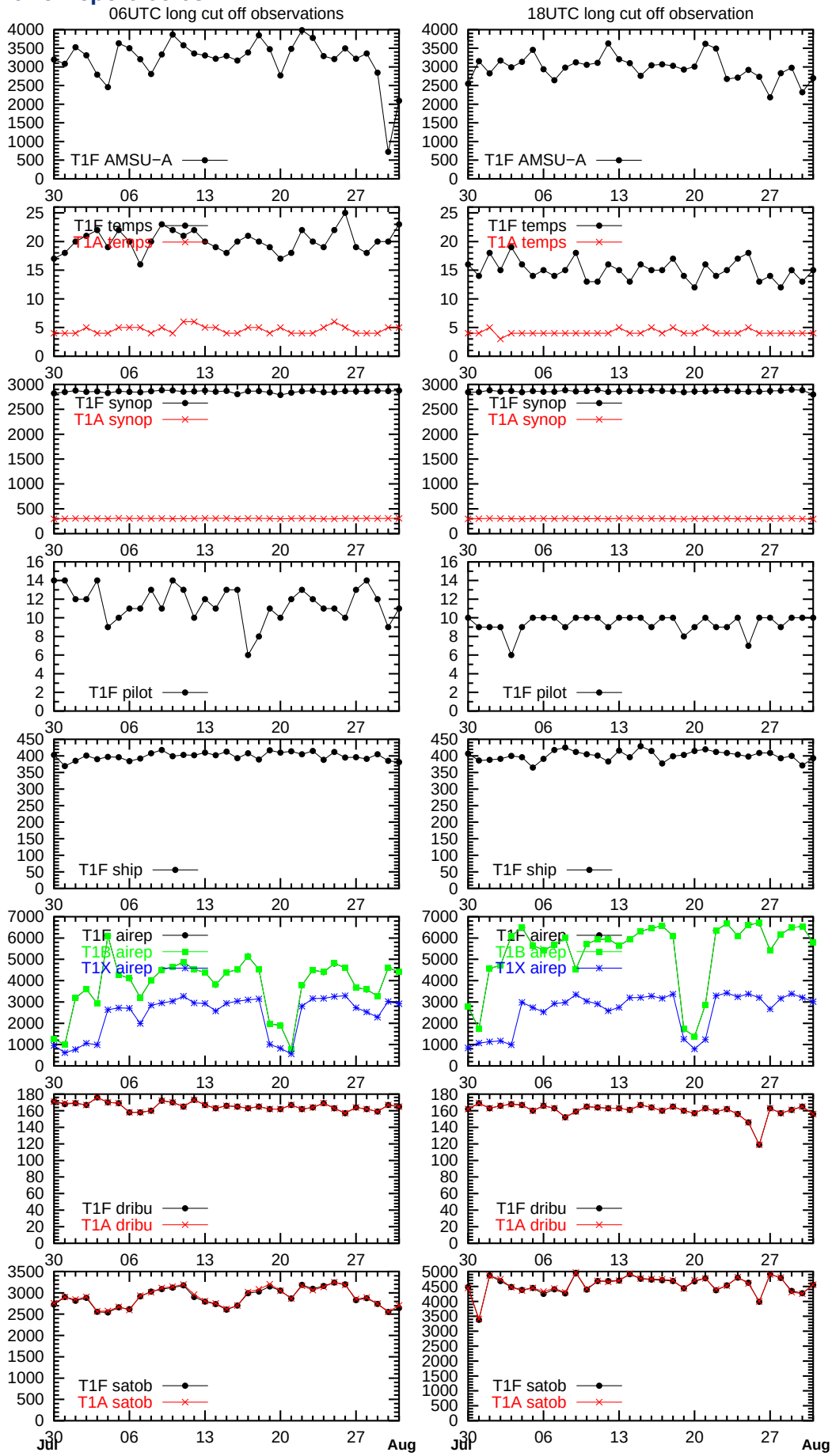

Figure 7: Observation usage for 06 UTC analyses (left) and 18 UTC analyses (right) with short cut off (used in the reassimilation cycles). Note that PILOT and SHIP data are used in the T1F experiment only.

illustrate the general trends of the bias behavior. Figures 23-28 show obs-verification based on daily scores of 00 UTC and 12 UTC forecasts for the variables: Mslp, 300 hPa temperature and wind, 850 hPa temperature, 700 hPa relative humidity and 500 hPa geopotential height. Furthermore, results for mslp based on daily scores of 06 UTC and 18 UTC forecasts are shown in Figure 29. Overlayed is the 90 % two sided confidence intervals. These plots are additional to the previous and made to see the significance of the differences for some of the parameters; they are the ones referred to when comments about significance of the results are made later in the report.

A comment about the verification of upper air temperatures at analysis time is appropriate. Some of the experiments (T1T, T1D, T1U and T1F) use radiosonde temperature data in the analyses, and as some of these data are used for verification these experiments are bound to have better upper air temperature scores for the analyses (0 h forecast lengths) than the experiments not including these data.

Figure 8 shows the verification scores for impact of wind and temperature from E-AMDAR (T1X), all aircraft (T1B) and the additional radiosondes (T1T). Figures 13, 14 and 15 provide additional profile information. For short forecast lead times, it is expected that the impact from E-AMDAR dominate the scores for T1B since the large majority of EWGLAM stations are located in the area for which most of the E-AMDAR data are measured and most of the other aircraft data comes from areas somewhat away from the EWGLAM stations. For long forecast lead times, the ACARS coming mainly from over USA is expected to have an important impact, in particular for a relative large limited area model such as T15, that covers a large part of USA. Depending on the weather situation, the air masses for which E-AMDAR have contributed to a given analysis may have moved outside the main verification area during a forecast. Contrary to this, the air masses for which ACARS (over North America) have contributed to a given analysis may have moved into the main verification area over Europe during a forecast. Therefore, the impact from all aircraft data is expected to be somewhat larger than the impact from E-AMDAR data alone.

In general, T1T and T1B have the better scores while T1X has scores in between those and the scores of the baseline experiment. For reasons mentioned above, T1T naturally has somewhat better analyses temperature scores than T1B and T1X. The upper air wind, temperature and geopotential scores are in general significantly better than the baseline experiment scores, at least up to 36 h forecast lead time. The inter comparison between T1B and T1X shows that the 300 hPa wind and temperature scores are significantly better for T1B, and that the 00 UTC/12 UTC mslp scores for long forecast lead times are better for T1B. However, the significance plots show that there are large day to day fluctuations in some of the scores for 48 h forecasts. The inter comparison between T1T and T1B show that aircraft data have almost as big an impact as the additional wind and temperature data from radiosondes. The impacts on 850 hPa temperature and 500 hPa geopotential are consistently higher from the radiosonde data than from the aircraft data, but it is not significant. T1B has significantly better scores than T1X for the shown 300 hPa temperatures, 36 h and 48 h 300 hPa wind speed, 12 h 850 hPa temperature, relative humidity and also for 12 h to 24 h mslp. Since aircraft data in principle are available at any time, and only very few radiosonde data are available for analyses except for the 00 UTC and 12 UTC analyses, some additional significance plots based on 06 UTC and 18 UTC forecasts are shown in Figure 30 for T1T, T1B and T1X in addition to the mslp plots in Figure 29. The verifications are done against 00 UTC and 12 UTC radiosonde data and therefore results are shown for the forecast lengths 6 h, 18 h, 30 h and 42 h. Figure 29 shows that T1B has better mslp scores than T1X, but only some of them (6 h, 18 h, 24 h and 48 h) are significantly better. The differences in mslp scores for T1T and T1B are generally small, but for 6 h and 18 h forecasts T1T has significantly better scores than T1B. Compared to the mslp scores for the baseline experiment (T1A), T1X and T1B have significantly better scores for forecast lengths up to 24 h and T1T has significantly better scores for 42 h and 48 h forecasts as well. Figure 30 shows that for 850 hPa temperature the differences in scores for T1T, T1B and T1X are small and not significant. T1T has significantly better 500 hPa geopotential scores than T1X for 6 h and 42 h forecasts, and otherwise the differences in 500 hPa geopotential

scores between T1T, T1B and T1X are insignificant. For the 300 hPa wind speed scores the only significant difference scores are: T1B is better than T1T and T1T is better than T1X for 6 h forecasts, and T1B is better than T1X for 42 h forecasts. For 300 hPa temperature T1B has significantly better scores than T1T for 6 h and 18 h forecasts, and significantly better scores than T1X for all forecast lengths except for 18 h.

Figure 9 shows the verification scores for impact of additional non-GUAN radiosonde data information: Additional wind data (T1W), additional wind and temperature data (T1T), and all data (T1D). Figures 16, 17 and 18 show additional profile information. In general T1D and T1T have the better scores, and T1W scores in between those and the scores from the baseline experiment. In general the upper air wind, temperature and geopotential scores, as well as the short lead forecast time 00 UTC/12 UTC mslp scores, are significantly better than the baseline experiment scores for T1T and T1D. T1W has typically significantly better scores than the comparable baseline experiment scores for short forecast lead times. The differences between T1T and T1D scores are in general insignificant. Overall T1T has significantly better upper air wind, temperature and geopotential scores than the corresponding T1W scores. So, the additional temperature data do have a significant positive impact compared to just adding the wind observations.

Figure 10 shows the verification scores for impact of wind and temperature from additional non-GUAN radiosondes (T1T), further adding wind and temperature from aircraft data (T1U), and for the full observing system (T1F). Figures 19, 20 and 21 show additional profile information. In general T1F has better scores than T1U that has somewhat better scores than T1T. The baseline (T1A) has the worst scores. For most variables the differences are significant between T1U and T1T for forecast lead times up to and including 24 h. T1F has significantly better mslp and relative humidity at 700 hPa scores up to and including 24 h, as well as better 500 hPa geopotential height scores for 24 h and 26 h forecast lead times than T1U. For the other parameters and forecast lead times the differences in T1F and T1U scores are not significant.

Finally, Figures 11 and 31 show that the impact from the few wind profiler data are insignificant. This may to some extent be due to the rather few stations (13) from which data are used. A larger number may be needed to see a general impact. However, impact(s) may be seen in some case studies. In addition, wind profiler data are normally not used operationally in any country using the HIRLAM data analysis and forecasting system. Therefore, no attempt to optimize the usage of these data have been made since the original implementation. This should of course be done to optimize use of the data, in particular if hourly data could be used in connection to using 4D-Var analyses. However, as the impact from wind data only from the non-GUAN radiosondes show, the impact from wind data alone is somewhat smaller than when temperature data is available as well.

3.2 Precipitation verification

Precipitation is verified by two means, by producing contingency tables and by calculating equitable threat scores, both for 12 h forecast periods.

Tables 7 to 12 show contingency tables of precipitation accumulated over 12 hours (from 6 to 18 hour forecasts, 18 to 30 hour forecasts, and 30 to 42 hour forecasts) for the given period, using either EWGLAM stations that do report 12 hours accumulated precipitation, or Danish stations. The numbers in these tables are obtained by counting the number of observed and predicted precipitation amounts in each of five classes. The five precipitation classes are (precipitation amounts in mm): $P1 < 0.2$, $0.2 \leq P2 < 1.0$, $1.0 \leq P3 < 5$, $5 \leq P4 < 10$ and $P5 \geq 10$. P is either F (forecast) or O (observation) in the tables. The “sum” rows and columns are the sums of the numbers in the given observation classes or forecast classes, respectively. Note that the observed values are uncorrected values. Thus, small observed precipitation values are most likely underestimated, and some “observed” 0 mm/12 h values may not be a real measurement at all, but a standard number used (this occasionally do happen for some Danish stations). The results based on this kind of comparisons are very

mixed and it is not possible to make any solid conclusions. Two noteworthy results are: 1) for the Danish station list the baseline experiment has the poorest results for the short range (6 h-18 h lead forecast time); 2) for the short forecast range (6 h-18 h lead forecast time) the experiments including aircraft data (T1B, T1X, T1U and T1F) have the best overall scores in terms of highest numbers in the diagonal.

The equitable threat score (ETS) measures the fraction of observed and/or forecast events that were correctly predicted, adjusted for hits associated with random change (see, e.g. `http://www.bom.gov.au/bmrc/wefor/staff/eee/verif/verif_web_page.html`). In terms if the definitions in the following table

	observed	
	no event	event
forecast no event	A	B
forecast event	C	D

we have ETS=(D−chance)/(B+C+D−chance) with chance=(C+D)*(B+D)/(A+B+C+D). This is sometimes written as: ETS=(R−chance)/(T−chance), where R is the total number of events observed **and** forecasted, T is total number of events observed **or** forecasted, and chance is given by chance=F*O/N where F is number of forecasted events, O the number of observed events and N is the total number of events plus non-events. The ETS score is between $-1/3$ and 1, 1 being the perfect score and 0 indicating no skill.

Tables 13 and 14 show the results by use of a Danish station list and an EWGLAM station list, respectively. Results for 6-18 h, 18-30 h and for 30-42 h are given for limits of very low precipitation amounts (0.3 mm/12 h), low precipitation amounts (1.5 mm/12 h) and for larger precipitation amounts (5 mm/12 h).

Both of these comparisons indicate a deficiency of the present humidity analysis. The model seems to act in a negative manner to the humidity increments which may be in imbalance with the overall fields.

The results for the Danish station list are very mixed. Part of this may be due to the relative small area and small statistical size compared to the full area and a single bad case may have a relatively larger impact on the result.

For the EWGLAM stations, for which the statistics are based on much higher numbers, we can note the following: 1) The difference between the better and worse scores for 18-30 h forecasts correspond at large to the differences between 6-18 h and 18-30 h forecasts for a given experiment. Similarly the difference between the better and worse scores for 30-42 h forecasts correspond at large to the differences between 18-30 h and 30-42 h forecasts for a given experiment. Thus the difference between the worse and better scores correspond to a gain of 12 h in forecast range. 2) T1U has better scores than T1T except for 6-18 h forecast range for ETS3. 3) T1B has (mostly marginally) better scores than T1T except for 6-18 h forecast range for ETS3. 4) T1U has (mostly marginally) better scores than T1B. 5) T1F has better scores than T1T except for 18-30 h forecast range for ETS1 where they have the same score. 6) Overall T1F and T1U have the better scores, and T1A and T1V the worse scores.

3.3 Field verification

Results from a field verification for which forecasts are compared to verifying analyses valid at the same time are summarized for selected parameters in Table 6 for 36 h and 48 h forecasts. The verifying analyses are the T1F initialized analyses for all the cases. The results are averages of 4 daily forecasts over the period studied here. The averages given are averages over grid points for the full area as well as for grid points in a European area defined by the southwest corner 12.5°W,35°N and northeast corner 35°E,75°N which is an area often used by

Table 6: Results from field verification. Top part is for averages over the full domain and the bottom part is for averages over a European area. The verifying analyses are T1F initialised analyses. The worse scores are marked in a bold, red font. The best scores are given with a bold, black font. The FCL column indicates the forecast length.

		T1A		T1V		T1W		T1T		T1D		T1X		T1B		T1U		T1F	
type	FCL	bias	rms	bias	rms	bias	rms	bias	rms	bias	rms	bias	rms	bias	rms	bias	rms	bias	rms
mslp	36	−0.13	**1.64**	−0.11	**1.64**	−0.14	1.58	−0.10	1.52	−0.11	1.52	−0.13	1.62	−0.11	1.56	**−0.08**	1.48	**−0.15**	**1.44**
mslp	48	**−0.15**	**1.99**	−0.12	**1.99**	−0.14	1.91	**−0.09**	1.85	−0.11	1.85	**−0.15**	1.96	−0.11	1.90	**−0.08**	1.81	**−0.16**	**1.76**
H500	36	3.1	**15.8**	3.3	**15.9**	2.7	15.1	2.7	14.5	2.9	14.5	2.8	15.4	3.0	15.0	2.9	14.1	2.7	**13.7**
H500	48	3.7	**20.0**	3.9	**20.1**	3.3	19.1	3.5	18.7	3.7	18.6	3.4	19.6	3.8	19.2	3.6	18.1	3.4	**17.6**
T850	36	0.18	**1.37**	0.17	**1.37**	0.15	1.33	0.11	1.28	0.11	1.27	0.16	**1.35**	0.17	1.32	0.12	1.25	0.11	**1.22**
T850	48	0.18	**1.54**	0.18	**1.53**	0.15	1.50	0.12	1.46	0.12	1.45	0.16	**1.52**	0.17	1.50	0.12	1.43	0.12	**1.41**
T500	36	0.19	**1.15**	0.19	**1.15**	0.17	1.10	0.20	1.07	0.22	1.07	0.19	1.13	0.17	1.09	0.18	**1.03**	0.23	**1.03**
T500	48	0.25	**1.35**	0.24	**1.35**	0.23	1.32	0.24	1.28	0.27	1.28	0.25	1.34	0.23	1.30	0.23	**1.25**	0.29	**1.24**
T300	36	−0.09	**1.21**	−0.09	**1.21**	**−0.09**	1.17	**−0.11**	1.14	−0.09	1.12	−0.06	1.19	**−0.01**	1.15	−0.04	1.10	0.03	**1.08**
T300	48	−0.07	**1.39**	−0.07	**1.38**	**−0.08**	1.35	**−0.09**	1.33	−0.08	1.32	−0.05	**1.38**	**−0.00**	1.34	−0.04	**1.30**	0.05	**1.28**
RH850	36	−1.1	16.2	−1.1	16.2	−1.0	15.8	−0.8	15.6	−0.6	15.5	−1.1	16.2	−1.1	15.8	−0.9	15.4	−0.6	15.0
RH850	48	−1.0	17.5	−1.0	17.4	−0.9	17.2	−0.8	17.0	−0.6	16.9	−1.0	17.5	−1.0	17.1	−0.8	16.9	−0.6	16.5
Average over European area (lon,lat): $(-12.5, 35) \rightarrow (35, 75)$																			
mslp	36	−0.44	**1.76**	−0.40	**1.78**	−0.40	1.66	**−0.28**	1.55	−0.34	1.58	**−0.45**	1.69	−0.39	1.64	**−0.29**	**1.50**	−0.43	**1.49**
mslp	48	−0.50	**2.24**	−0.45	**2.25**	−0.45	2.10	**−0.31**	2.00	−0.37	2.04	**−0.53**	2.14	−0.45	2.11	−0.33	1.96	−0.49	**1.91**
H500	36	0.5	18.3	0.9	**18.6**	0.6	17.1	1.2	16.2	1.5	16.3	0.1	17.3	0.9	16.9	1.3	15.4	1.5	**15.1**
H500	48	1.0	**23.5**	**1.5**	**23.7**	1.1	22.1	**2.1**	21.3	**2.4**	21.5	**0.4**	22.4	**1.5**	22.2	**2.1**	20.6	**2.1**	**20.0**
T850	36	**0.15**	**1.44**	**0.16**	**1.45**	0.11	1.38	**0.04**	1.32	**0.05**	1.31	0.14	1.40	0.14	1.38	**0.04**	1.28	0.09	**1.25**
T850	48	**0.14**	**1.64**	**0.15**	**1.64**	0.11	1.58	**0.05**	1.54	0.06	1.53	0.12	1.60	0.12	1.58	**0.05**	1.49	0.10	**1.48**
T500	36	**0.15**	**1.27**	**0.15**	**1.28**	**0.16**	1.22	0.21	1.16	0.27	1.18	**0.16**	1.23	0.18	1.21	0.23	**1.14**	**0.30**	**1.12**
T500	48	**0.23**	**1.52**	**0.23**	**1.51**	**0.23**	1.46	0.28	1.41	0.34	1.43	**0.24**	1.48	0.25	1.44	0.30	1.38	**0.37**	**1.36**
T300	36	**−0.18**	1.33	**−0.18**	**1.34**	**−0.17**	1.28	**−0.16**	1.23	−0.11	1.22	−0.12	1.28	−0.09	1.27	−0.11	**1.20**	**−0.04**	**1.19**
T300	48	**−0.16**	**1.53**	**−0.16**	**1.54**	**−0.15**	1.49	**−0.15**	1.44	−0.11	1.46	−0.11	1.49	−0.07	1.48	−0.09	**1.43**	**−0.02**	**1.42**
RH850	36	−1.8	16.8	−1.8	16.8	−1.6	16.4	−1.3	16.1	−0.8	15.9	−1.8	16.6	−1.7	16.3	−1.3	15.7	−0.9	15.3
RH850	48	−1.8	18.2	−1.8	18.1	−1.6	17.9	−1.4	17.7	−1.1	17.6	−1.9	18.0	−1.8	17.8	−1.4	17.4	−1.1	17.0

ECMWF. The results support the findings in obs-verification in the sense that T1A (baseline) and T1V (baseline plus wind profilers) have the worse scores for most parameters and that the full system (T1F) has the superior rms-scores. T1U (baseline plus wind and temperature from other radiosondes as well as aircrafts) typically has the second best rms-scores. It should be noted that T1F may have a small advantage since this verification use the T1F analyses, but it is believed to be only marginal.

3.4 Case studies

August 2005 had a number of episodes where some part or most of Denmark had a substantial amount of precipitation. Here we focus on one case where all parts of Denmark had precipitation within 24 h. Furthermore a case with a low north west of Scotland is studied. Here we focus on 00 UTC August 24, 2005 and 48 h forecasts valid at this time. Similar plots of 36 h forecasts show much smaller differences between the different experiments and are therefore not shown here.

Figures 32 and 33 show analyses and 48 h forecasts, respectively, of mslp and 10 m wind valid at 00 UTC August 24. Figure 34 shows differences of the 48 h mslp forecasts against the T1F analysis valid at this time. The mslp pressure of the center low in the analyses and in the 48 h forecasts are given in the following table:

experiment	T1A	T1V	T1W	T1T	T1D	T1X	T1B	T1U	T1F
Analysis (hPa)	970.0	969.6	969.2	970.3	971.1	969.4	969.7	971.7	970.8
48 h forecasts (hPa)	959.2	959.5	961.4	964.9	964.8	958.8	961.4	965.9	970.3

There are some differences in the analyses both in the center low pressure and also in the shapes. There is a buoy pressure measurement very close to the center showing 971.0 hPa. Since no other pressure measurements are available anywhere close to the center, the minimum value is expected to be fairly close to this observed value.

For the 48 h forecasts the full system do very well and is somewhat better than the second best mslp forecast. Both the center low pressure and the position of it are good. For all other forecasts the center low pressure is too low. The experiments including radiosonde wind and temperature (T1T, T1D and T1U) are a little better than the others in this respect but not as good as the full system. The position of the low is also too westerly in all forecasts but only a little in the forecast from the full system. In this respect, T1U seems to be second best.

Figures 35 and 36 show forecasted 12 h accumulated precipitation (6 h to 18 h forecasts) valid at 18 UTC August 5, 2005, and forecasted 12 h accumulated precipitation (18 h to 30 h forecasts) valid at 06 UTC August 6, 2005, respectively. Corresponding observations from SYNOP stations and from the Danish SVK (Spildevandskomiteen, see e.g. Nielsen and Cappelen, 2006 (in Danish)) net are shown in Figures 37 and 38. The observations show large variations in the amounts of precipitation over the area, in particular for the values valid at 18 UTC August 5, 2005. The differences in the forecasted accumulated precipitation and the position(s) of the largest precipitation amounts varies considerable between the experiments for both the 6 h to 18 h forecasts and the 18 h to 30 h forecasts. However, none of the experiments stand out as being particularly good. For the 6 h-18 h forecasts most experiments indicate higher than average amounts of precipitation in the most southern part of Jutland/northernmost part of Germany. This is in agreement with the observations even though they have somewhat higher values than forecasted. (31 mm/12 h and 25 mm/12 h observed in Glücksburg and Skrydstrup, respectively). For this region, T1A (baseline) and T1V (baseline plus wind profiler) are poorest, and T1X (baseline plus E-AMDAR) is the only experiment showing larger than 16 mm/12 h forecasted values, but closer to the Helgoland observation of 24 mm/12 h than to Glücksburg.

None of the 18 h-30 h forecasts are good. Some of them do, however, show a tendency of large precipitation

close to Bornholm. T1X (baseline plus E-AMDAR) do show a band of larger precipitation amounts from Lolland via eastern Zealand and into the south western part of Sweden in agreement with observations, even though there is no forecast values close to the observed 31 mm/12 h in Torup.

This case study do show the general trend that it is very hard to get convective precipitation forecasted correct and that small differences in the analyses can trigger the convective precipitation in quite different manners.

3.5 Comparisons of wind speed and temperature observations with first guess fields

For the use of observations in an analysis system such as the HIRLAM 3D-Var system it is important that the background (or first guess) and observation error statistics are specified correctly. Recently, a study (Navascués *et al.*, 2006) based on the method of Desroziers *et al.*, 2005, was initiated within the HIRLAM community in order to tune these errors, since they are known not to be optimal. One of the assumptions that are made, is that the observations are bias-free and that the error distributions of both the background and the observations are Gaussian. Figures 39 and 40 show the statistics of wind speed data from Meteosat-8, aircraft and radiosondes compared with the first guess fields (from the control experiment, T1F) interpolated to the observation points. The statistics are shown for three vertical 'layers'. The observational data are the data used in the analyses, data rejected in the analyses are not used in making the statistics. The figures show that the "quality" of the observations – as compared to the model fields – are similar for the 3 data types. If anything, the radiosonde wind speeds are a little worse. However, only few AMV and aircraft winds are available above ca. 200 hPa, in opposition to radiosonde wind data. Two of problems in the present use of radiosonde data are that all data are assumed to be valid at the same time, and that they are assumed to be valid at the same horizontal position. Both of these assumptions are invalid. During the ascent of a balloon it can drift many kilometer (even grid points) away from the original horizontal position. This will inevitable cause erroneous analysis increments in some cases.

Similar, Figure 41 shows the statistics of temperature data from radiosondes and aircraft. It is quite clear from this figure that there is a better agreement between aircraft temperatures and the first guess field temperatures than between radiosonde temperatures and the first guess field temperatures. Again, this may very well be a consequence of the assumption of constant horizontal position of the radiosonde measurements.

4 Conclusions

The present study has resulted in a number of interesting results. The summer runs confirm to a large extent the conclusions from the winter runs. Besides showing that radiosonde data are still a core part of todays meteorological observation system some of the major conclusions are

- The baseline setup has rather poor overall scores compared to most other setups.
- The use of E-AMDAR data gives only approximately half the impact (over Europe) of using all aircraft data. For some parameters the impact is significantly larger and for other parameters the impact is small.
- The use of wind data alone from the additional non-GUAN radiosondes give approximately half the impact from using both wind and temperature from the additional radiosonde data.
- Additional use of humidity from the additional non-GUAN radiosondes give an insignificant impact.
- The use of aircraft wind and temperature data give approximately the same impact as the additional radiosonde wind and temperature data.

- The use of both aircraft and the additional radiosonde wind and temperature data leads to significant better scores compared to using only one of the two components.

- For the long 06 UTC and 18 UTC forecasts for which the analyses have data available from only very few radiosonde stations, the impact from aircraft data are significantly larger than data from the non-GUAN radiosonde stations for only a few forecast lengths and parameters. Thus, the impact for the summer period is somewhat smaller than for the winter period.

- Addition of the (very few) additional wind profiler data gives an insignificant impact. However, regular monitoring of the data from the different stations should be made, and based on this a revised list of observation errors and which stations to be included in the whitelist can be estimated. Furthermore, restrictions such as is done in Aladin (between 400 hPa and 700 hPa; Roger Randriamampianina (OMSZ), private communication) to which part of the atmosphere where the data are used could be considered as well.

Thus, aircraft data and the extra radiosonde data are not redundant data in the DMI-HIRLAM analysis and forecasting system, but to a very high extent complementary data. Radiosonde data may also in the future be very important data. Besides being useful by themselves in assimilation they are of importance to anchor the bias correction of satellite radiances in a setup with adaptive bias correction, and of course for verification purposes.

It also seems important to have temperature information in addition to wind data, as the radiosonde data experiments show. In a future study it would be interesting to have an additional experiment with temperature data (and no wind data) from non-GUAN radiosonde stations.

Occasionally some satellite data are missing which furthermore results in a baseline setup that may be more sensitive to additional data than for a setup using more satellite data as expected in the future. It should also be noted that the amount of AMSU-A data over sea and sea ice is rather low for the 00 UTC analyses with the present satellite configuration. This is expected to be much better in the very near future, when data from METOP-A become available. The number of aircraft data in Europe during night is limited, since many airports do not allow aircrafts to land or depart during the night. This could be important if aircraft data are supposed to replace some radiosonde stations.

Studies like this should be repeated in the future, when more satellite data become available (with the above remark about the 00 UTC in mind), and also when the assimilation system undergoes a large change, such as the expected near future introduction of 4D-Var analyses in limited area models, that can take advantage of more of the data that are available at least hourly.

Acknowledgments

This study has been supported by EUCOS. The experiments have been made at ECMWF, partly via allocation of computer resources to a Special Project entitled 'EUCOS/EUMETSAT Data Impact Studies'. Thanks to Roger Randriamampianina (OMSZ) for providing the revised diagnostic tool from ECMWF for the significance test. Discussions at the EUCOS meetings in connection to this project have also been very valuable. Henrik Vedel is acknowledged for careful reading of the manuscript and for useful suggestions for improving it.

References

Amstrup, Bjarne. 2000. *EUCOS observing systems experiments with the DMI-HIRLAM Optimum Interpolation analysis and forecasting system*. DMI Scientific Report 00-19. Danish Meteorological Institute.

Amstrup, Bjarne. 2001. *Impact of ATOVS AMSU-A radiance data in the DMI-HIRLAM 3D-Var analysis and forecasting system*. DMI Scientific Report 01-06. Danish Meteorological Institute.

Amstrup, Bjarne. 2004. Impact of NOAA15 and NOAA16 ATOVS AMSU-A radiance data in the DMI-HIRLAM 3D-VAR data assimilation system – November and December 2003. *Hirlam Newsletter*, **45**, 235–247.

Amstrup, Bjarne. 2005. *First experiences with RTTOV8 for assimilating AMSU-A data in the DMI 3D-Var data assimilation system*. `http://cimss.ssec.wisc.edu/itwg/itsc/itsc14/proceedings/`.

Amstrup, Bjarne. 2006a. *EUCOS space/terrestrial OSE study using the DMI-HIRLAM 3D-VAR data assimilation system. Part I: A winter period*. DMI Scientific Report 06-07. Danish Meteorological Institute.

Amstrup, Bjarne. 2006b. Note on the use of bias predictors for bias correction of AMSU-A data in DMI-HIRLAM. *Hirlam Newsletter*, **51**, 141–152.

Amstrup, Bjarne and Mogensen, Kristian S. 2000. Observing system experiments with the DMI HIRLAM Optimum Interpolation analysis/three-dimensional variational analysis and forecasting system. *HIRLAM Technical Report*, **46**.

Amstrup, Bjarne and Mogensen, Kristian S. 2004. Observing system experiments with the DMI HIRLAM 3D-VAR data assimilation system in a winter and summer period in 2002. *Unpublised results*.

Andersson, E., Hólm, E., Bauer, P., Beljaars, A., Kelly, G. A., McNally, A. P., Simmons, A. J., Thépaut, J-N. and Tompkins, A. M. 2006. *Analysis and forecast impact of the main humidity observing systems*. Technical Memorandum 493. ECMWF.

Bauer, Peter, Lopez, Philippe, Benedetti, Angela, Salmond, Deborah and Moreau, Emmanuel. 2006a. Implementation of 1D+4D-Var assimilation of precipitation-affected microwave radiances at ECMWF. I: 1D-Var. *Quart. J. Roy. Meteorol. Soc.*, **132**, 2277–2306.

Bauer, Peter, Lopez, Philippe, Salmond, Deborah, Benedetti, Angela, Saarinen, Sami and Bonazzola, Marine. 2006b. Implementation of 1D+4D-Var assimilation of precipitation-affected microwave radiances at ECMWF. II: 4D-Var. *Quart. J. Roy. Meteorol. Soc.*, **132**, 2307–2332.

Berre, Loïk. 2000. Estimation of Synoptic and Mesoscale Forecast Error Covariances in a Limited-Area Model. *Mon. Weather Rev.*, **128**, 644–667.

Bormann, Niels and Thépaut, Jean-Noël. 2004. Impact of MODIS Polar Winds in ECMWF's 4DVAR Data Assimilation System. *Monthly Weather Review*, **132**, 929–940.

Bormann, Niels, Saarinen, Sami, Kelly, Graeme and Thépaut, Jean-Noël. 2003. The Spatial Structure of Observation Errors in Atmospheric Motion Vectors from Geostationary Satellite Data. *Mon. Weather Rev.*, **131**, 706–718.

Bouttier, F. and Kelly, G. 2001. Observing-system experiments in the ECMWF 4D-Var data assimilation system. *Quart. J. Roy. Meteorol. Soc.*, **127**, 1469–1488.

Cardinali, Carla, Isaksen, Lars and Andersson, Erik. 2003. Use and Impact of Automated Aircraft Data in a Global 4DVAR Data Assimilation System. *Mon. Weather Rev.*, **131**, 1865–1877.

Deblonde, Godelieve. 1999. Variational Assimilation of SSM/I Total Precipitable Water Retrievals in the CMC Analysis System. *Mon. Weather Rev.*, **127**, 1458–1476.

Desroziers, G., Berre, L., Chapnik, B. and Poli, P. 2005. Diagnosis of observation, background and analysis-error statistics in observation space. *Quart. J. Roy. Meteorol. Soc.*, **131**, 3385–3396.

English, S. J., Renshaw, R. J., Dibben, P. C., Smith, A. J., Rayer, P. J., Poulsen, C., Saunders, R. W. and Eyre, J. R. 2000. A comparison of the impact of TOVS and ATOVS satellite sounding data on the acuracy of numerical weather forecasts. *Quart. J. Roy. Meteorol. Soc.*, **126**, 2911–2931.

Feddersen, Henrik. 2004. "Horizontal" reduction of pressure to mean sea level. *Hirlam Newsletter*, **46**, 73–77.

Fourrié, Nadia, Marchal, David, Rabier, Florence, Chapnik, Bernard and Desroziers, Gerald. 2006. Impact study of the 2003 North Atlantic THORPEX Regional Campaign. *Quart. J. Roy. Meteorol. Soc.*, **132**, 275–295.

Geleyn, J.-F. 1998. Interpolation of wind, temperature and humidity values from the model levels to the height of measurement. *Tellus*, **40A**, 347–351.

Gérard, E. and Saunders, R. W. 1999. Four-dimensional variational assimilation of Special Sensor Microwave/Imager total column water vapour in the ECMWF model. *Quart. J. Roy. Meteorol. Soc.*, **125**, 3077–3101.

Graham, Richard, Anderson, Simon, Grant, Roger and Bader, Michael. 1998. Recent Data Impact Studies at UKMO - a review. *Pages 55–69 of: Proceedings of CGC/WMO workshop. Impact of various observing systems on numerical weather prediction. WMO/TD No. 868.*

Guerrero, C. Geijo and Amstrup, B. 2005. Assimilation of M8-AMV data in the HIRLAM-NWP model. *Hirlam Newsletter*, **49**, 12–21.

Gustafsson, N., Berre, L., Hörnquist, S., Huang, X.-Y., Lindskog, M., Navascués, B., Mogensen, K. S. and Thorsteinsson, S. 2001. Three-dimensional variational data assimilation for a limited area model. Part I: General formulation and the background error constraint. *Tellus*, **53A**, 425–446.

Harris, B. A. and Kelly, G. 2001. A satellite radiance-bias correction scheme for data assimilation. *Quart. J. Roy. Meteorol. Soc.*, **127**, 1453–1468.

Healy, S. B. and Thépaut, J.-N. 2006. Assimilation experiments with CHAMP GPS radio occultation measurements. *Quart. J. Roy. Meteorol. Soc.*, **132**, 605–623.

Huang, Xiang-Yu, Mogensen, Kristian Sten and Yang, Xiaohua. 2002 (March). First-Guess at the Appropriate Time: the HIRLAM Implementation and Experiments. *Pages 28–43 of: HIRLAM Workshop Report of HIRLAM Workshop on Variational Data Assimilation and Remote Sensing*.

Isaksen, Lars and Janssen, Peter A.E.M. 2004. Impact of ERS scatterometer winds in ECMWF's assimilation system. *Quart. J. Roy. Meteorol. Soc.*, **130**, 1793–1814.

Köpken, Christina, Thépaut, Jean-Noël and Kelly, Graeme. 2003. *Assimilation of Geostationary WV Radiances from GOES and Meteosat at ECMWF*. EUMETSAT/ECMWF Fellowship Programme, Research Report No. 14. ECMWF.

Lacroix, Bruno, Randriamamoianina, Roger and Charpentier, Etienne. 1998. Most recent impact studies at Metéo-France. *Pages 107–113 of: Proceedings of CGC/WMO workshop. Impact of various observing systems on numerical weather prediction. WMO/TD No. 868.*

Langland, Rolf H. and Baker, Nancy L. 2004. Estimation of observation impact using the NRL atmospheric variational data assimilation adjoint system. *Tellus*, **56A**, 189–201.

Lindberg, Karina. 2005. The effects of the modifications aimed to reduce noise in the semi-Lagrangian scheme in DMI-HIRLAM and the first preliminary tests of the SETTLS scheme in HIRLAM. *Hirlam Newsletter*, **48**, 128–134.

Lindskog, M., Gustafsson, N., Navascués, B., Mogensen, K. S., Huang, X.-Y., Yang, X., Andræ, U., Berre, L., Thorsteinsson, S. and Rantakokko, J. 2001. Three-dimensional variational data assimilation for a limited area model. Part II: Observation handling and assimilation experiments. *Tellus*, **53A**, 447–468.

Marécal, Virginie and Mahfouf, Jean-François. 2003. Experiments on 4D-Var assimilation of rainfall data using an incremental formulation. *Quart. J. Roy. Meteorol. Soc.*, **129**, 3137–3160.

McNally, A. P., Watts, P. D., Smith, J. A., Engelen, R., Kelly, G. A., Thépaut, J. N. and Matricardi, M. 2006. The assimilation of AIRS radiance data at ECMWF. *Quart. J. Roy. Meteorol. Soc.*, **132**, 935–957.

Navascués, Beatriz, Lindskog, Magnus, Yang, Xiaohua and Amstrup, Bjarne. 2006. Diagnosis of error statistics in the HIRLAM 3D-VAR. *HIRLAM Technical Report*, **66**.

Nielsen, Maja Kjørup and Cappelen, John. 2006. *Drift af Spildevandskomitéens Regnmålersystem – Årsnotat 2005*. DMI Technical Report 06-03. Danish Meteorological Institute.

Okamoto, Kozo and Derber, John C. 2006. Assimilation of SSM/I Radiances in the NCEP Global Data Assimilation System. *Monthly Weather Review*, **134**, 2612–2631.

Portabella, M. and Stoffelen, A. 2004. A probabilistic approach for SeaWinds data assimilation. *Quart. J. Roy. Meteorol. Soc.*, **130**, 127–152.

Sass, B. H. 2002. *A research version of the STRACO cloud scheme*. DMI Technical Report 02-10. Danish Meteorological Institute.

Schyberg, Harald, Landelius, Tomas, Thorsteinsson, Sigurdur, Tveter, Frank Thomas, Vignes, Ole, Amstrup, Bjarne, Gustafsson, Nils, Järvinen, Heikki and Lindskog, Magnus. 2003. Assimilation of ATOVS data in the HIRLAM 3D-VAR System. *HIRLAM Technical Report*, **60**.

Tomassini, M., Kelly, G. and Saunders, R. 1999. Use and Impact of Satellite Atmospheric Motion Winds on ECMWF Analyses and Forecasts. *Mon. Wea. Rew.*, **127**, 971–986.

Undén, Per, Rontu, Laura, Järvinen, Heikki, Lynch, Peter, Calvo, Javier, Cats, Gerard, Cuxart, Joan, Eerola, Kalle, Fortelius, Carl, Garcia-Moya, Jose Antonio, Jones, Colin, Lenderlink, Geert, McDonald, Aidan, McGrath, Ray, Navascues, Beatrix, Nielsen, Niels Woetmann, Ødegaard, Viel, Rodriguez, Ernesto, Rummukainen, Markku, Rõõm, Rein, Sattler, Kai, Sass, Bent Hansen, Savijärvi, Hannu, Schreuer, Ben Wichers, Sigg, Robert, The, Han and Tijm, Aleksander. 2002. *HIRLAM-5 Scientific Documentation*. HIRLAM Scientific Report.

Vedel, Henrik and Huang, Xiang-Yu. 2004. Impact of Ground Based GPS data on Numerical Weather Prediction. *J. Meteorol. Soc. Japan*, **82**, 459–472.

Vignes, Ole, Tveter, Frank Thomas and Schyberg, Harald. 2005. *Results from the Winter 2003/2004 HIRLAM Analysis Impact Study*. met.no report 06. Norwegian Meteorological Institute.

Yang, Xiaohua, Pedersen, Claus, Amstrup, Bjarne, Andersen, Bjarne, Feddersen, Henrik, Kmit, Maryanne, Korsholm, Ulrik, Lindberg, Karina, Mogensen, Kristian S., Sass, Bent Hansen, Sattler, Kai and Nielsen, Niels Woetmann. 2005a. *The DMI-HIRLAM upgrade in June 2004*. DMI Technical Report 05-09. Danish Meteorological Institute.

Yang, Xiaohua, Kmit, Maryanne, Sass, Bent Hansen, Amstrup, Bjarne, Lindberg, Karina, Pedersen, Claus, Korsholm, Ulrik and Nielsen, Niels Woetmann. 2005b. *The DMI-HIRLAM upgrade in May 2005*. DMI Technical Report 05-10. Danish Meteorological Institute.

Table 7: Contingency tables for 20050730-20050831 (6–18 h forecasts). Danish station list.

T1A 20050730-20050831 (64.7 %)						
obs→ / ↓ for	O1	O2	O3	O4	O5	sum
F1	**530**	23	8	2	0	563
F2	217	**42**	21	6	4	290
F3	125	55	**54**	16	10	260
F4	12	7	26	**26**	10	81
F5	0	2	5	11	**9**	27
sum	884	129	114	61	33	1221
%FO	60	33	47	43	27	54

T1B 20050730-20050831 (66.3 %)						
obs→ / ↓ for	O1	O2	O3	O4	O5	sum
F1	**546**	18	6	1	0	571
F2	214	**49**	22	6	4	295
F3	116	54	**62**	25	10	267
F4	8	7	22	**24**	12	73
F5	0	1	2	5	**7**	15
sum	884	129	114	61	33	1221
%FO	62	38	54	39	21	56

T1W 20050730-20050831 (66.6 %)						
obs→ / ↓ for	O1	O2	O3	O4	O5	sum
F1	**510**	24	7	1	0	542
F2	248	**38**	23	3	2	314
F3	119	61	**62**	20	9	271
F4	5	5	21	**28**	12	71
F5	**2**	1	1	9	**10**	23
sum	884	129	114	61	33	1221
%FO	58	29	54	46	30	53

T1T 20050730-20050831 (65.5 %)						
obs→ / ↓ for	O1	O2	O3	O4	O5	sum
F1	**523**	23	6	1	0	553
F2	228	**41**	20	2	2	293
F3	123	59	**69**	25	12	288
F4	8	5	17	**24**	10	64
F5	**2**	1	2	9	**9**	23
sum	884	129	114	61	33	1221
%FO	59	32	61	39	27	55

T1D 20050730-20050831 (67.3 %)						
obs→ / ↓ for	O1	O2	O3	O4	O5	sum
F1	**540**	29	7	1	0	577
F2	222	**35**	22	4	2	285
F3	114	60	**66**	21	14	275
F4	8	5	18	**25**	9	65
F5	0	0	1	10	**8**	19
sum	884	129	114	61	33	1221
%FO	61	27	58	41	24	55

T1U 20050730-20050831 (65.1 %)						
obs→ / ↓ for	O1	O2	O3	O4	O5	sum
F1	**519**	21	8	1	0	549
F2	241	**43**	18	6	3	311
F3	118	60	**60**	20	10	268
F4	6	5	26	**25**	14	76
F5	0	0	2	9	**6**	17
sum	884	129	114	61	33	1221
%FO	59	33	53	41	18	53

T1F 20050730-20050831 (66.0 %)						
obs→ / ↓ for	O1	O2	O3	O4	O5	sum
F1	**533**	25	5	2	0	565
F2	238	**36**	18	3	3	298
F3	103	62	**57**	17	12	251
F4	9	6	30	**28**	10	83
F5	**1**	0	4	11	**8**	24
sum	884	129	114	61	33	1221
%FO	60	28	50	46	24	54

T1V 20050730-20050831 (66.8 %)						
obs→ / ↓ for	O1	O2	O3	O4	O5	sum
F1	**515**	20	5	3	0	543
F2	240	**47**	28	5	2	322
F3	121	54	**61**	19	10	265
F4	7	6	19	**25**	9	66
F5	**1**	2	1	9	**12**	25
sum	884	129	114	61	33	1221
%FO	58	36	54	41	36	54

T1X 20050730-20050831 (67.1 %)						
obs→ / ↓ for	O1	O2	O3	O4	O5	sum
F1	**531**	22	3	1	0	557
F2	231	**43**	18	3	1	296
F3	114	56	**72**	24	11	277
F4	7	6	16	**27**	14	70
F5	**1**	2	5	6	**7**	21
sum	884	129	114	61	33	1221
%FO	60	33	63	44	21	56

T1Y 20050730-20050831 (66.0 %)						
obs→ / ↓ for	O1	O2	O3	O4	O5	sum
F1	**530**	20	7	1	0	558
F2	229	**44**	16	5	4	298
F3	119	57	**65**	23	10	274
F4	6	7	25	**26**	11	75
F5	0	1	1	6	**8**	16
sum	884	129	114	61	33	1221
%FO	60	34	57	43	24	55

Table 8: Contingency tables for 20050730-20050831 (18–30 h forecasts). Danish station list.

T1A 20050730-20050831 (65.7 %)						
obs→ / ↓ for	O1	O2	O3	O4	O5	sum
F1	**543**	27	8	1	**1**	580
F2	217	**39**	20	5	3	284
F3	127	51	**59**	21	6	264
F4	13	10	15	**18**	10	66
F5	**3**	1	7	12	**5**	28
sum	903	128	109	57	25	1222
%FO	60	30	54	32	20	54

T1B 20050730-20050831 (67.7 %)						
obs→ / ↓ for	O1	O2	O3	O4	O5	sum
F1	**556**	27	9	5	**1**	598
F2	216	**41**	22	8	3	290
F3	119	51	**62**	16	10	258
F4	12	9	11	**15**	5	52
F5	0	0	5	13	**6**	24
sum	903	128	109	57	25	1222
%FO	62	32	57	26	24	56

T1W 20050730-20050831 (66.2 %)						
obs→ / ↓ for	O1	O2	O3	O4	O5	sum
F1	**543**	24	9	0	**2**	578
F2	228	**42**	15	6	1	292
F3	116	55	**67**	20	6	264
F4	16	6	17	**29**	11	79
F5	0	1	1	2	**5**	9
sum	903	128	109	57	25	1222
%FO	60	33	61	51	20	56

T1T 20050730-20050831 (65.0 %)						
obs→ / ↓ for	O1	O2	O3	O4	O5	sum
F1	**538**	26	9	1	**1**	575
F2	225	**47**	22	3	3	300
F3	121	49	**59**	23	6	258
F4	16	4	16	**25**	12	73
F5	**3**	2	3	5	**3**	16
sum	903	128	109	57	25	1222
%FO	60	37	54	44	12	55

T1D 20050730-20050831 (64.1 %)						
obs→ / ↓ for	O1	O2	O3	O4	O5	sum
F1	**537**	33	11	2	**2**	585
F2	213	**37**	15	5	3	273
F3	131	46	**61**	18	3	259
F4	18	11	18	**22**	12	81
F5	**4**	1	4	10	**5**	24
sum	903	128	109	57	25	1222
%FO	59	29	56	39	20	54

T1U 20050730-20050831 (69.0 %)						
obs→ / ↓ for	O1	O2	O3	O4	O5	sum
F1	**565**	30	10	2	0	607
F2	213	**36**	23	10	6	288
F3	111	52	**61**	16	3	243
F4	14	10	15	**24**	11	74
F5	0	0	0	5	**5**	10
sum	903	128	109	57	25	1222
%FO	63	28	56	42	20	57

T1F 20050730-20050831 (67.7 %)						
obs→ / ↓ for	O1	O2	O3	O4	O5	sum
F1	**560**	32	6	2	**1**	601
F2	221	**41**	23	11	4	300
F3	115	49	**64**	9	7	244
F4	7	6	13	**24**	10	60
F5	0	0	3	11	**3**	17
sum	903	128	109	57	25	1222
%FO	62	32	59	42	12	57

T1V 20050730-20050831 (63.9 %)						
obs→ / ↓ for	O1	O2	O3	O4	O5	sum
F1	**514**	22	4	1	**1**	542
F2	236	**49**	27	8	2	322
F3	135	50	**59**	17	9	270
F4	17	7	17	**23**	8	72
F5	**1**	0	2	8	**5**	16
sum	903	128	109	57	25	1222
%FO	57	38	54	40	20	53

T1X 20050730-20050831 (64.7 %)						
obs→ / ↓ for	O1	O2	O3	O4	O5	sum
F1	**551**	29	7	2	0	589
F2	209	**38**	24	5	6	282
F3	130	51	**55**	17	5	258
F4	10	9	18	**22**	8	67
F5	**3**	1	5	11	**6**	26
sum	903	128	109	57	25	1222
%FO	61	30	50	39	24	55

T1Y 20050730-20050831 (66.4 %)						
obs→ / ↓ for	O1	O2	O3	O4	O5	sum
F1	**542**	28	11	2	**1**	584
F2	226	**45**	21	10	3	305
F3	126	48	**61**	18	7	260
F4	9	7	9	**14**	9	48
F5	0	0	7	13	**5**	25
sum	903	128	109	57	25	1222
%FO	60	35	56	25	20	55

Table 9: Contingency tables for 20050730-20050831 (30–42 h forecasts). Danish station list.

T1A 20050730-20050831 (60.7 %)						
obs→ / ↓ for	O1	O2	O3	O4	O5	sum
F1	**501**	21	7	1	**1**	531
F2	210	**40**	15	4	3	272
F3	163	56	**67**	27	9	322
F4	13	9	20	**19**	10	71
F5	**11**	4	1	7	**3**	26
sum	898	130	110	58	26	1222
%FO	56	31	61	33	12	52

T1B 20050730-20050831 (63.5 %)						
obs→ / ↓ for	O1	O2	O3	O4	O5	sum
F1	**542**	31	10	4	**2**	589
F2	207	**44**	21	8	7	287
F3	135	43	**52**	15	5	250
F4	13	9	22	**19**	11	74
F5	**1**	3	5	12	**1**	22
sum	898	130	110	58	26	1222
%FO	60	34	47	33	4	54

T1W 20050730-20050831 (64.8 %)						
obs→ / ↓ for	O1	O2	O3	O4	O5	sum
F1	**538**	22	7	2	**2**	571
F2	216	**40**	23	3	2	284
F3	130	58	**60**	29	8	285
F4	13	10	17	**19**	9	68
F5	**1**	0	3	5	**5**	14
sum	898	130	110	58	26	1222
%FO	60	31	55	33	19	54

T1T 20050730-20050831 (66.2 %)						
obs→ / ↓ for	O1	O2	O3	O4	O5	sum
F1	**565**	32	8	1	**2**	608
F2	190	**37**	18	5	5	255
F3	131	53	**66**	31	7	288
F4	11	7	15	**20**	9	62
F5	**1**	1	3	1	**3**	9
sum	898	130	110	58	26	1222
%FO	63	28	60	34	12	57

T1D 20050730-20050831 (65.7 %)						
obs→ / ↓ for	O1	O2	O3	O4	O5	sum
F1	**560**	26	8	1	**1**	596
F2	193	**48**	22	8	3	274
F3	127	49	**62**	33	8	279
F4	15	7	18	**15**	13	68
F5	**3**	0	0	1	**1**	5
sum	898	130	110	58	26	1222
%FO	62	37	56	26	4	56

T1U 20050730-20050831 (65.0 %)						
obs→ / ↓ for	O1	O2	O3	O4	O5	sum
F1	**561**	25	14	2	**1**	603
F2	190	**44**	20	10	5	269
F3	138	53	**51**	20	7	269
F4	8	8	23	**22**	13	74
F5	**1**	0	2	4	**0**	7
sum	898	130	110	58	26	1222
%FO	62	34	46	38	0	55

T1F 20050730-20050831 (65.7 %)						
obs→ / ↓ for	O1	O2	O3	O4	O5	sum
F1	**555**	29	13	2	**1**	600
F2	206	**41**	15	2	2	266
F3	127	52	**61**	30	7	277
F4	10	8	17	**17**	11	63
F5	0	0	4	7	**5**	16
sum	898	130	110	58	26	1222
%FO	62	32	55	29	19	56

T1V 20050730-20050831 (62.4 %)						
obs→ / ↓ for	O1	O2	O3	O4	O5	sum
F1	**511**	26	4	3	**2**	546
F2	214	**41**	24	3	2	284
F3	146	55	**57**	26	10	294
F4	22	4	23	**20**	8	77
F5	**5**	4	2	6	**4**	21
sum	898	130	110	58	26	1222
%FO	57	32	52	34	15	52

T1X 20050730-20050831 (64.0 %)						
obs→ / ↓ for	O1	O2	O3	O4	O5	sum
F1	**540**	28	8	2	**1**	579
F2	199	**46**	18	5	4	272
F3	142	45	**63**	22	10	282
F4	15	10	21	**23**	8	77
F5	**2**	1	0	6	**3**	12
sum	898	130	110	58	26	1222
%FO	60	35	57	40	12	55

T1Y 20050730-20050831 (64.1 %)						
obs→ / ↓ for	O1	O2	O3	O4	O5	sum
F1	**543**	34	13	4	**2**	596
F2	207	**44**	22	5	6	284
F3	129	41	**57**	25	6	258
F4	16	9	17	**15**	10	67
F5	**3**	2	1	9	**2**	17
sum	898	130	110	58	26	1222
%FO	60	34	52	26	8	54

Table 10: Contingency tables for 20050730-20050831 (6–18 h forecasts). EWGLAM station list.

T1A 20050730-20050831						
obs→ / ↓ for	O1	O2	O3	O4	O5	sum
F1	**10257**	402	152	34	**29**	10874
F2	2326	**477**	328	76	50	3257
F3	1420	551	**804**	301	192	3268
F4	206	98	276	**198**	155	933
F5	**71**	34	104	131	**235**	575
sum	14280	1562	1664	740	661	18907
%FO	72	31	48	27	36	63

T1B 20050730-20050831						
obs→ / ↓ for	O1	O2	O3	O4	O5	sum
F1	**10416**	392	144	26	**24**	11002
F2	2231	**470**	332	76	47	3156
F3	1394	579	**787**	299	186	3245
F4	181	90	293	**214**	161	939
F5	**58**	31	108	125	**243**	565
sum	14280	1562	1664	740	661	18907
%FO	73	30	47	29	37	64

T1W 20050730-20050831						
obs→ / ↓ for	O1	O2	O3	O4	O5	sum
F1	**10456**	383	135	38	**25**	11037
F2	2220	**461**	323	69	53	3126
F3	1349	596	**823**	293	179	3240
F4	193	94	284	**216**	145	932
F5	**62**	28	99	124	**259**	572
sum	14280	1562	1664	740	661	18907
%FO	73	30	49	29	39	65

T1T 20050730-20050831						
obs→ / ↓ for	O1	O2	O3	O4	O5	sum
F1	**10351**	385	131	28	**27**	10922
F2	2267	**469**	329	77	43	3185
F3	1414	585	**813**	280	164	3256
F4	186	90	287	**234**	173	970
F5	**62**	33	104	121	**254**	574
sum	14280	1562	1664	740	661	18907
%FO	72	30	49	32	38	64

T1D 20050730-20050831						
obs→ / ↓ for	O1	O2	O3	O4	O5	sum
F1	**10466**	400	152	28	**26**	11072
F2	2199	**465**	308	76	47	3095
F3	1378	564	**821**	292	176	3231
F4	183	101	278	**209**	164	935
F5	**54**	32	105	135	**248**	574
sum	14280	1562	1664	740	661	18907
%FO	73	30	49	28	38	65

T1U 20050730-20050831						
obs→ / ↓ for	O1	O2	O3	O4	O5	sum
F1	**10475**	405	149	27	**29**	11085
F2	2242	**453**	330	67	37	3129
F3	1335	581	**818**	317	187	3238
F4	180	90	258	**205**	167	900
F5	**48**	33	109	124	**241**	555
sum	14280	1562	1664	740	661	18907
%FO	73	29	49	28	36	64

T1F 20050730-20050831						
obs→ / ↓ for	O1	O2	O3	O4	O5	sum
F1	**10391**	390	131	30	**27**	10969
F2	2287	**483**	312	64	49	3195
F3	1387	571	**877**	301	166	3302
F4	162	87	264	**226**	172	911
F5	**53**	31	80	119	**247**	530
sum	14280	1562	1664	740	661	18907
%FO	73	31	53	31	37	65

T1V 20050730-20050831						
obs→ / ↓ for	O1	O2	O3	O4	O5	sum
F1	**10334**	389	166	39	**23**	10951
F2	2203	**487**	324	77	65	3156
F3	1466	560	**798**	278	183	3285
F4	208	90	272	**202**	156	928
F5	**69**	36	104	144	**234**	587
sum	14280	1562	1664	740	661	18907
%FO	72	31	48	27	35	64

T1X 20050730-20050831						
obs→ / ↓ for	O1	O2	O3	O4	O5	sum
F1	**10302**	388	128	36	**28**	10882
F2	2304	**455**	341	64	44	3208
F3	1410	607	**837**	295	198	3347
F4	203	80	250	**222**	159	914
F5	**61**	32	108	123	**232**	556
sum	14280	1562	1664	740	661	18907
%FO	72	29	50	30	35	64

T1Y 20050730-20050831						
obs→ / ↓ for	O1	O2	O3	O4	O5	sum
F1	**10447**	382	149	29	**29**	11036
F2	2223	**497**	308	80	47	3155
F3	1360	561	**826**	303	185	3235
F4	190	95	285	**205**	160	935
F5	**60**	27	96	123	**240**	546
sum	14280	1562	1664	740	661	18907
%FO	73	32	50	28	36	65

Table 11: Contingency tables for 20050730-20050831 (18–30 h forecasts). EWGLAM station list.

T1A 20050730-20050831						
obs→ / ↓for	O1	O2	O3	O4	O5	sum
F1	**10232**	421	189	50	**32**	10924
F2	2303	**462**	318	89	65	3237
F3	1485	520	**759**	284	218	3266
F4	211	109	260	**189**	162	931
F5	**83**	42	120	121	**177**	543
sum	14314	1554	1646	733	654	18901
%FO	71	30	46	26	27	63

T1B 20050730-20050831						
obs→ / ↓for	O1	O2	O3	O4	O5	sum
F1	**10400**	419	163	49	**28**	11059
F2	2225	**440**	335	76	55	3131
F3	1439	569	**791**	304	196	3299
F4	176	95	235	**195**	167	868
F5	**74**	31	122	109	**208**	544
sum	14314	1554	1646	733	654	18901
%FO	73	28	48	27	32	64

T1W 20050730-20050831						
obs→ / ↓for	O1	O2	O3	O4	O5	sum
F1	**10319**	411	172	44	**43**	10989
F2	2300	**463**	345	91	52	3251
F3	1423	525	**778**	304	214	3244
F4	196	114	240	**187**	145	882
F5	**76**	41	111	107	**200**	535
sum	14314	1554	1646	733	654	18901
%FO	72	30	47	26	31	63

T1T 20050730-20050831						
obs→ / ↓for	O1	O2	O3	O4	O5	sum
F1	**10318**	426	162	40	**33**	10979
F2	2328	**445**	314	96	56	3239
F3	1404	553	**828**	313	200	3298
F4	194	93	233	**187**	171	878
F5	**70**	37	109	97	**194**	507
sum	14314	1554	1646	733	654	18901
%FO	72	29	50	26	30	63

T1D 20050730-20050831						
obs→ / ↓for	O1	O2	O3	O4	O5	sum
F1	**10280**	406	158	48	**36**	10928
F2	2360	**440**	328	80	51	3259
F3	1408	575	**828**	313	209	3333
F4	202	103	246	**188**	173	912
F5	**64**	30	86	104	**185**	469
sum	14314	1554	1646	733	654	18901
%FO	72	28	50	26	28	63

T1U 20050730-20050831						
obs→ / ↓for	O1	O2	O3	O4	O5	sum
F1	**10379**	408	155	31	**25**	10998
F2	2308	**453**	336	89	53	3239
F3	1371	587	**807**	303	204	3272
F4	186	83	252	**206**	161	888
F5	**70**	23	96	104	**211**	504
sum	14314	1554	1646	733	654	18901
%FO	73	29	49	28	32	64

T1F 20050730-20050831						
obs→ / ↓for	O1	O2	O3	O4	O5	sum
F1	**10309**	417	170	33	**24**	10953
F2	2299	**477**	331	87	44	3238
F3	1436	532	**775**	298	217	3258
F4	207	99	277	**199**	156	938
F5	**63**	29	93	116	**213**	514
sum	14314	1554	1646	733	654	18901
%FO	72	31	47	27	33	63

T1V 20050730-20050831						
obs→ / ↓for	O1	O2	O3	O4	O5	sum
F1	**10249**	422	174	49	**37**	10931
F2	2290	**448**	352	86	55	3231
F3	1489	547	**756**	313	220	3325
F4	203	113	263	**190**	157	926
F5	**83**	24	101	95	**185**	488
sum	14314	1554	1646	733	654	18901
%FO	72	29	46	26	28	63

T1X 20050730-20050831						
obs→ / ↓for	O1	O2	O3	O4	O5	sum
F1	**10313**	427	179	51	**33**	11003
F2	2281	**450**	331	83	55	3200
F3	1428	540	**783**	277	216	3244
F4	210	101	247	**205**	164	927
F5	**82**	36	106	117	**186**	527
sum	14314	1554	1646	733	654	18901
%FO	72	29	48	28	28	63

T1Y 20050730-20050831						
obs→ / ↓for	O1	O2	O3	O4	O5	sum
F1	**10386**	430	173	47	**28**	11064
F2	2253	**449**	327	79	62	3170
F3	1411	545	**779**	304	203	3242
F4	194	97	264	**187**	154	896
F5	**70**	33	103	116	**207**	529
sum	14314	1554	1646	733	654	18901
%FO	73	29	47	26	32	64

Table 12: Contingency tables for 20050730-20050831 (30–42 h forecasts). EWGLAM station list.

T1A 20050730-20050831						
obs→ / ↓ for	O1	O2	O3	O4	O5	sum
F1	**10269**	454	220	66	**49**	11058
F2	2247	**429**	367	99	69	3211
F3	1527	507	**745**	306	205	3290
F4	229	118	212	**166**	156	881
F5	**78**	36	89	96	**159**	458
sum	14350	1544	1633	733	638	18898
%FO	72	28	46	23	25	62

T1B 20050730-20050831						
obs→ / ↓ for	O1	O2	O3	O4	O5	sum
F1	**10285**	448	204	45	**39**	11021
F2	2315	**417**	367	98	59	3256
F3	1439	525	**750**	302	203	3219
F4	234	113	216	**180**	163	906
F5	**77**	41	96	108	**174**	496
sum	14350	1544	1633	733	638	18898
%FO	72	27	46	25	27	62

T1W 20050730-20050831						
obs→ / ↓ for	O1	O2	O3	O4	O5	sum
F1	**10349**	440	202	49	**52**	11092
F2	2267	**436**	365	96	48	3212
F3	1439	525	**764**	306	220	3254
F4	214	104	206	**184**	149	857
F5	**81**	39	96	98	**169**	483
sum	14350	1544	1633	733	638	18898
%FO	72	28	47	25	26	63

T1T 20050730-20050831						
obs→ / ↓ for	O1	O2	O3	O4	O5	sum
F1	**10322**	481	212	62	**40**	11117
F2	2251	**397**	360	91	66	3165
F3	1504	513	**740**	316	192	3265
F4	198	111	229	**168**	165	871
F5	**75**	42	92	96	**175**	480
sum	14350	1544	1633	733	638	18898
%FO	72	26	45	23	27	62

T1D 20050730-20050831						
obs→ / ↓ for	O1	O2	O3	O4	O5	sum
F1	**10278**	446	200	62	**42**	11028
F2	2324	**422**	367	84	63	3260
F3	1460	536	**729**	310	192	3227
F4	200	105	237	**180**	176	898
F5	**88**	35	100	97	**165**	485
sum	14350	1544	1633	733	638	18898
%FO	72	27	45	25	26	62

T1U 20050730-20050831						
obs→ / ↓ for	O1	O2	O3	O4	O5	sum
F1	**10372**	442	194	46	**38**	11092
F2	2280	**446**	368	91	54	3239
F3	1427	509	**762**	317	199	3214
F4	205	102	219	**171**	175	872
F5	**66**	45	90	108	**172**	481
sum	14350	1544	1633	733	638	18898
%FO	72	29	47	23	27	63

T1F 20050730-20050831						
obs→ / ↓ for	O1	O2	O3	O4	O5	sum
F1	**10425**	416	195	52	**42**	11130
F2	2263	**450**	338	89	48	3188
F3	1380	545	**775**	306	209	3215
F4	189	100	228	**197**	158	872
F5	**93**	33	97	89	**181**	493
sum	14350	1544	1633	733	638	18898
%FO	73	29	47	27	28	64

T1V 20050730-20050831						
obs→ / ↓ for	O1	O2	O3	O4	O5	sum
F1	**10239**	463	216	65	**38**	11021
F2	2279	**421**	359	108	78	3245
F3	1520	525	**723**	298	192	3258
F4	230	95	221	**169**	153	868
F5	**82**	40	114	93	**177**	506
sum	14350	1544	1633	733	638	18898
%FO	71	27	44	23	28	62

T1X 20050730-20050831						
obs→ / ↓ for	O1	O2	O3	O4	O5	sum
F1	**10267**	471	215	53	**44**	11050
F2	2315	**414**	354	95	60	3238
F3	1475	522	**755**	319	207	3278
F4	210	106	210	**171**	157	854
F5	**83**	31	99	95	**170**	478
sum	14350	1544	1633	733	638	18898
%FO	72	27	46	23	27	62

T1Y 20050730-20050831						
obs→ / ↓ for	O1	O2	O3	O4	O5	sum
F1	**10345**	450	204	47	**37**	11083
F2	2257	**434**	345	94	58	3188
F3	1469	519	**772**	309	214	3283
F4	191	100	211	**190**	157	849
F5	**88**	41	101	93	**172**	495
sum	14350	1544	1633	733	638	18898
%FO	72	28	47	26	27	63

Table 13: Equitable threat scores (ETS) for the August period runs. ETS1 is for a limit of 0.3 mm/12 h, ETS2 is for a limit of 1.5 mm/12 h and ETS3 is for a limit of 5.0 mm/12 h. The smallest value and values within 0.0025 of this value for a given forecast range and limit is shown in red. The best value as well as values within 0.0025 of this value for a given forecast range and limit is marked with bold black font.

Danish stations									
	6–18 h			18–30 h			30–42 h		
model	ETS1	ETS2	ETS3	ETS1	ETS2	ETS3	ETS1	ETS2	ETS3
T1A	**0.253**	**0.311**	0.346	0.246	0.265	0.310	**0.198**	**0.249**	0.239
T1B	0.270	0.341	**0.324**	0.256	0.274	**0.298**	0.215	0.268	0.279
T1D	0.267	0.343	0.381	**0.219**	0.287	0.320	0.253	0.272	**0.205**
T1T	**0.251**	0.348	0.370	0.234	0.272	0.325	**0.258**	0.287	0.240
T1U	**0.251**	**0.377**	0.372	**0.269**	**0.250**	0.341	0.233	**0.247**	0.278
T1W	0.263	0.348	**0.425**	0.243	0.296	0.351	0.242	0.261	0.264
T1V	0.262	0.336	0.390	0.224	0.284	0.317	0.209	0.274	0.228
T1X	**0.273**	0.369	0.379	0.226	0.275	0.335	0.227	0.270	0.267
T1Y	0.266	0.335	0.346	0.240	**0.300**	0.331	0.212	0.262	0.239
T1F	0.266	0.349	0.359	0.243	**0.298**	**0.405**	0.245	**0.290**	**0.294**

Table 14: Equitable threat scores (ETS) for the August period runs. ETS1 is for a limit of 0.3 mm/12 h, ETS2 is for a limit of 1.5 mm/12 h and ETS3 is for a limit of 5.0 mm/12 h. The smallest value and values within 0.0025 of this value for a given forecast range and limit is shown in red. The best value as well as values within 0.0025 of this value for a given forecast range and limit is marked with bold black font.

EWGLAM stations									
	6–18 h			18–30 h			30–42 h		
model	ETS1	ETS2	ETS3	ETS1	ETS2	ETS3	ETS1	ETS2	ETS3
T1A	**0.329**	0.347	**0.294**	0.314	**0.324**	0.259	**0.292**	**0.294**	**0.238**
T1B	0.344	0.361	0.311	0.329	0.341	0.288	0.309	0.318	0.258
T1D	0.343	0.359	0.318	0.326	0.339	0.275	0.301	0.306	0.257
T1T	0.338	0.359	0.329	0.328	0.336	0.273	0.303	0.308	0.253
T1U	**0.349**	**0.372**	0.315	**0.333**	0.344	**0.293**	0.311	0.323	**0.265**
T1W	0.347	0.353	0.312	0.322	0.328	0.262	0.306	0.301	0.251
T1V	0.333	**0.334**	0.304	**0.310**	**0.323**	**0.255**	**0.291**	0.298	0.242
T1X	0.335	0.359	0.312	0.317	0.333	0.276	0.300	0.311	0.249
T1Y	0.346	0.359	0.305	0.328	0.338	0.276	0.311	0.310	0.260
T1F	**0.351**	0.362	**0.335**	0.328	**0.354**	0.286	**0.315**	**0.328**	**0.264**

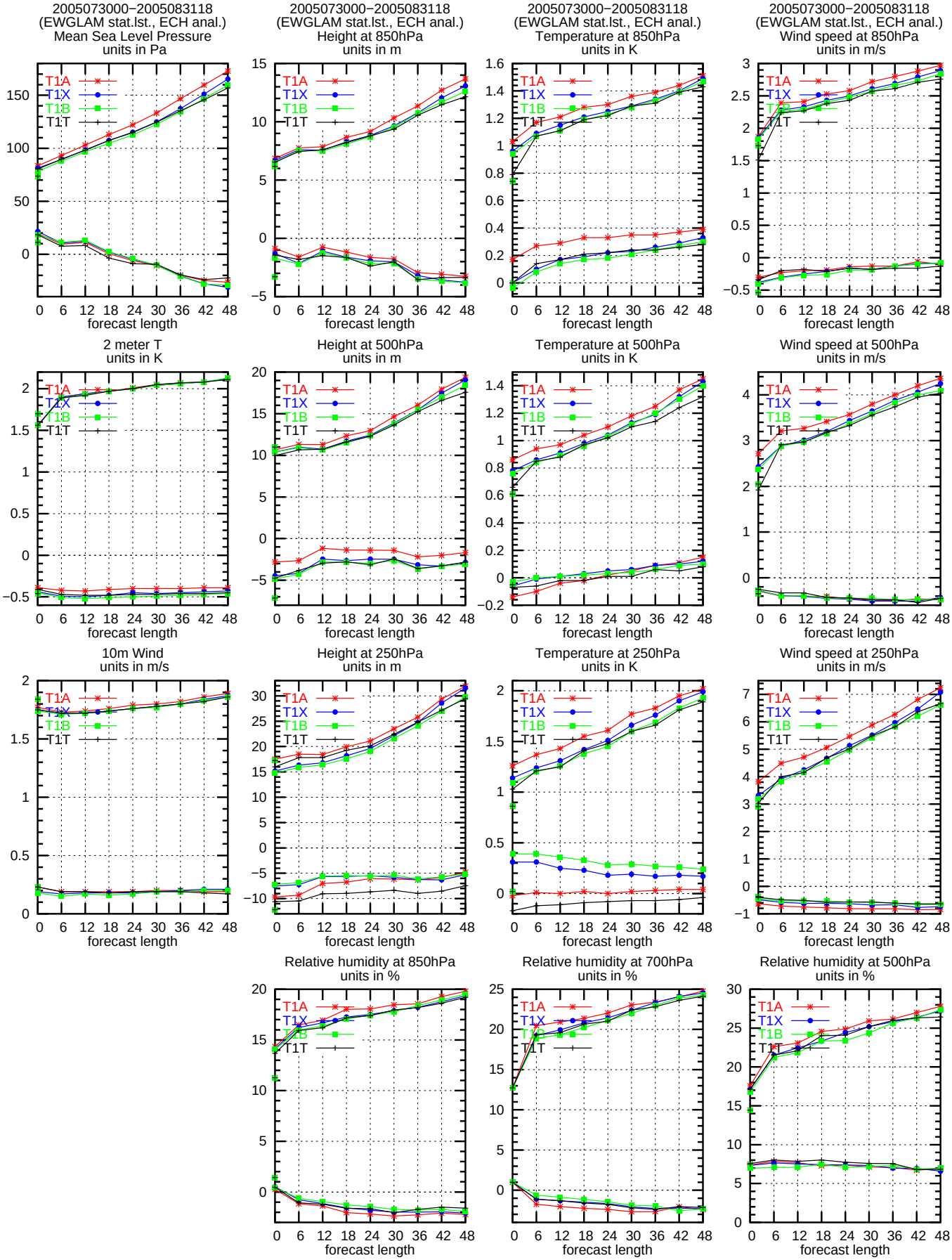

Figure 8: Obs-verification of control run (T1A), 'additional radiosonde wind and temperature' (T1T) run, 'all aircraft' (T1B) run, and 'E-AMDAR' (T1X) run. EWGLAM station list.

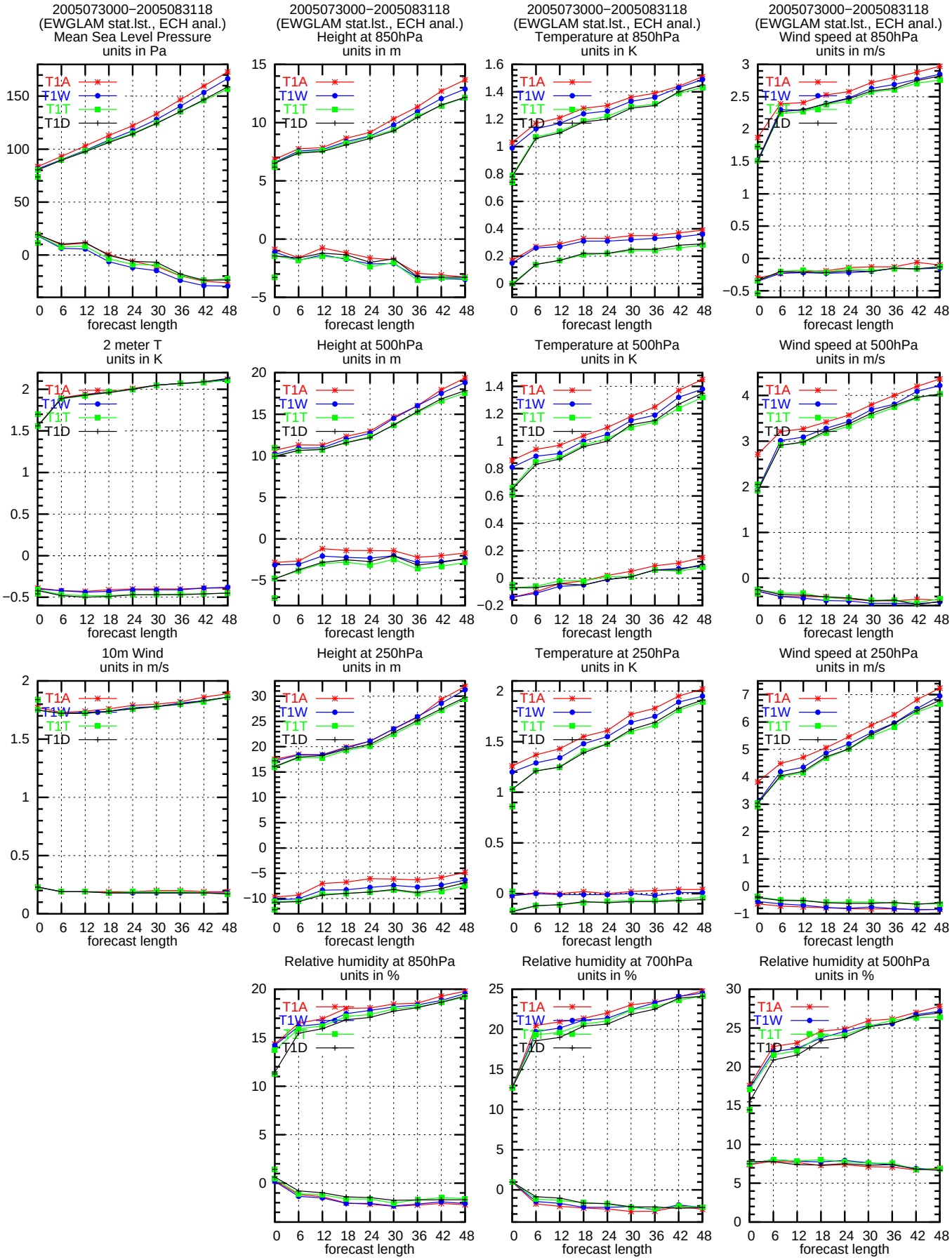

Figure 9: Obs-verification of control run (T1A), 'additional radiosonde wind' (T1W) run, 'additional radiosonde wind and temperature' (T1T) run, and 'all TEMP' run (T1D). EWGLAM station list.

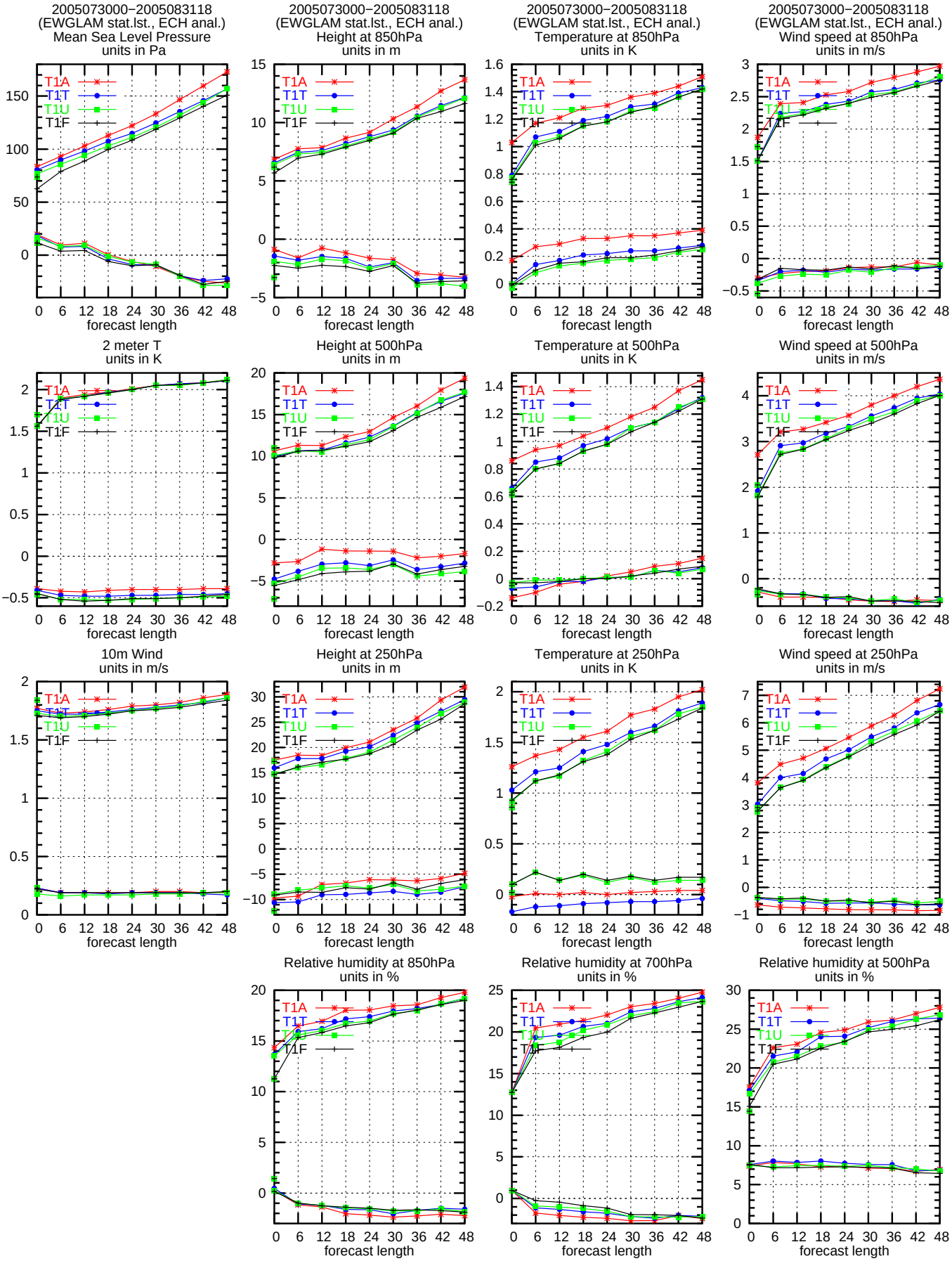

Figure 10: Obs-verification of the control run (T1A), the 'additional radiosonde wind and temperature' (T1T) run, 'additional radiosonde and aircraft wind and temperature' (T1U) run, and the 'full system' (T1F) run. EWGLAM station list.

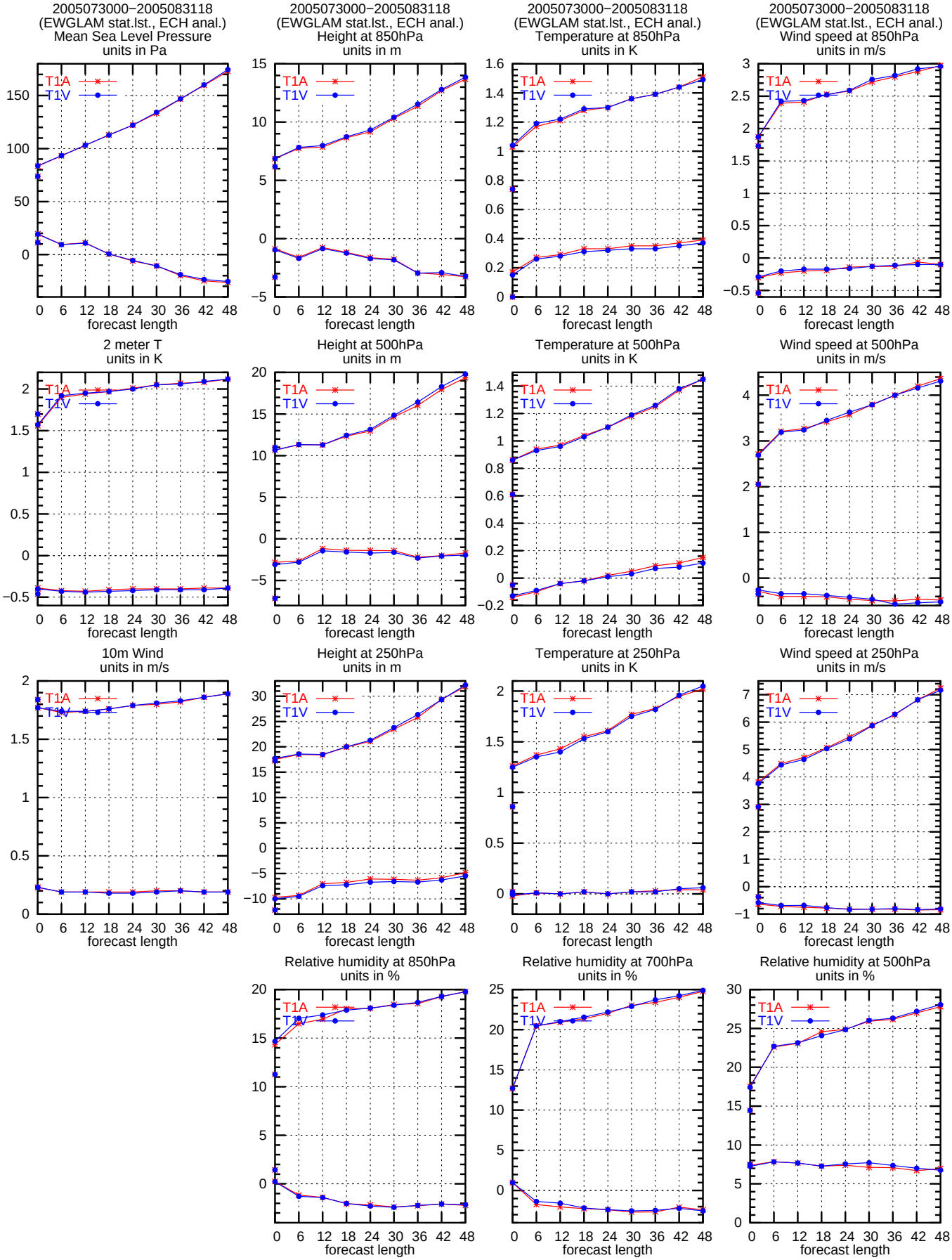

Figure 11: Obs-verification of the baseline (T1A) run and the 'wind profiler' (T1V) run. EWGLAM station list.

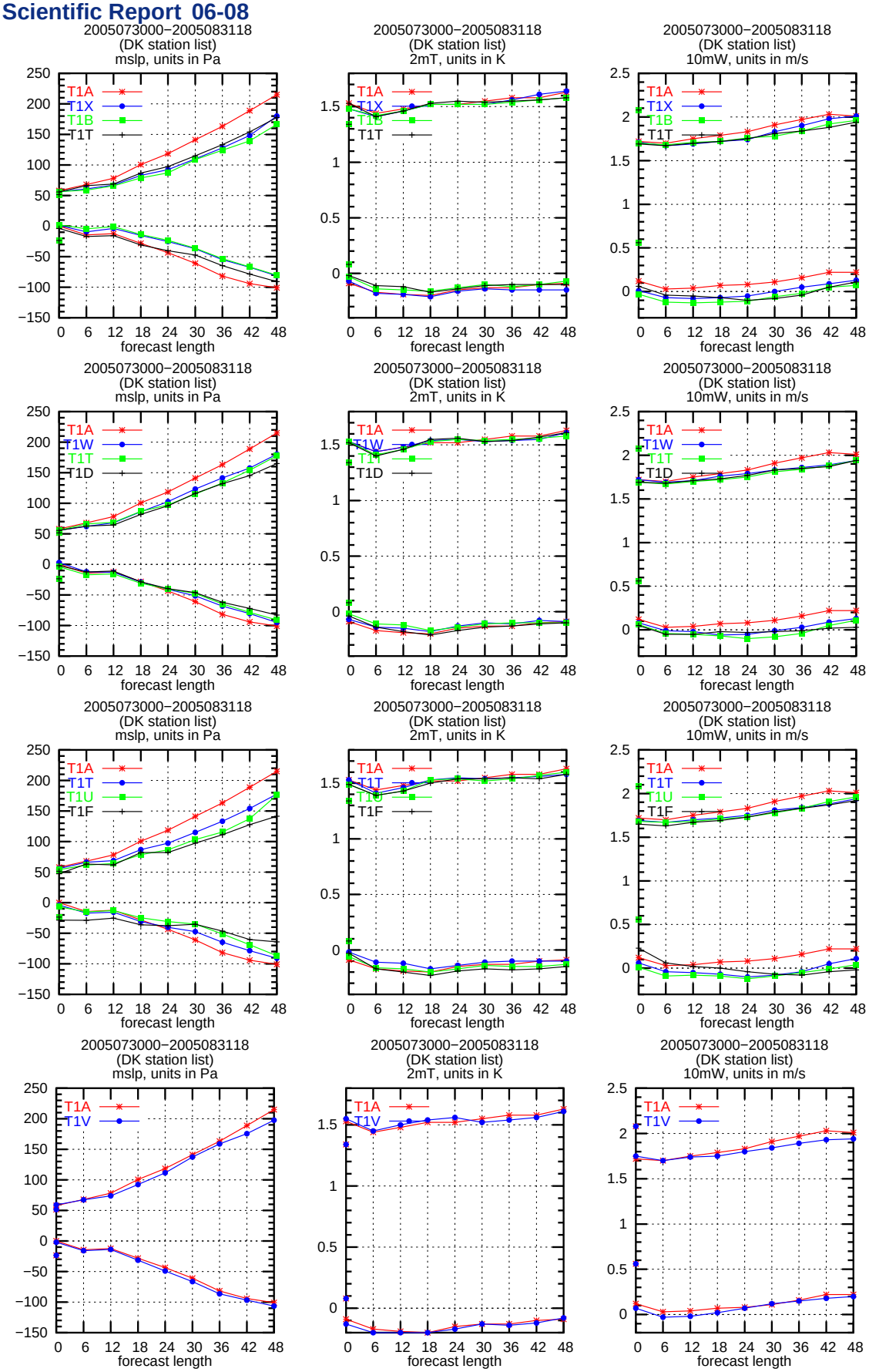

Figure 12: Obs-verification of surface parameters using a Danish station list. (T1F: all observations used; T1A: baseline run; T1B: T1A + aircraft; T1W: T1A + wind from other radiosondes; T1T: T1A + wind and temperature data from other radiosondes; T1D: T1A + data from all other radiosondes; T1X: T1A + E-AMDAR data; T1V: T1A + wind profiler data).

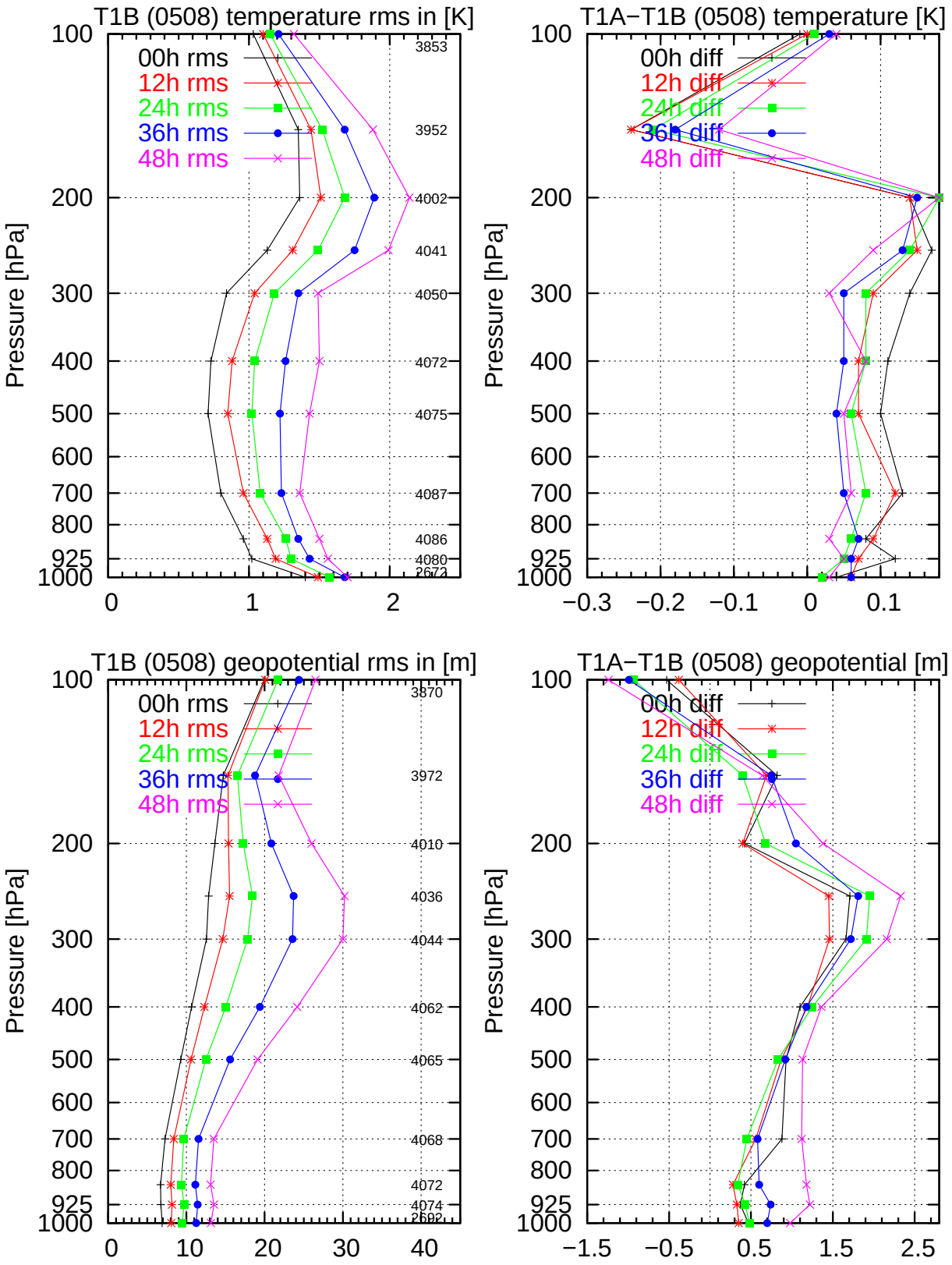

Figure 13: Rms scores for T1B (all AIREPs, left) and differences in rms-scores between T1A (baseline experiment) and T1B (right) at analysis time and for the 12, 24, 36 and 48 hour forecasts as a function of pressure in the August 2005 period. Top row is for temperature and bottom row is geopotential. Positive values in the difference plots where T1B has better rms-scores.

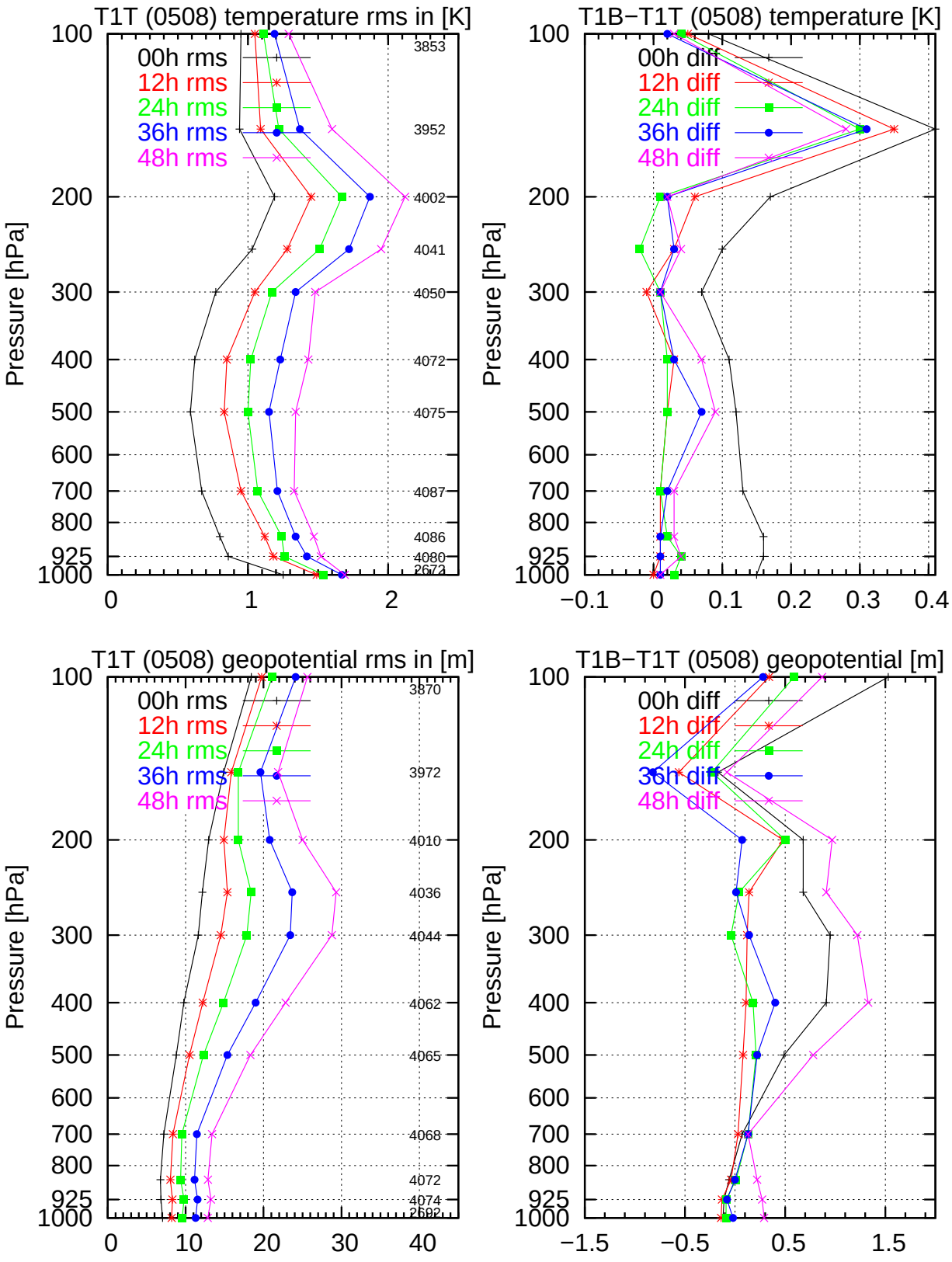

Figure 14: Rms scores for T1T (wind and temperature from radiosondes, left) and differences in rms-scores between T1B (all AIREPs) and T1T (right) at analysis time and for the 12, 24, 36 and 48 hour forecasts as a function of pressure in the August 2005 period. Top row is for temperature and bottom row is geopotential. Positive values in the difference plots where T1T has better rms-scores.

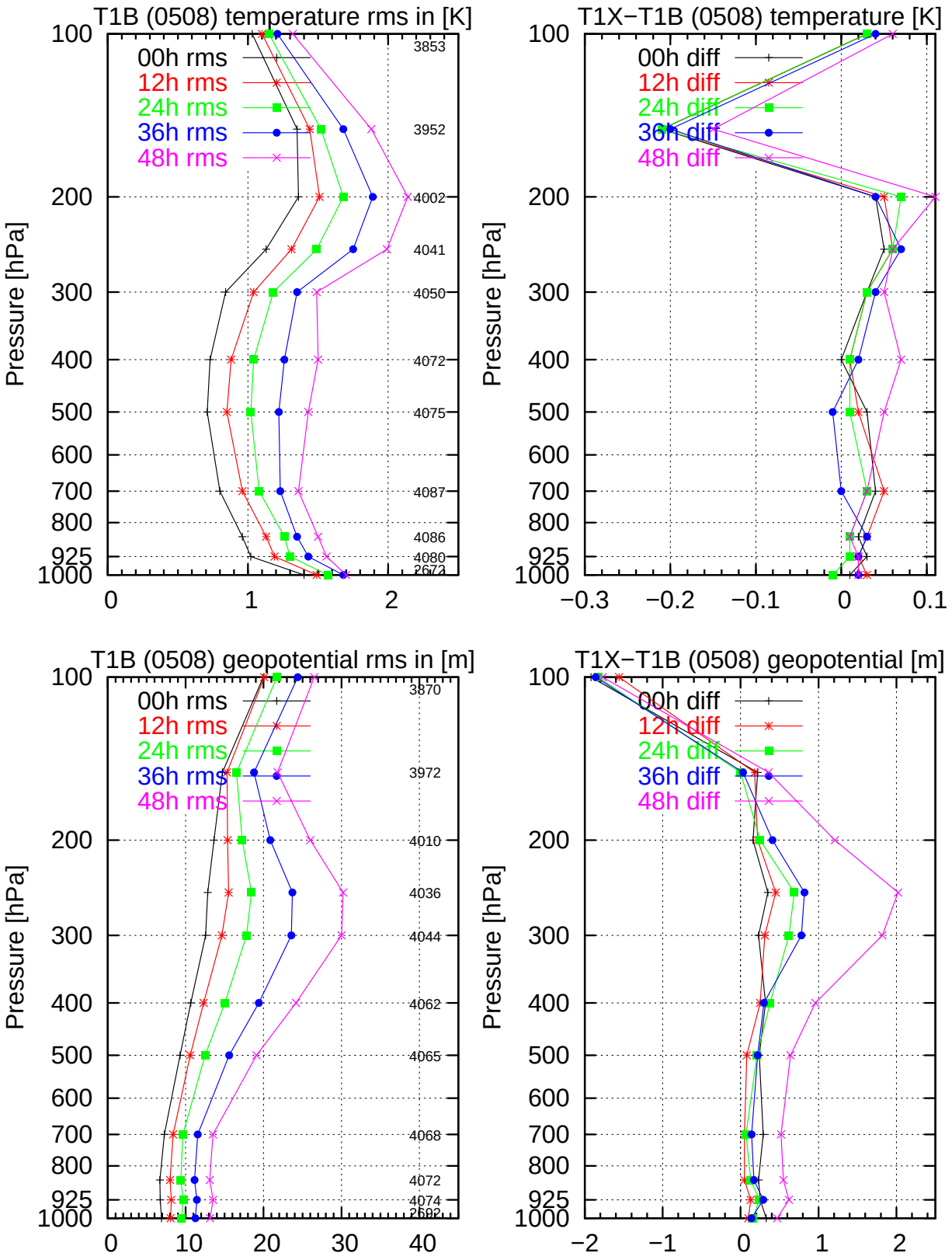

Figure 15: Rms scores for T1B (all AIREPs, left) and differences in rms-scores between T1X (all E-AMDAR) and T1B (right) at analysis time and for the 12, 24, 36 and 48 hour forecasts as a function of pressure in the August 2005 period. Top row is for temperature and bottom row is geopotential. Positive values in the difference plots where T1B has better rms-scores.

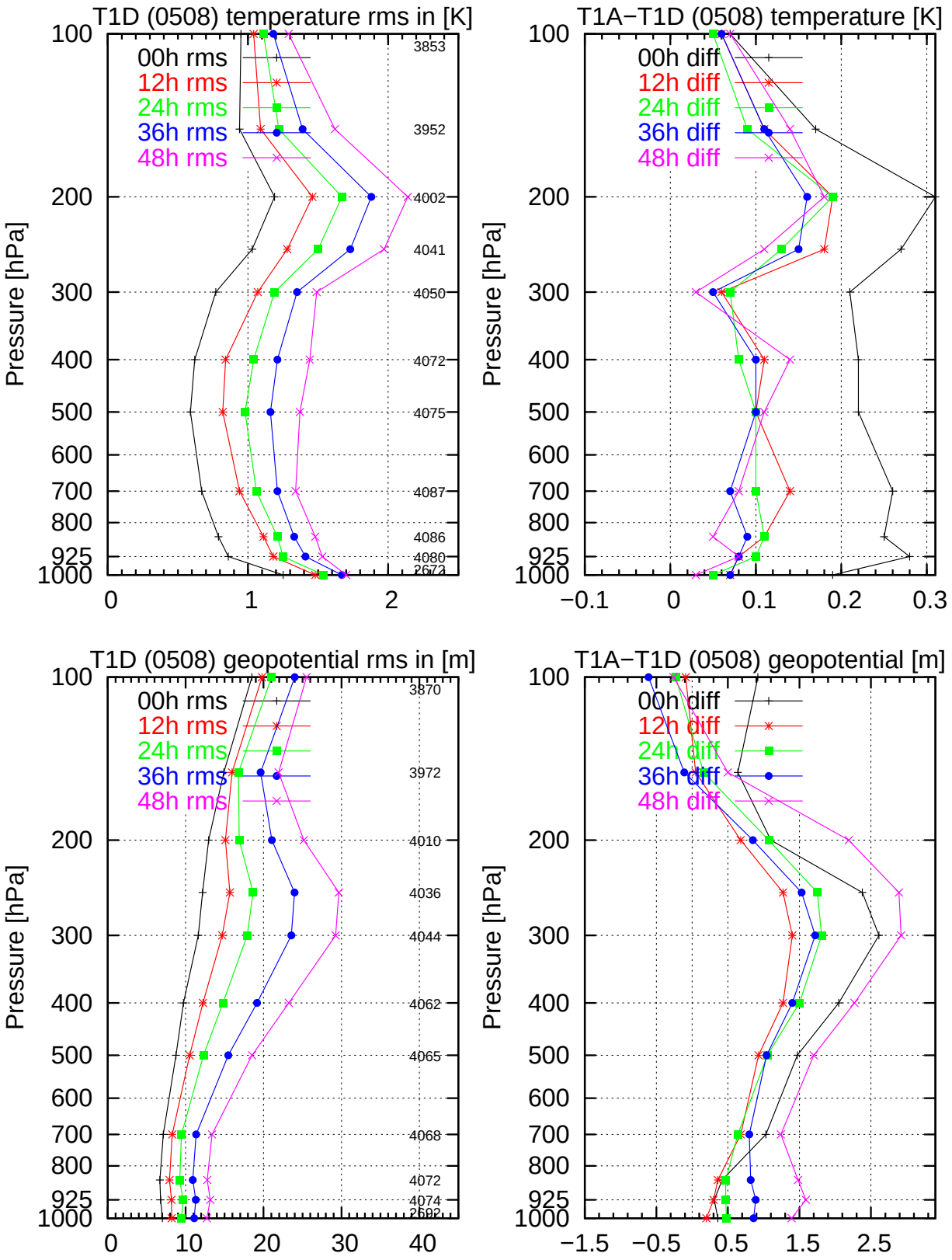

Figure 16: Rms scores for T1D (all TEMPs, left) and differences in rms-scores between T1A (baseline experiment) and T1D (right) at analysis time and for the 12, 24, 36 and 48 hour forecasts as a function of pressure in the August 2005 period. Top row is for temperature and bottom row is geopotential. Positive values in the difference plots where T1D has better rms-scores.

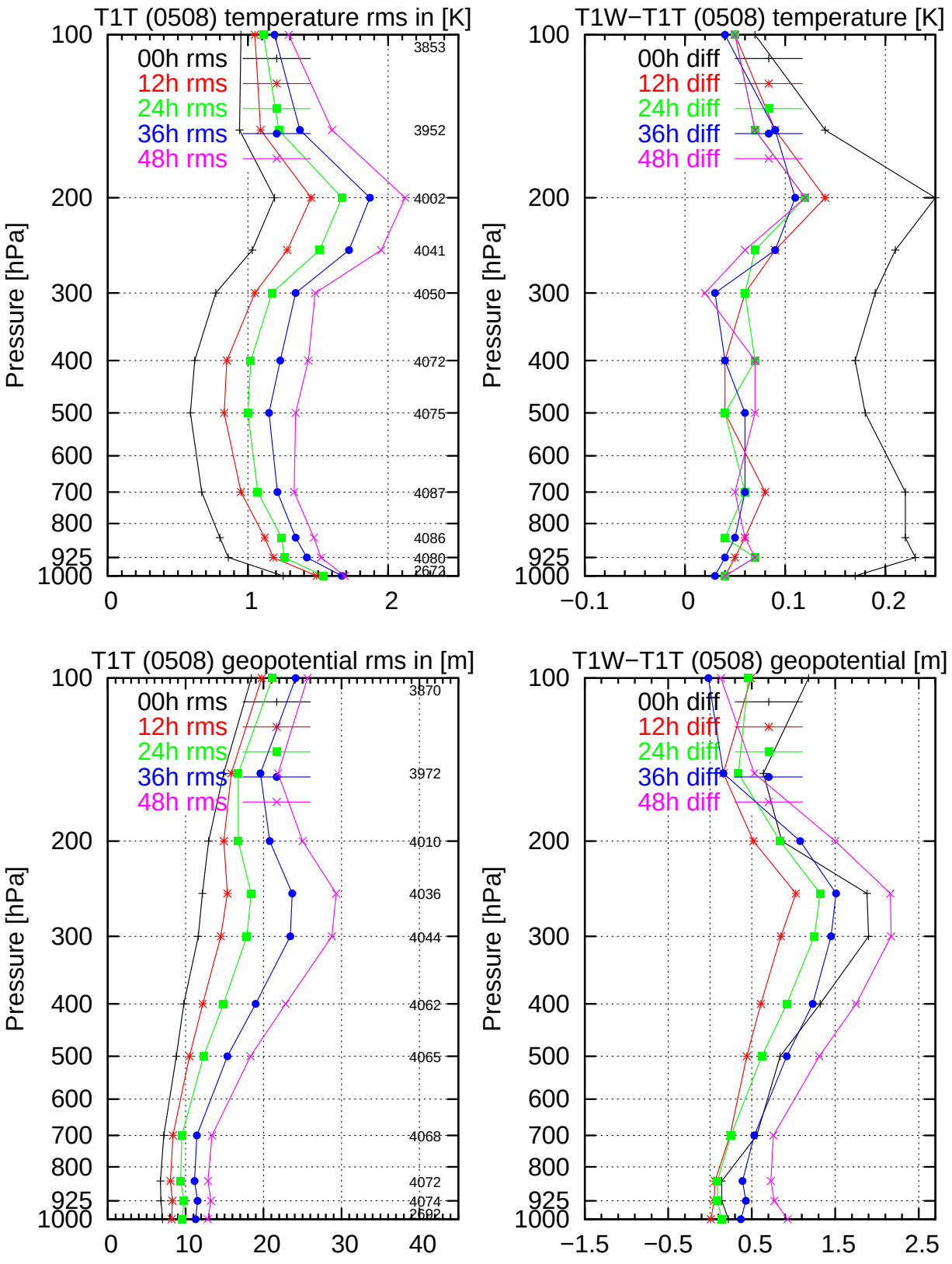

Figure 17: Rms scores for T1T (baseline + additional radiosonde wind and temperature data, left) and differences in rms-scores between T1W (baseline + additional radiosonde wind data) and T1T (right) at analysis time and for the 12, 24, 36 and 48 hour forecasts as a function of pressure in the August 2005 period. Top row is for temperature and bottom row is geopotential. Positive values in the difference plots where T1T has better rms-scores.

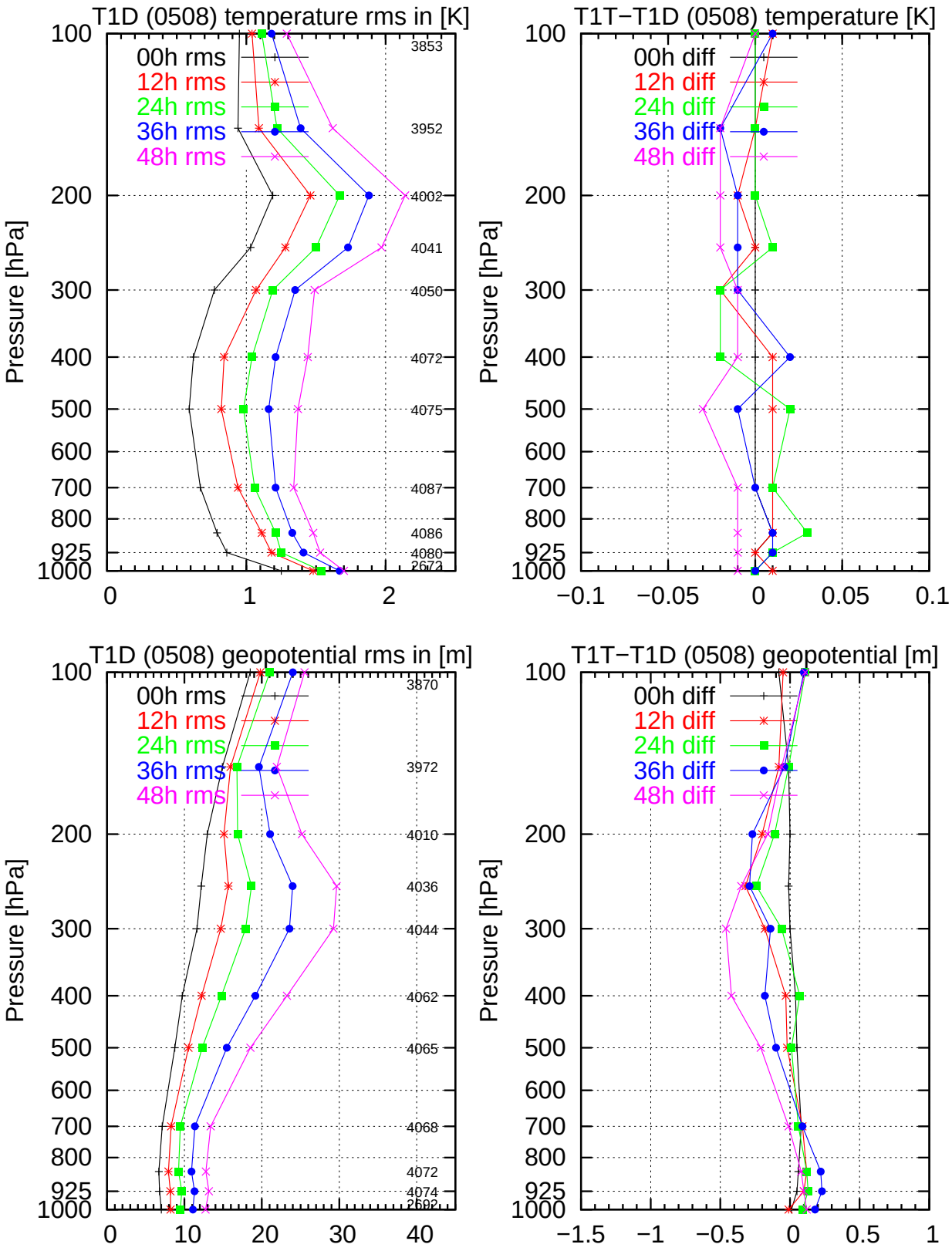

Figure 18: Rms scores for T1D (all radiosonde data, left) and differences in rms-scores between T1T (baseline + additional radiosonde wind and temperature data) and T1D (right) at analysis time and for the 12, 24, 36 and 48 hour forecasts as a function of pressure in the August 2005 period. Top row is for temperature and bottom row is geopotential. Positive values in the difference plots where T1D has better rms-scores.

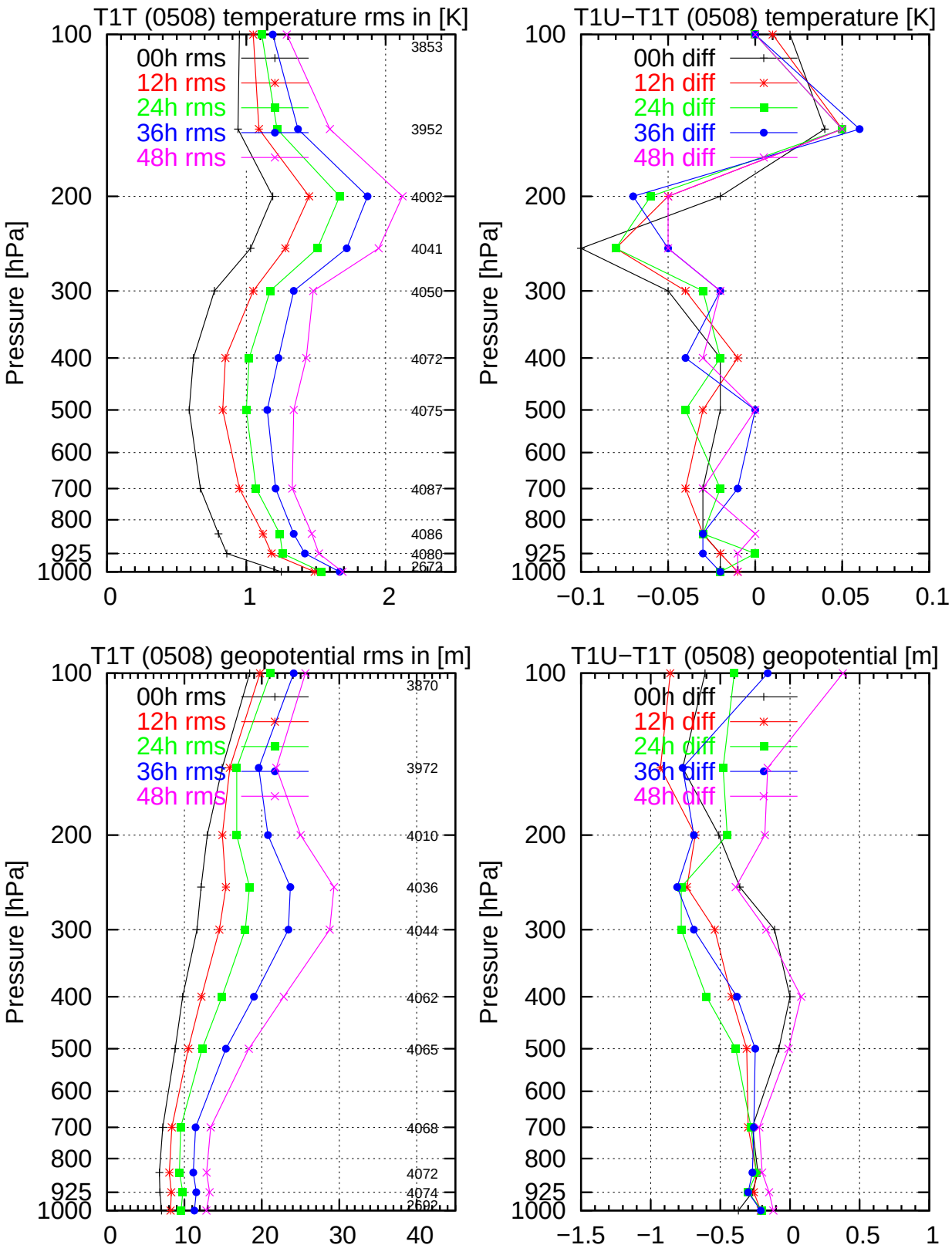

Figure 19: Rms scores for T1T (baseline + additional radiosonde wind and temperature data) and differences in rms-scores between T1U (baseline + additional radiosonde and aircraft wind and temperature data) and T1T (right) at analysis time and for the 12, 24, 36 and 48 hour forecasts as a function of pressure in the August 2005 period. Top row is for temperature and bottom row is geopotential. Positive values in the difference plots where T1T has better rms-scores.

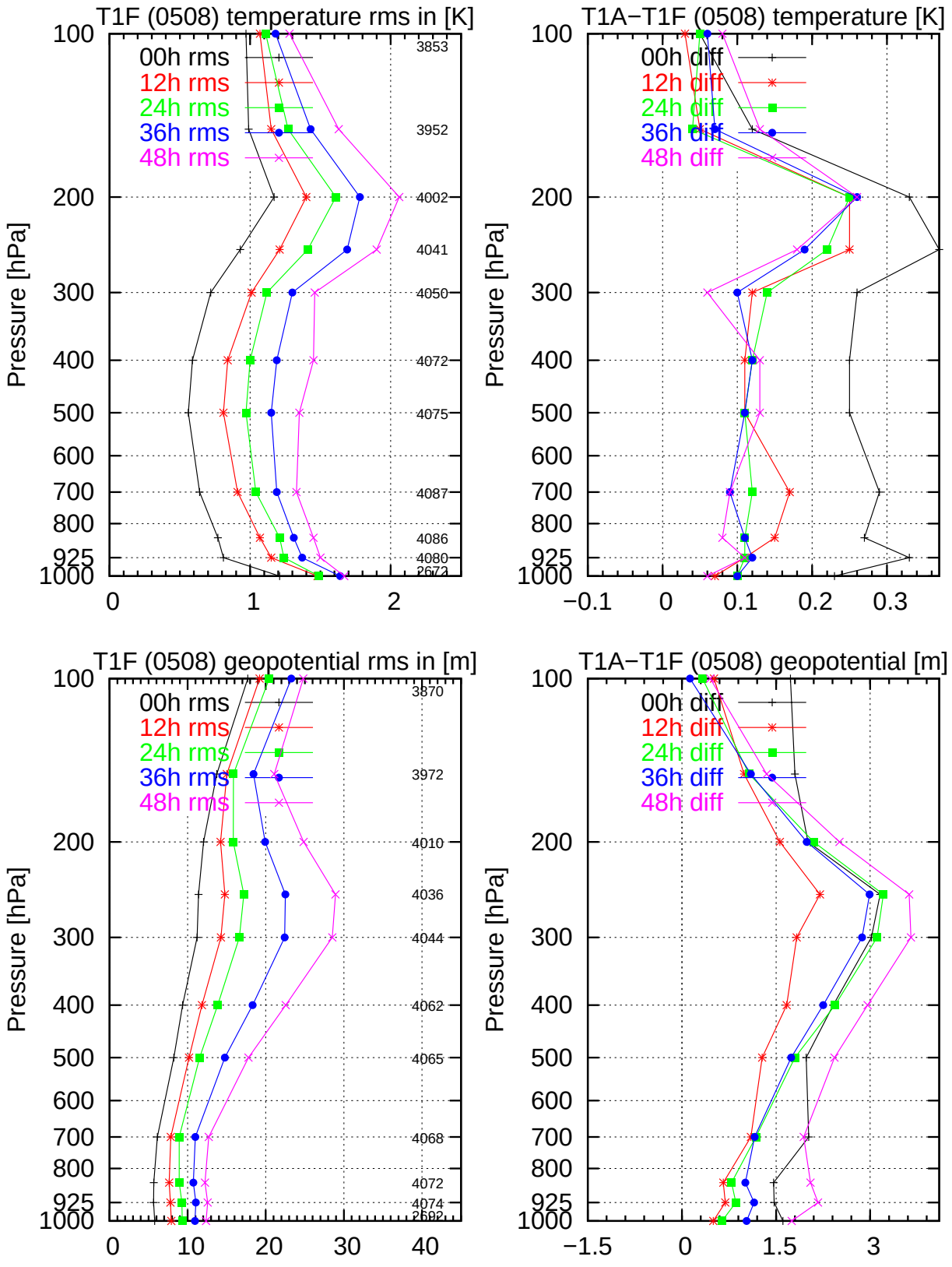

Figure 20: Rms scores for T1F (full system, left) and differences in rms-scores between T1A (baseline experiment) and T1F (right) at analysis time and for the 12, 24, 36 and 48 hour forecasts as a function of pressure in the August 2005 period. Top row is for temperature and bottom row is geopotential. Positive values in the difference plots where T1F has better rms-scores.

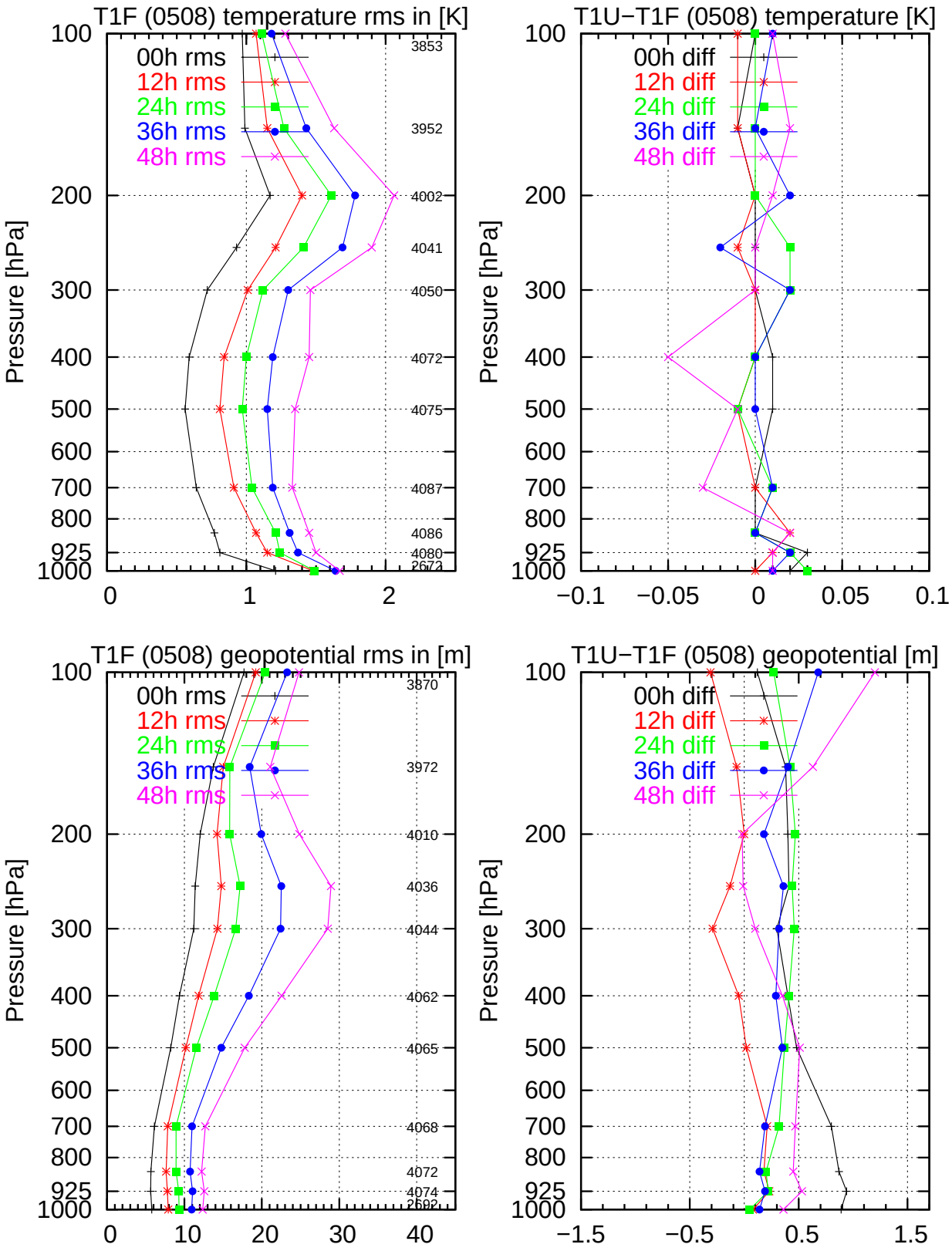

Figure 21: Rms scores for T1F (full system, left) and differences in rms-scores between T1U (baseline + additional radiosonde and aircraft wind and temperature data) and T1F (right) at analysis time and for the 12, 24, 36 and 48 hour forecasts as a function of pressure in the August 2005 period. Top row is for temperature and bottom row is geopotential. Positive values in the difference plots where T1F has better rms-scores.

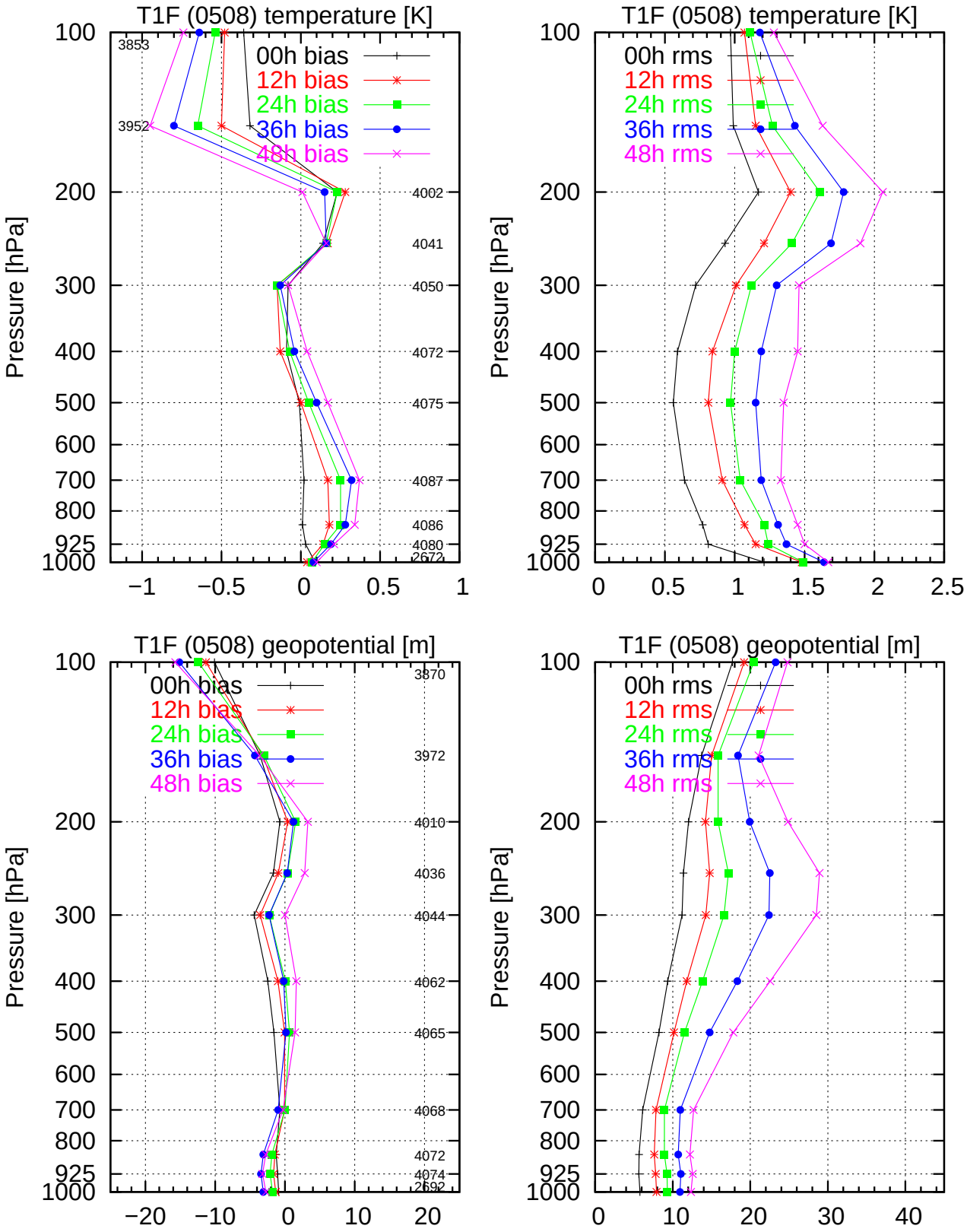

Figure 22: Bias (left) and rms scores at analysis time and for the 12, 24, 36 and 48 hour forecasts of the full system (T1F) experiment as a function of pressure in the August 2005 period. Top row is for temperature and bottom row is geopotential. (The numbers in small print in the bias plots indicate the number of observations used).

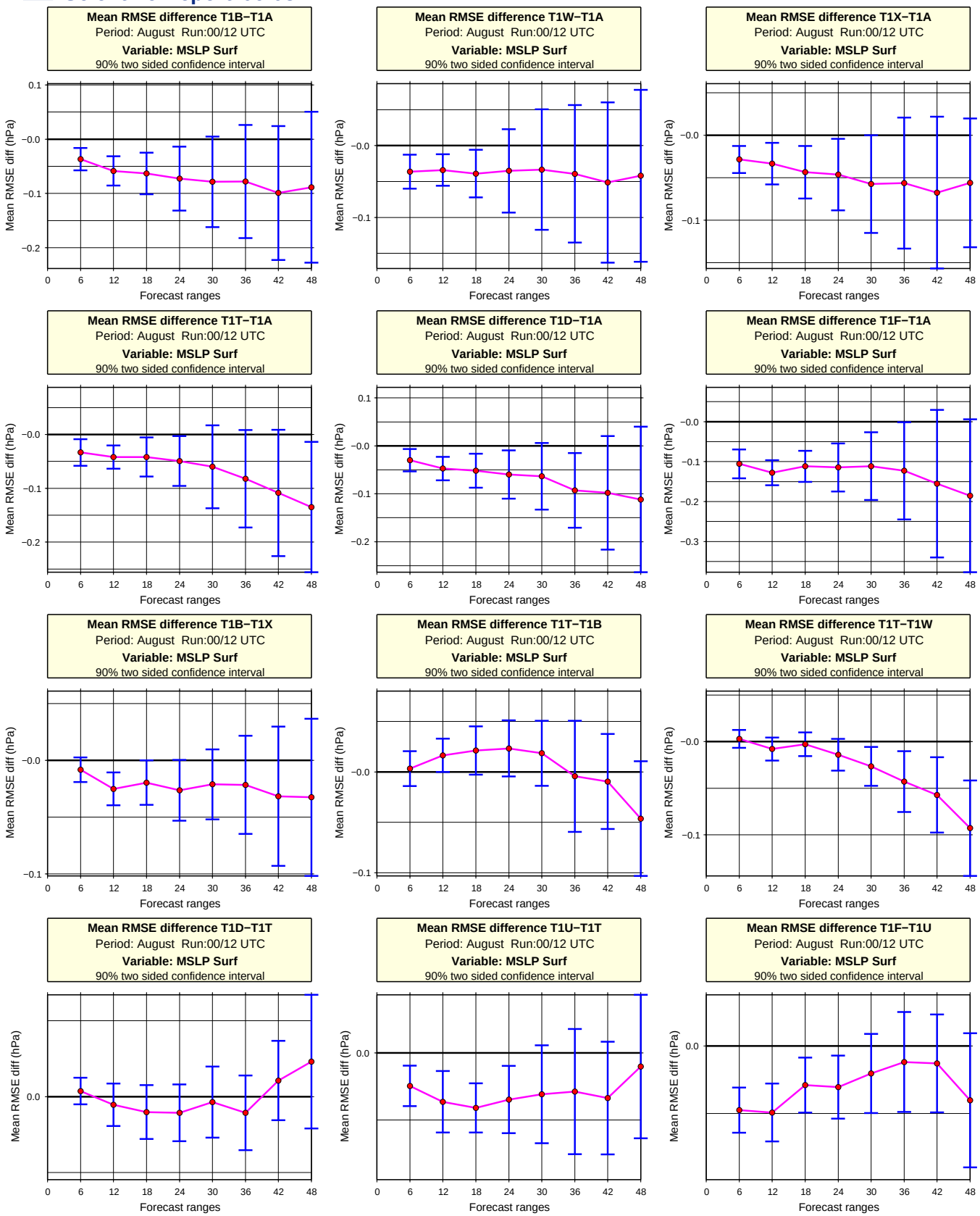

Figure 23: Significance test based on daily scores of mslp for 00 UTC and 12 UTC runs. 90 % two sided confidence interval. The first model run is better than the second run if the mean is negative. (T1F: all observations used; T1A: baseline run; T1B: T1A + aircraft; T1W: T1A + wind from other radiosondes; T1T: T1A + wind and temperature data from other radiosondes; T1D: T1A + data from all other radiosondes; T1X: T1A + E-AMDAR data; T1V: T1A + wind profiler data).

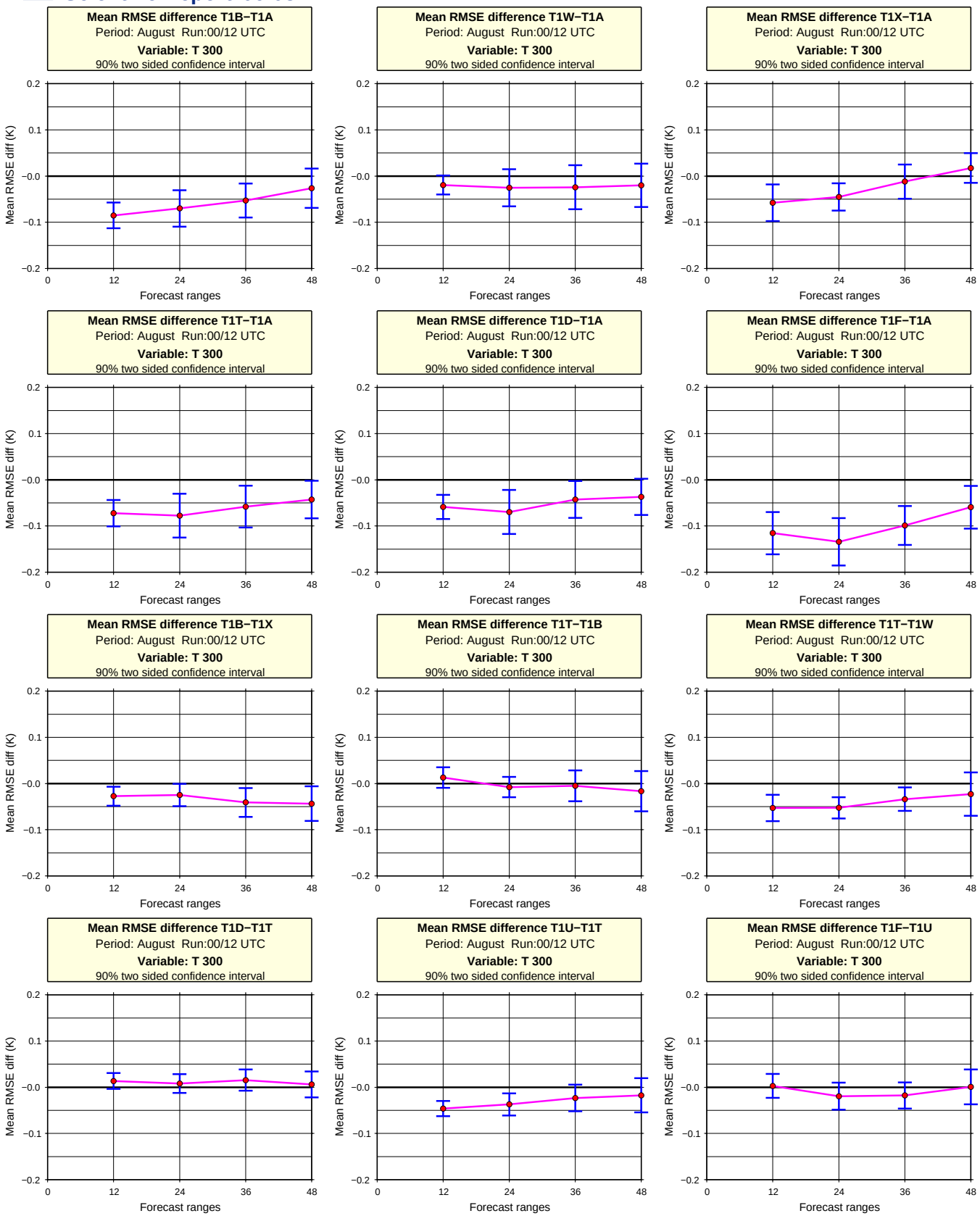

Figure 24: Significance test based on daily scores of 300 hPa temperature. 90 % two sided confidence interval. The first model run is better than the second run if the mean is negative. (T1F: all observations used; T1A: baseline run; T1B: T1A + aircraft; T1W: T1A + wind from other radiosondes; T1T: T1A + wind and temperature data from other radiosondes; T1D: T1A + data from all other radiosondes; T1X: T1A + E-AMDAR data; T1V: T1A + wind profiler data; T1U: T1T + all aircraft data).

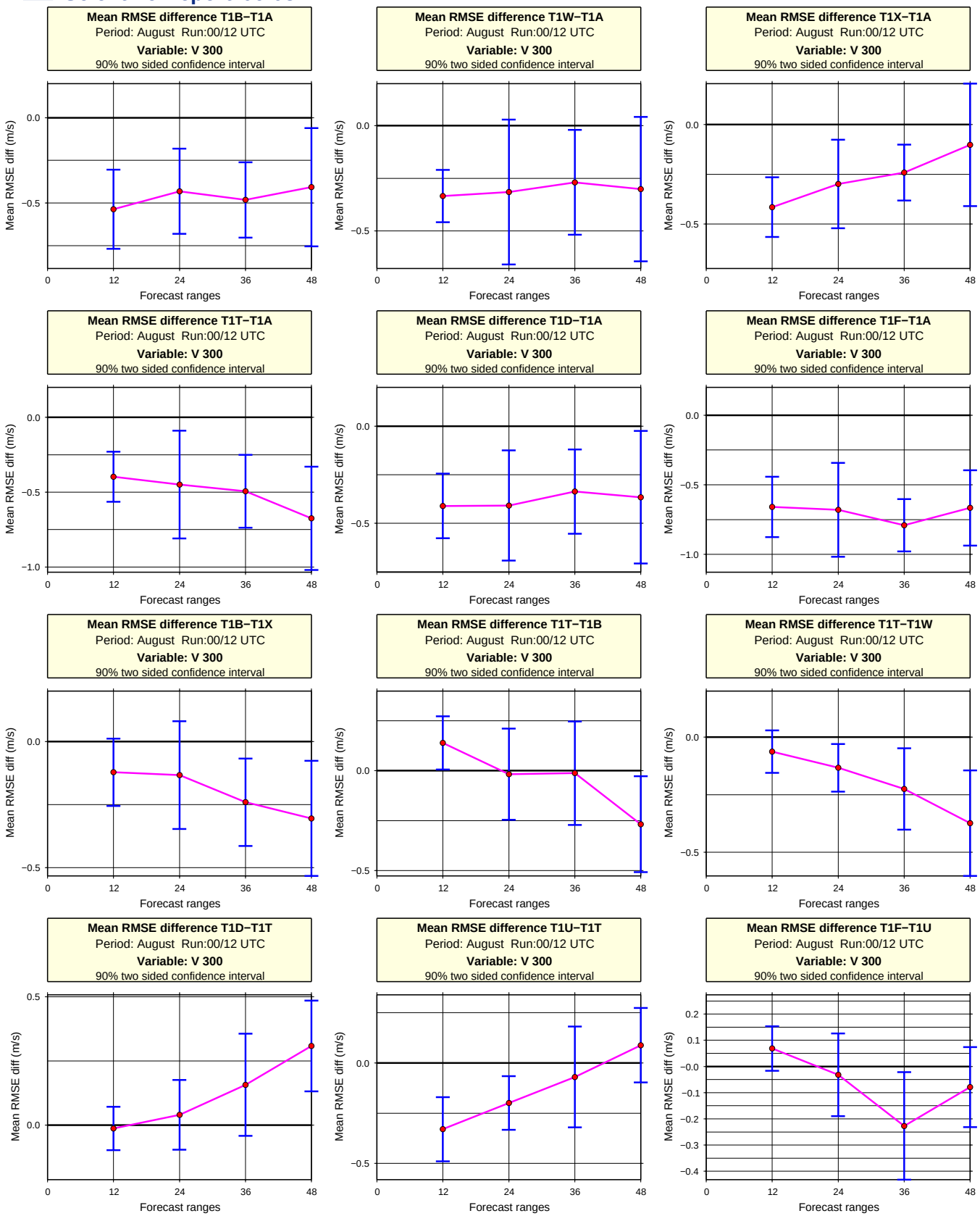

Figure 25: Significance test based on daily scores of 300 hPa wind speed. 90 % two sided confidence interval. The first model run is better than the second run if the mean is negative. (T1F: all observations used; T1A: baseline run; T1B: T1A + aircraft; T1W: T1A + wind from other radiosondes; T1T: T1A + wind and temperature data from other radiosondes; T1D: T1A + data from all other radiosondes; T1X: T1A + E-AMDAR data; T1V: T1A + wind profiler data; T1U: T1T + all aircraft data).

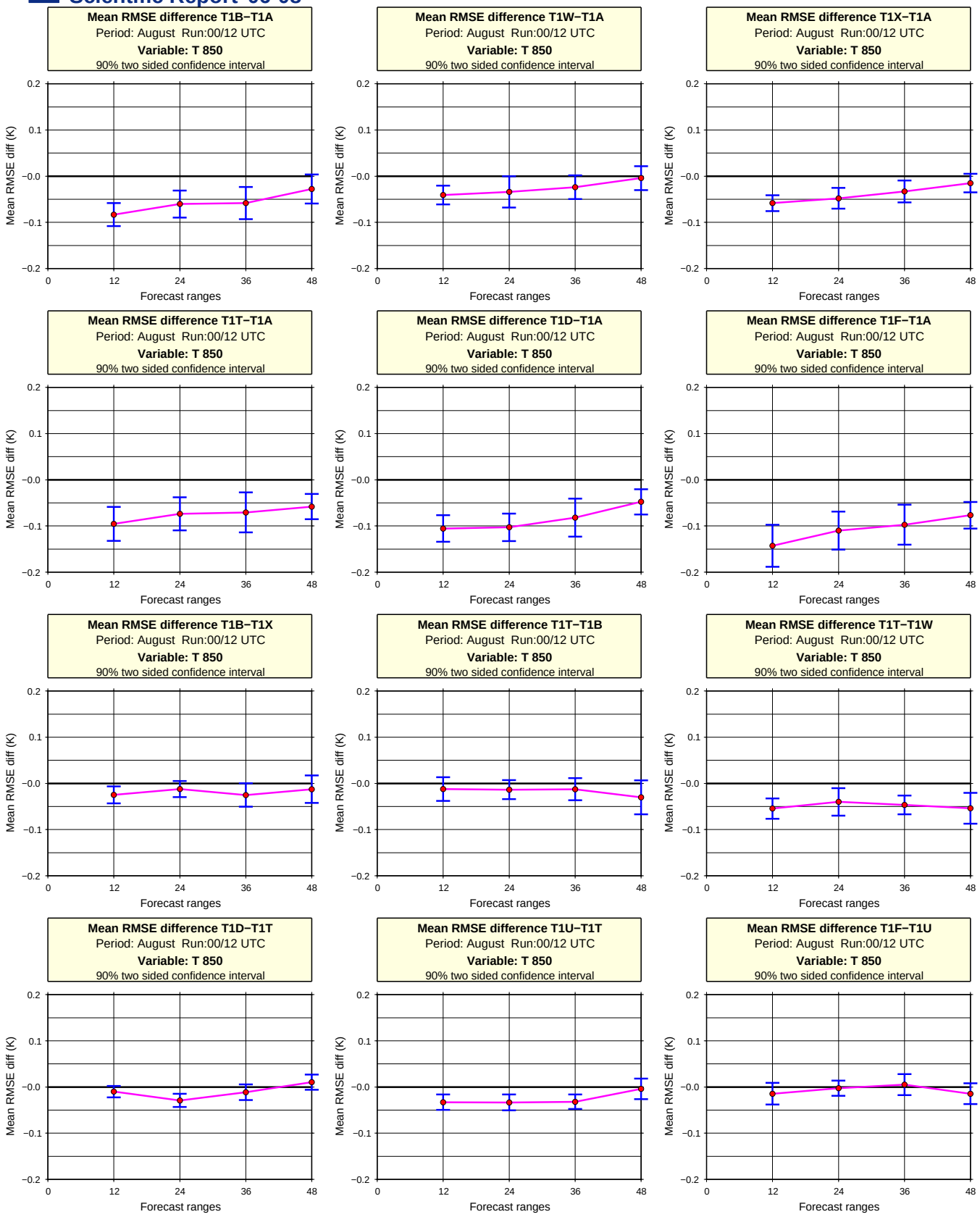

Figure 26: Significance test based on daily scores of 850 hPa temperature. 90 % two sided confidence interval. The first model run is better than the second run if the mean is negative. (T1F: all observations used; T1A: baseline run; T1B: T1A + aircraft; T1W: T1A + wind from other radiosondes; T1T: T1A + wind and temperature data from other radiosondes; T1D: T1A + data from all other radiosondes; T1X: T1A + E-AMDAR data; T1V: T1A + wind profiler data; T1U: T1T + all aircraft data).

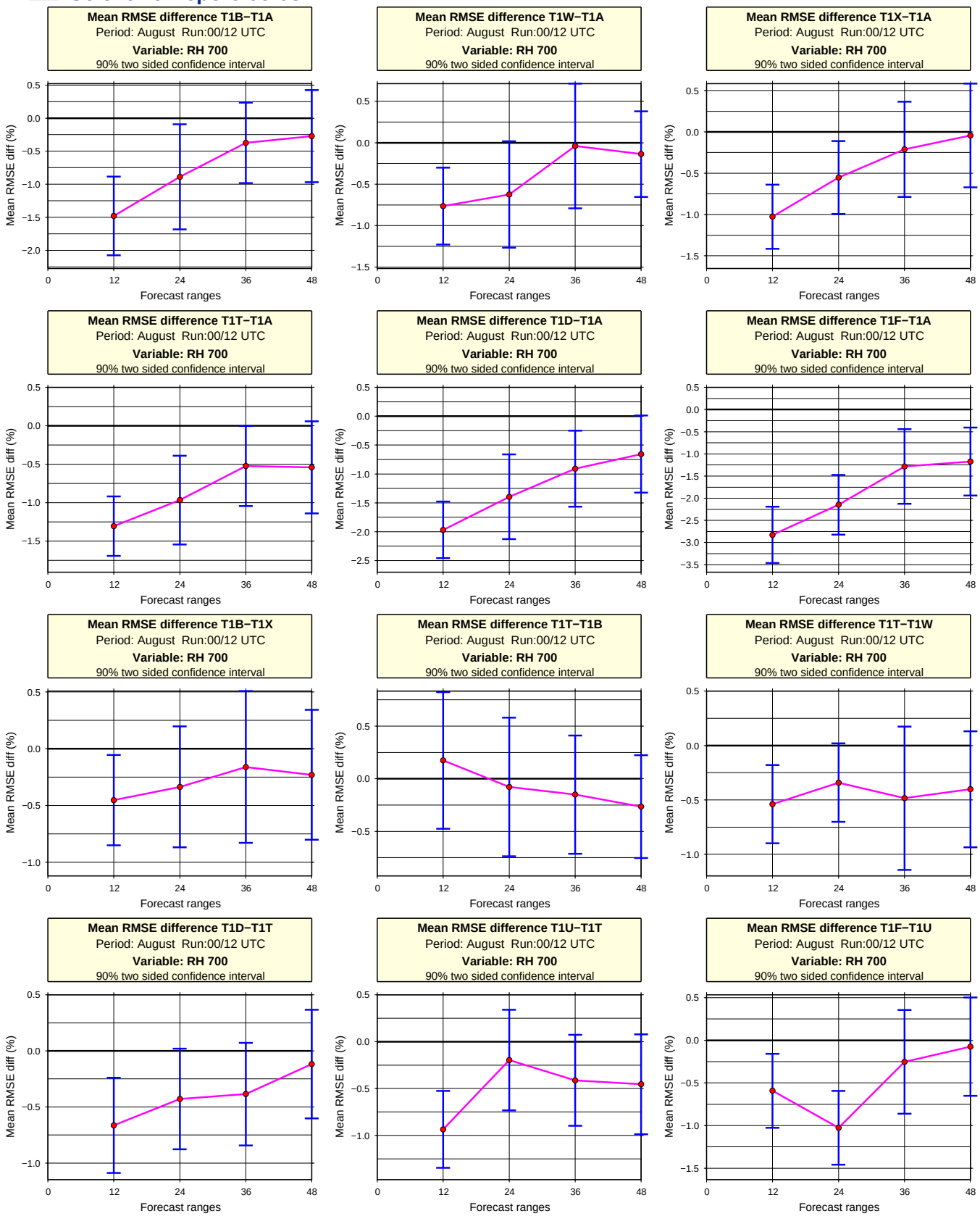

Figure 27: Significance test based on daily scores of 700 hPa relative humidity. 90 % two sided confidence interval. The first model run is better than the second run if the mean is negative. (T1F: all observations used; T1A: baseline run; T1B: T1A + aircraft; T1W: T1A + wind from other radiosondes; T1T: T1A + wind and temperature data from other radiosondes; T1D: T1A + data from all other radiosondes; T1X: T1A + E-AMDAR data; T1V: T1A + wind profiler data; T1U: T1T + all aircraft data)

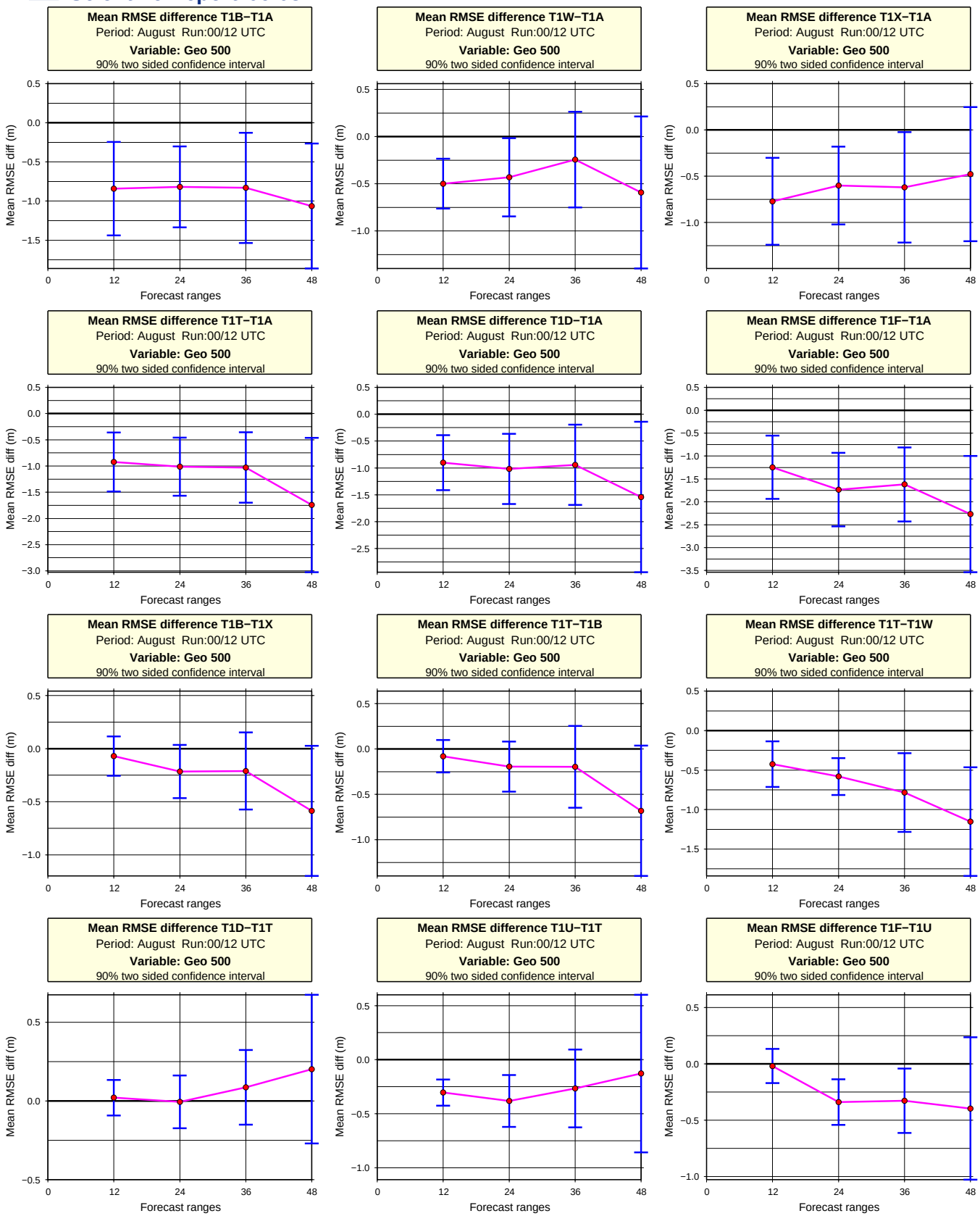

Figure 28: Significance test based on daily scores of 500 hPa geopotential height. 90 % two sided confidence interval. The first model run is better than the second run if the mean is negative. (T1F: all observations used; T1A: baseline run; T1B: T1A + aircraft; T1W: T1A + wind from other radiosondes; T1T: T1A + wind and temperature data from other radiosondes; T1D: T1A + data from all other radiosondes; T1X: T1A + E-AMDAR data; T1V: T1A + wind profiler data; T1U: T1T + all aircraft data)

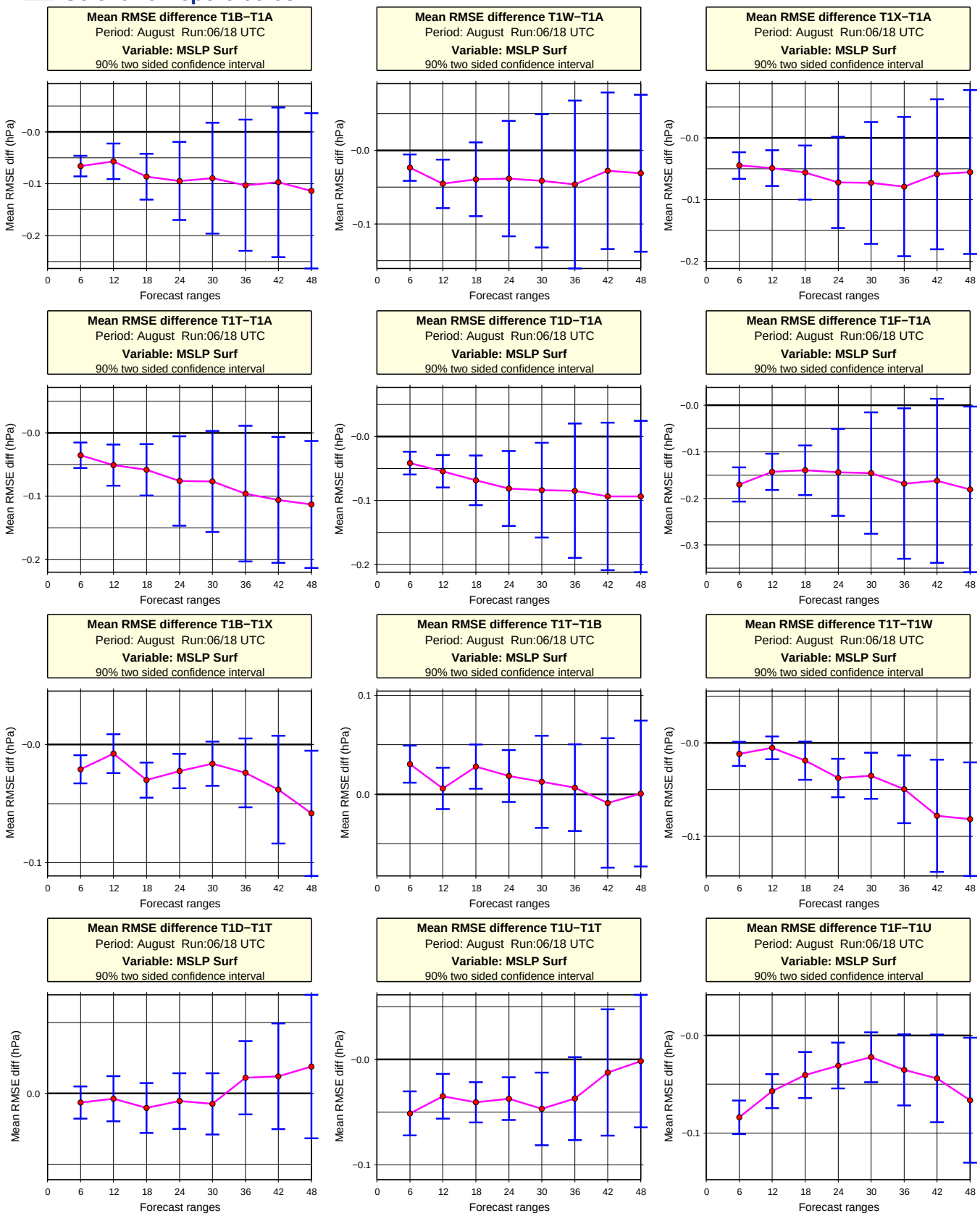

Figure 29: Significance test based on daily scores of mslp for 06 UTC and 18 UTC runs. 90 % two sided confidence interval. The first model run is better than the second run if the mean is negative. (T1F: all observations used; T1A: baseline run; T1B: T1A + aircraft; T1W: T1A + wind from other radiosondes; T1T: T1A + wind and temperature data from other radiosondes; T1D: T1A + data from all other radiosondes; T1X: T1A + E-AMDAR data; T1V: T1A + wind profiler data).

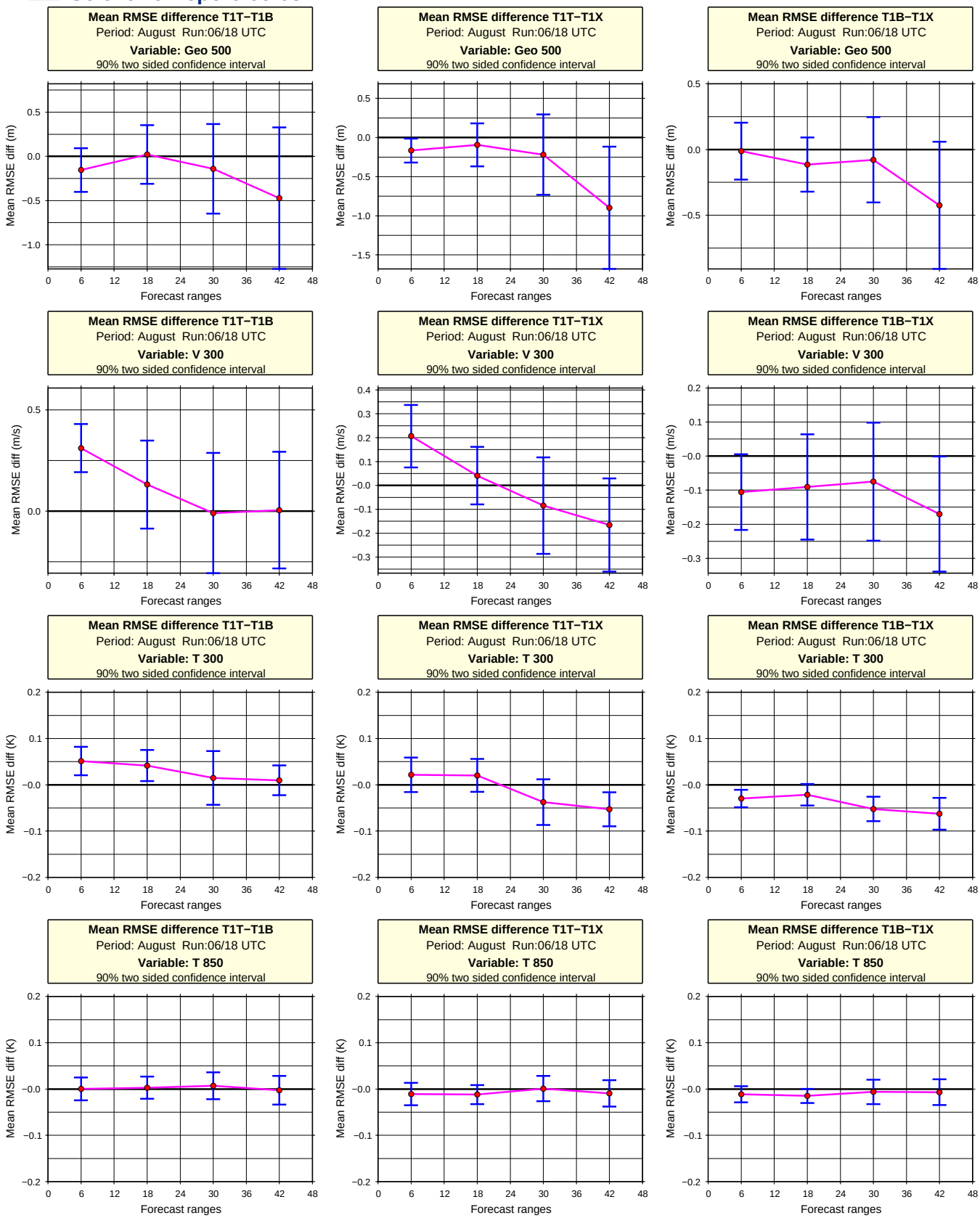

Figure 30: Significance test based on daily scores of selected parameters for 06 UTC and 18 UTC runs only. 90 % two sided confidence interval. The first model run is better than the second run if the mean is negative. Top row is for 500 hPa geopotential height, second row from top is for 300 hPa wind speed, third row is for 300 hPa temperature and bottom row is for 850 hPa temperature. (T1B: baseline + aircraft; T1T: baseline + wind and temperature data from non-GUAN radiosondes; T1X: baseline + E-AMDAR data).

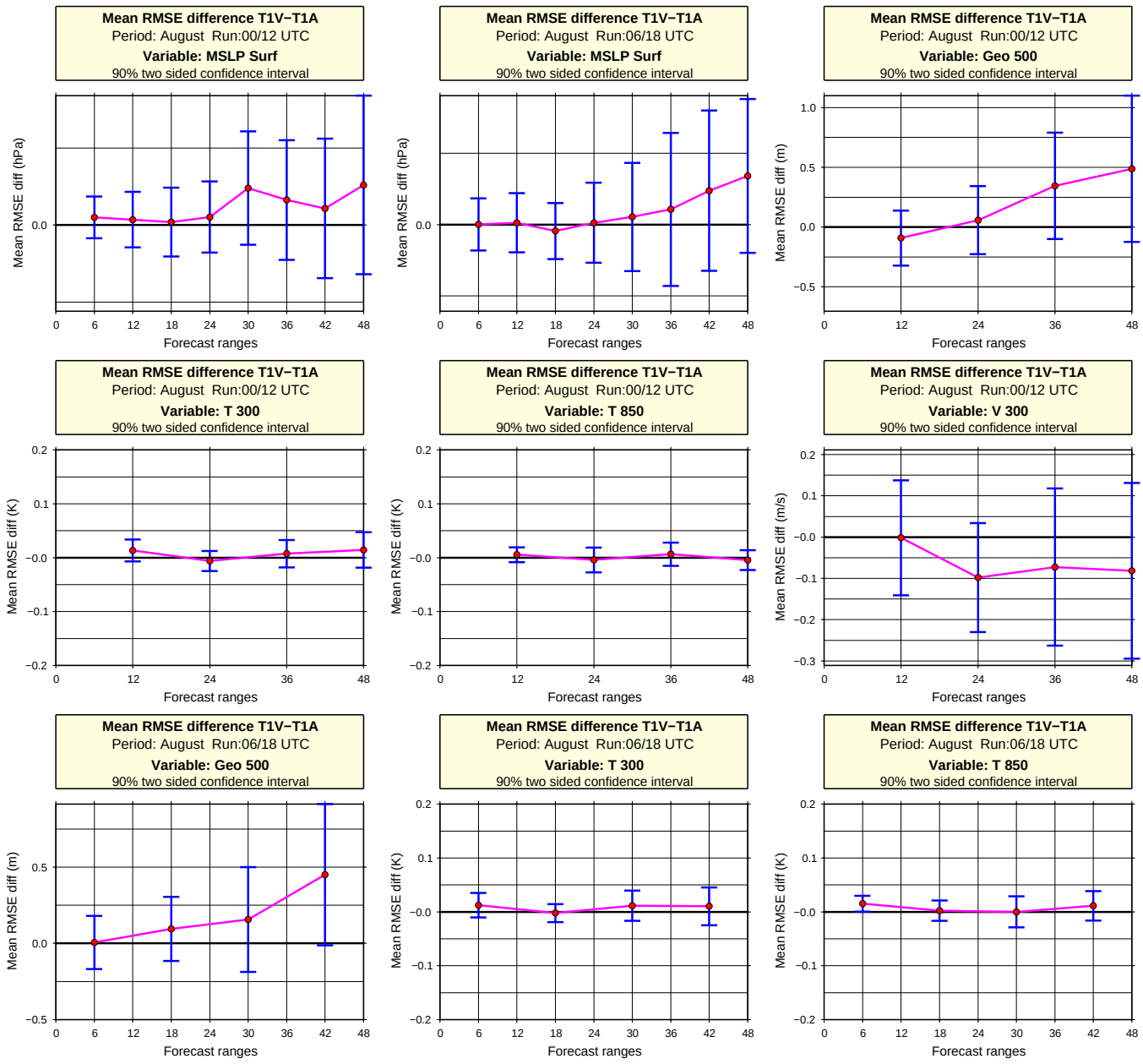

Figure 31: Significance test based on daily scores of selected parameters for T1V (baseline + wind profiler data) and T1A (baseline). 90 % two sided confidence interval. T1V is better than T1A if the mean is negative. See text in plots for parameters and whether it is for 00 UTC and 12 UTC runs or for 06 UTC and 18 UTC runs.

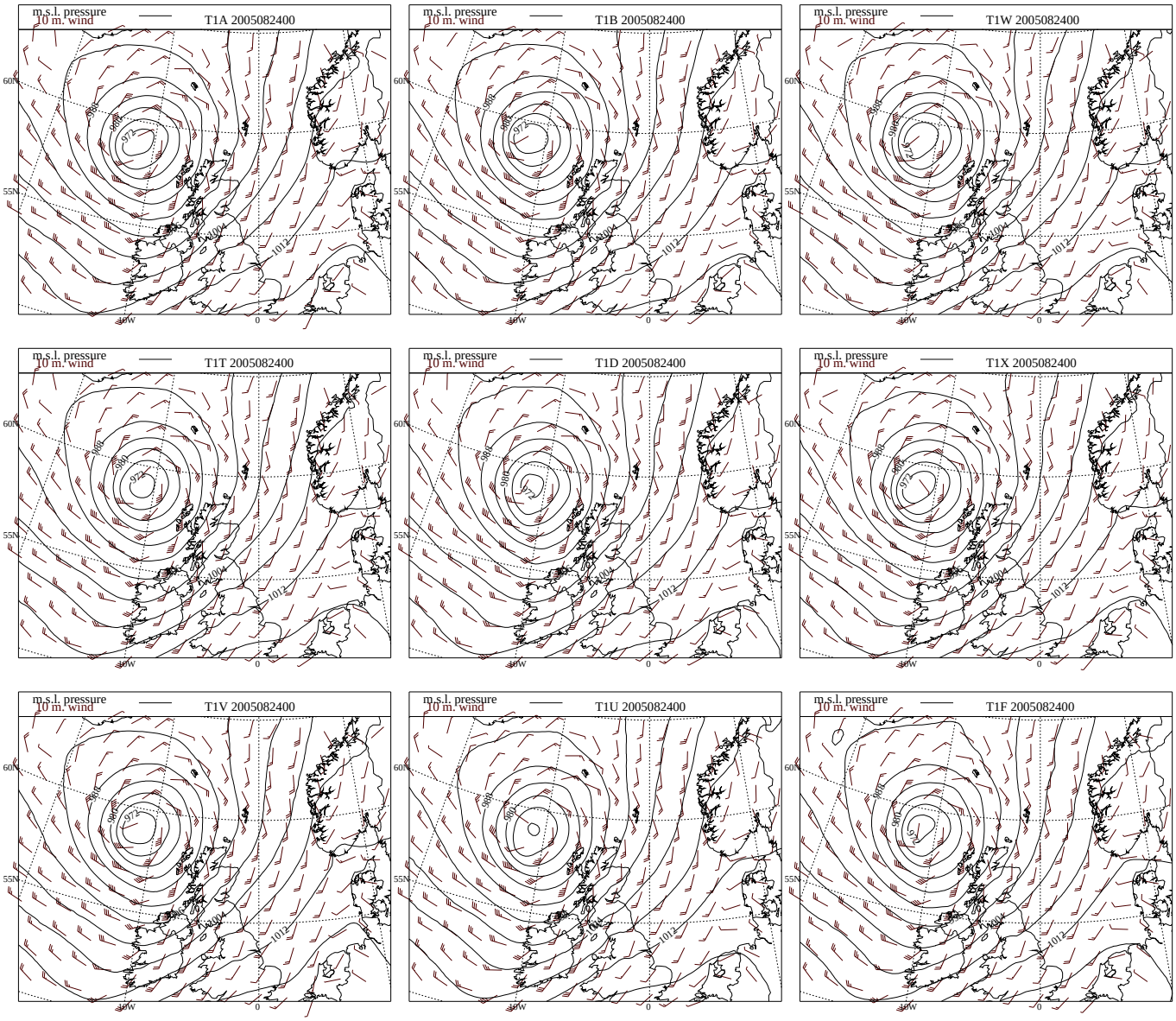

Figure 32: Mslp analyses and 10 m wind valid at 00 UTC August 24, 2005. (T1F: all observations used; T1A: baseline run; T1B: T1A + aircraft; T1W: T1A + wind from other radiosondes; T1T: T1A + wind and temperature data from other radiosondes; T1D: T1A + data from all other radiosondes; T1X: T1A + E-AMDAR data; T1V: T1A + wind profiler data; T1U: T1T + all aircraft data). Mslp contours for every 4 hPa and WMO standard wind arrows.

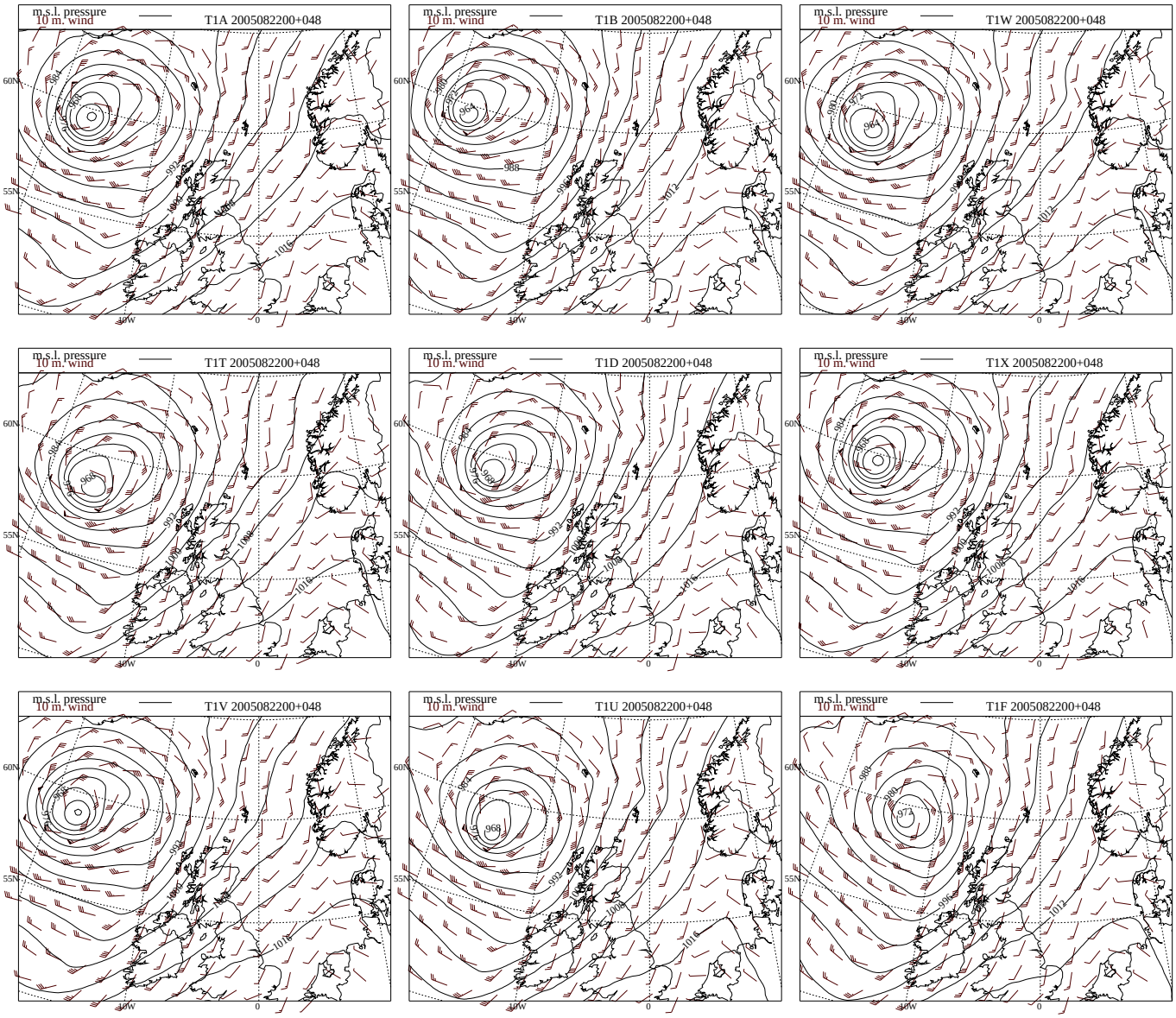

Figure 33: 48 h mslp and 10 m wind forecasts valid at 00 UTC August 24, 2005. (T1F: all observations used; T1A: baseline run; T1B: T1A + aircraft; T1W: T1A + wind from other radiosondes; T1T: T1A + wind and temperature data from other radiosondes; T1D: T1A + data from all other radiosondes; T1X: T1A + E-AMDAR data; T1V: T1A + wind profiler data; T1U: T1T + all aircraft data). Mslp contours for every 4 hPa and WMO standard wind arrows.

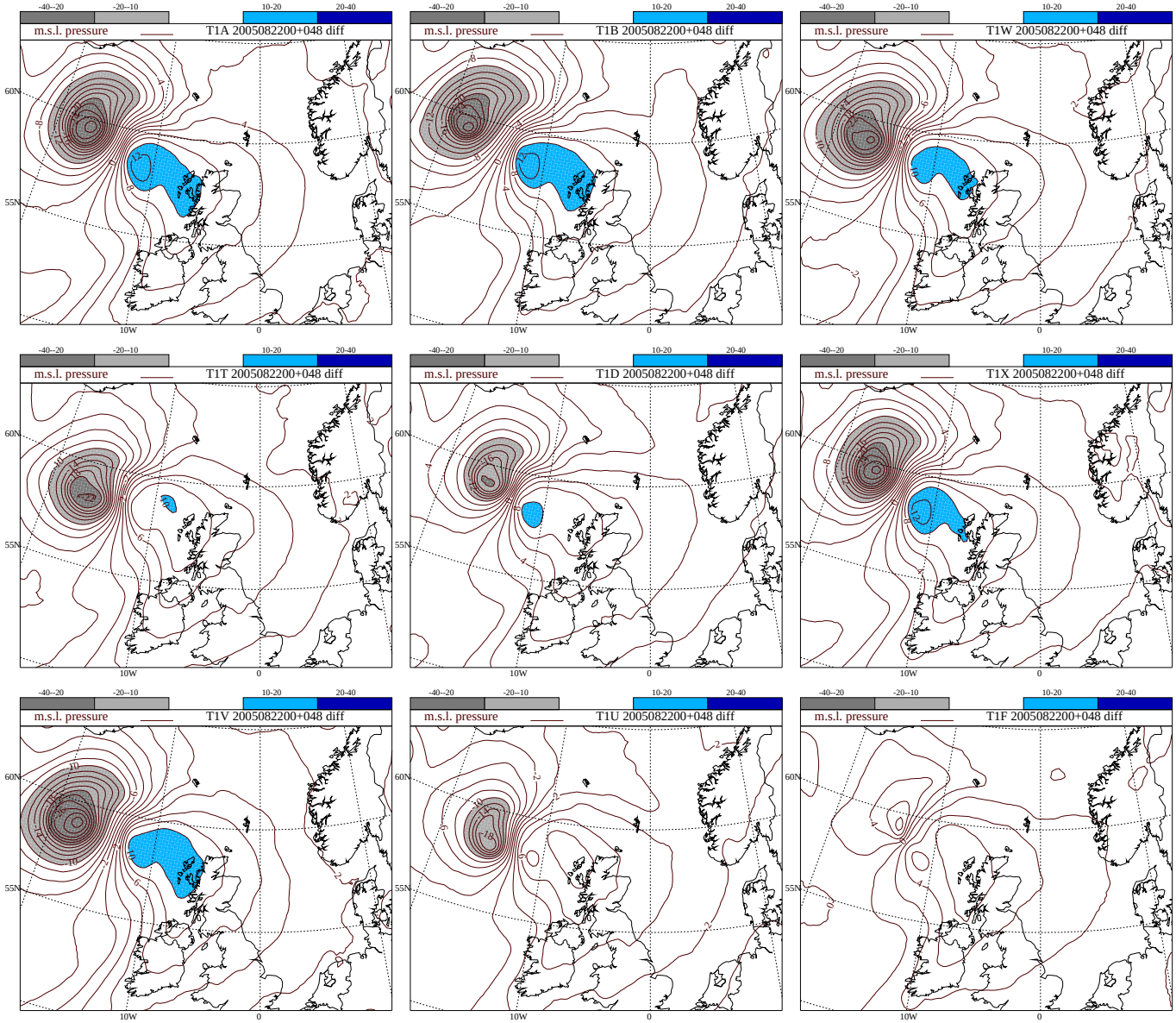

Figure 34: 48 h mslp forecast differences against the T1F analysis valid at 00 UTC August 24, 2005. (T1F: all observations used; T1A: baseline run; T1B: T1A + aircraft; T1W: T1A + wind from other radiosondes; T1T: T1A + wind and temperature data from other radiosondes; T1D: T1A + data from all other radiosondes; T1X: T1A + E-AMDAR data; T1V: T1A + wind profiler data; T1U: T1T + all aircraft data). Mslp difference contours for every 2 hPa. Light grey areas for values between -10 hPa and -20 hPa, dark grey areas for values between -20 hPa and -40 hPa, light blue areas for values between 10 hPa and 20 hPa, and dark blue areas for values between 20 hPa and 40 hPa.

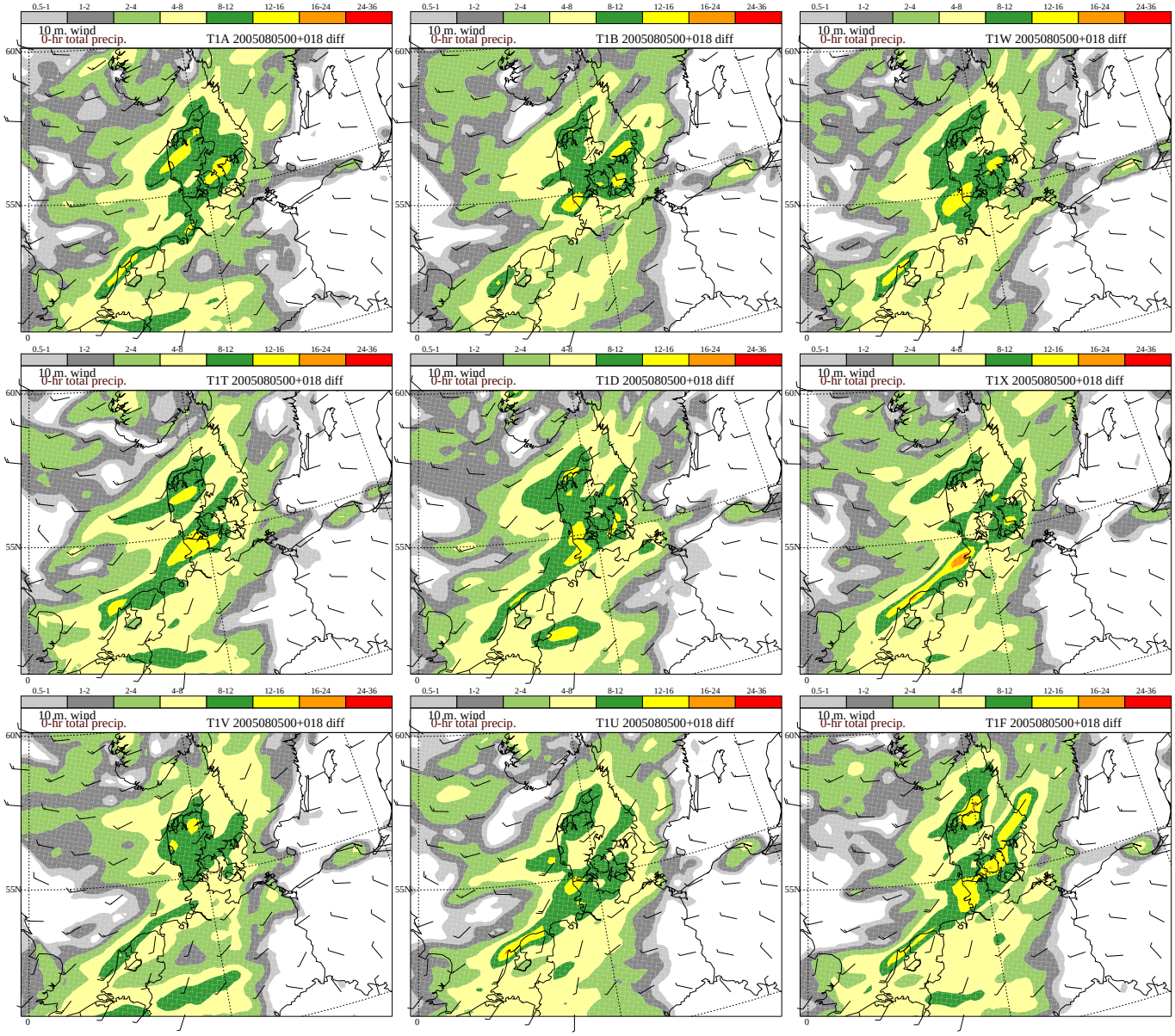

Figure 35: Forecasted (6 h-18 h) 12 h accumulated precipitation valid on 18 UTC August 5, 2005. (T1F: all observations used; T1A: baseline run; T1B: T1A + aircraft; T1W: T1A + wind from other radiosondes; T1T: T1A + wind and temperature data from other radiosondes; T1D: T1A + data from all other radiosondes; T1X: T1A + E-AMDAR data; T1V: T1A + wind profiler data; T1U: T1T + all aircraft data).

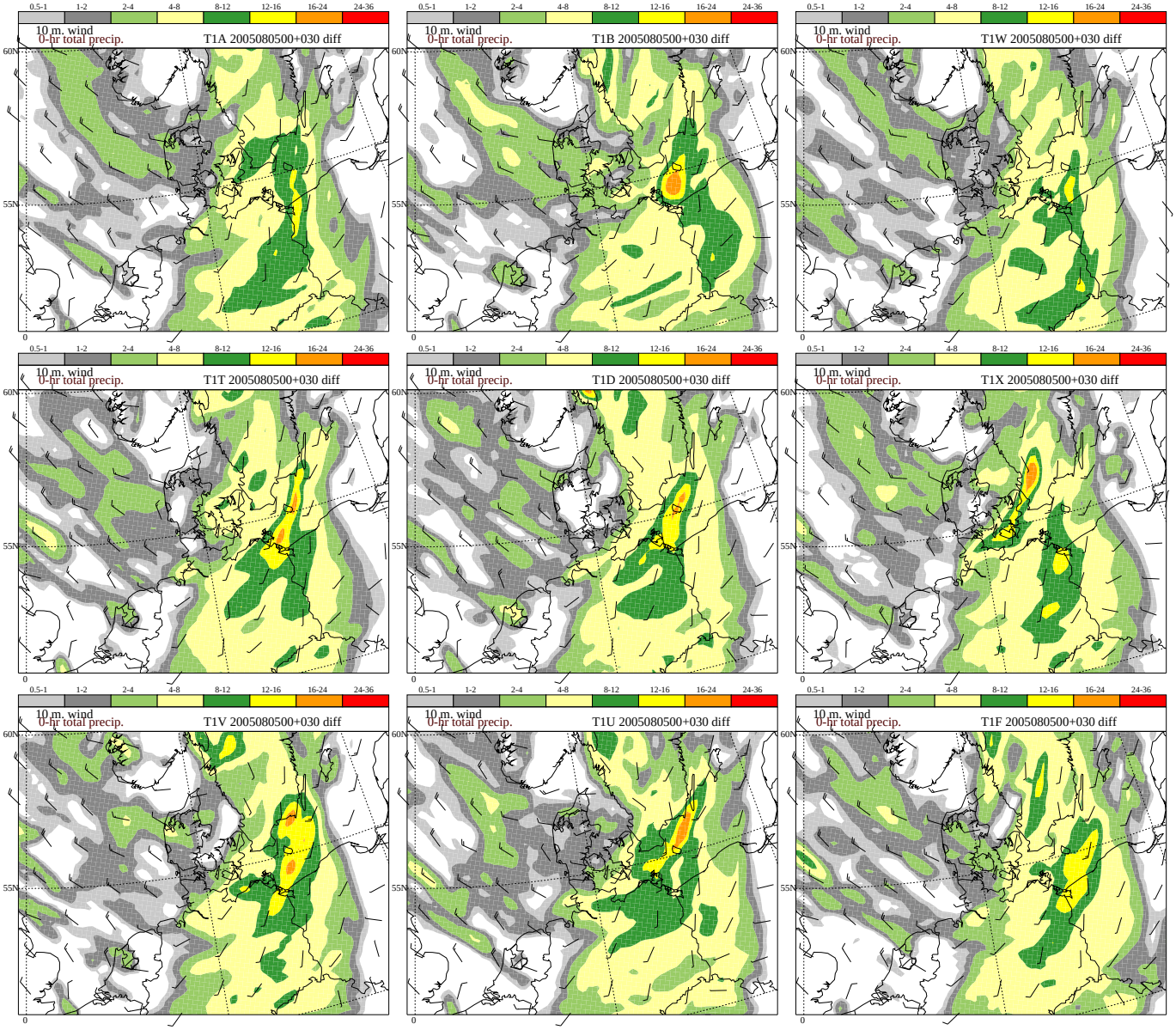

Figure 36: Forecasted (18 h-30 h) 12 h accumulated precipitation valid on 06 UTC August 6, 2005. (T1F: all observations used; T1A: baseline run; T1B: T1A + aircraft; T1W: T1A + wind from other radiosondes; T1T: T1A + wind and temperature data from other radiosondes; T1D: T1A + data from all other radiosondes; T1X: T1A + E-AMDAR data; T1V: T1A + wind profiler data; T1U: T1T + all aircraft data).

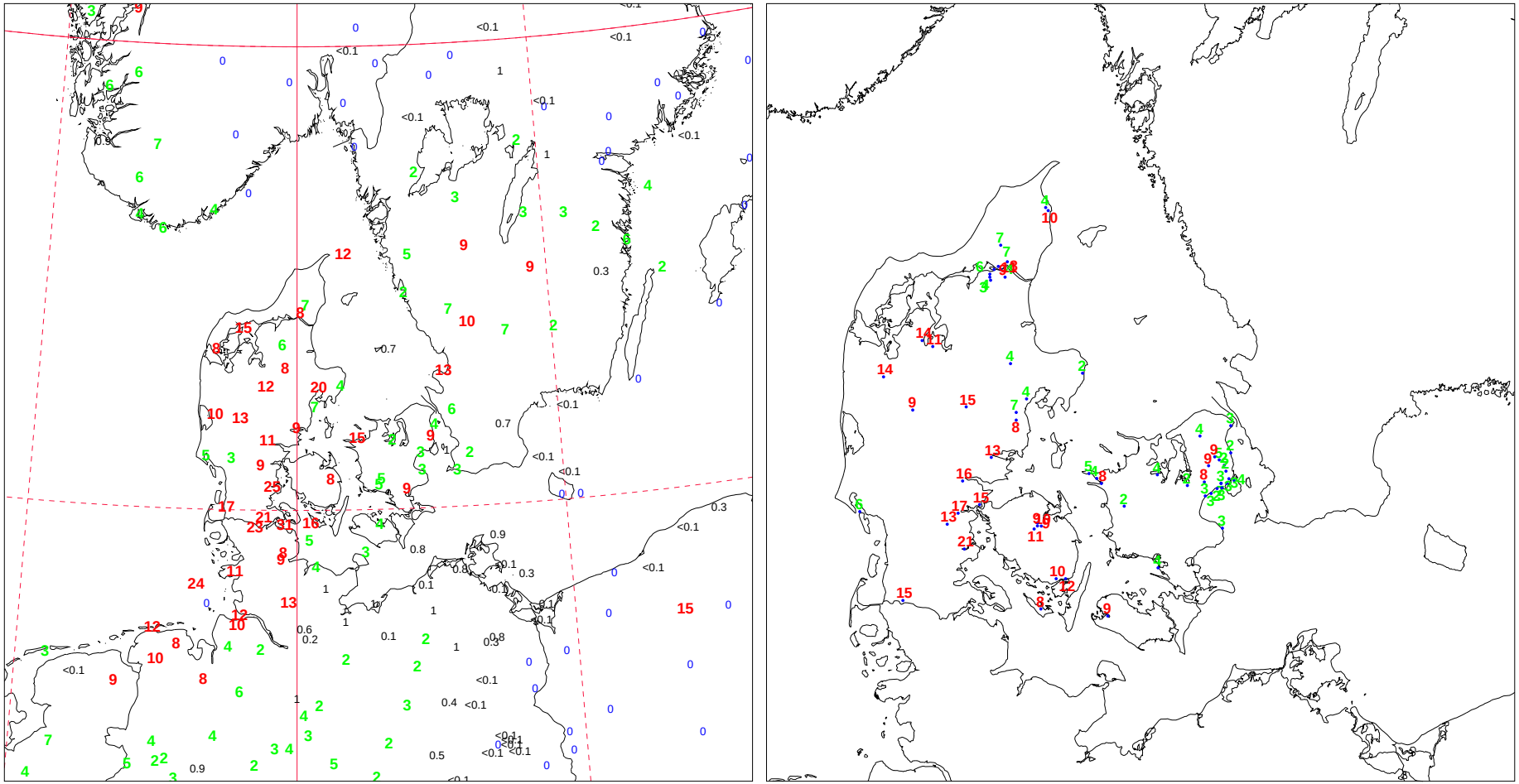

5. august 2005, 18:00 UTC

05. august 2005, 18:00 UTC

Figure 37: Observed 12 h accumulated precipitation on 18 UTC August 5, 2005. Data are from SYNOP stations (left) and from the SVK (Spildevandskomiteen, see e.g. Nielsen and Cappelen, 2006) system. Values larger than or equal to 8 mm have a bold, red and larger font. Values between more than 1 mm and less than 8 mm have a bold, green and larger font. Zero values have a blue font. Data from the SVK system is only shown if the observed value is at least 2 mm.

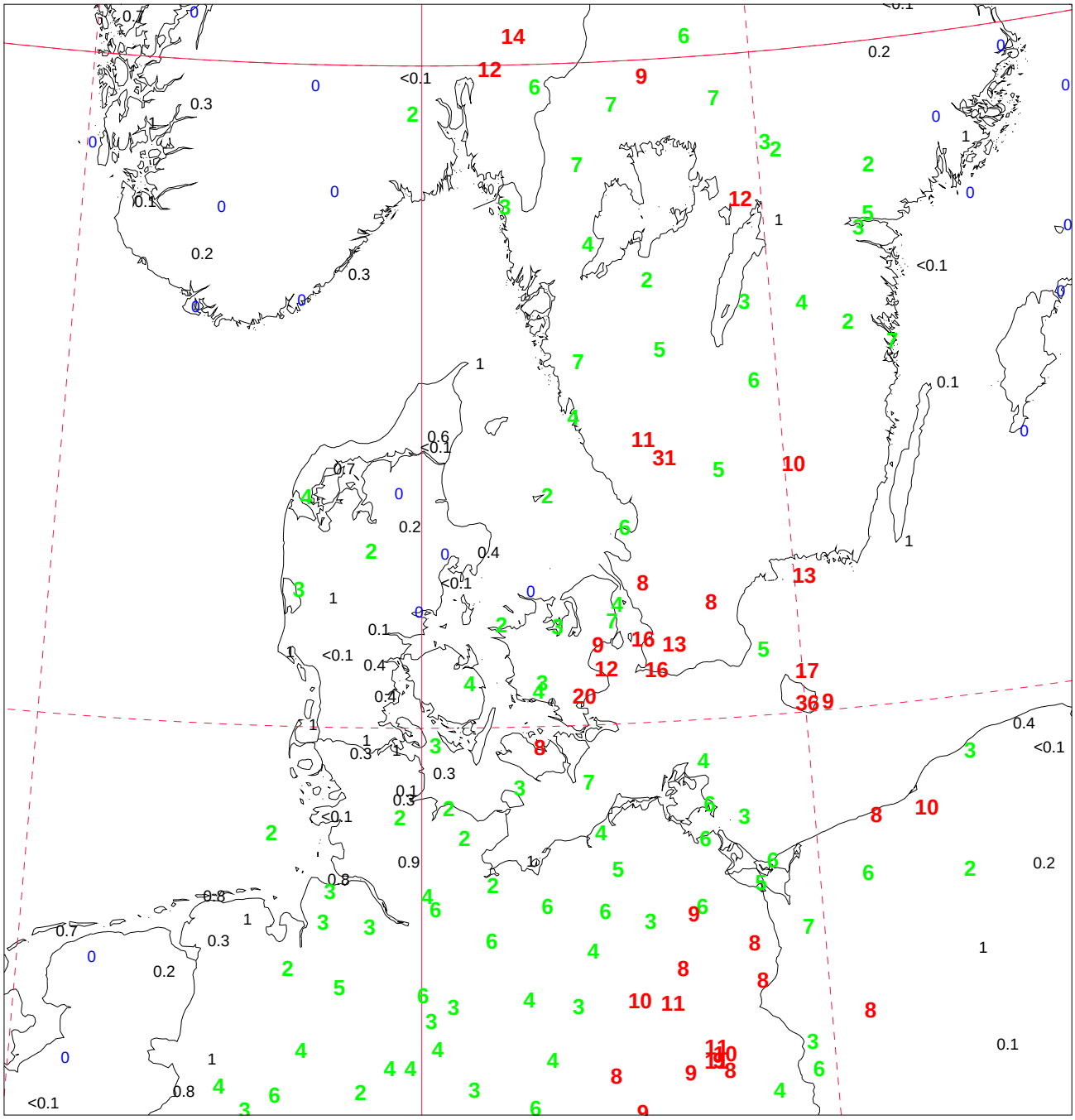

Figure 38: Observed (from SYNOP stations) 12 h accumulated precipitation on 06 UTC August 6, 2005. Values larger than or equal to 8 mm have a bold, red and larger font. Values between more than 1 mm and less than 8 mm have a bold, green and larger font. Zero values have a blue font.

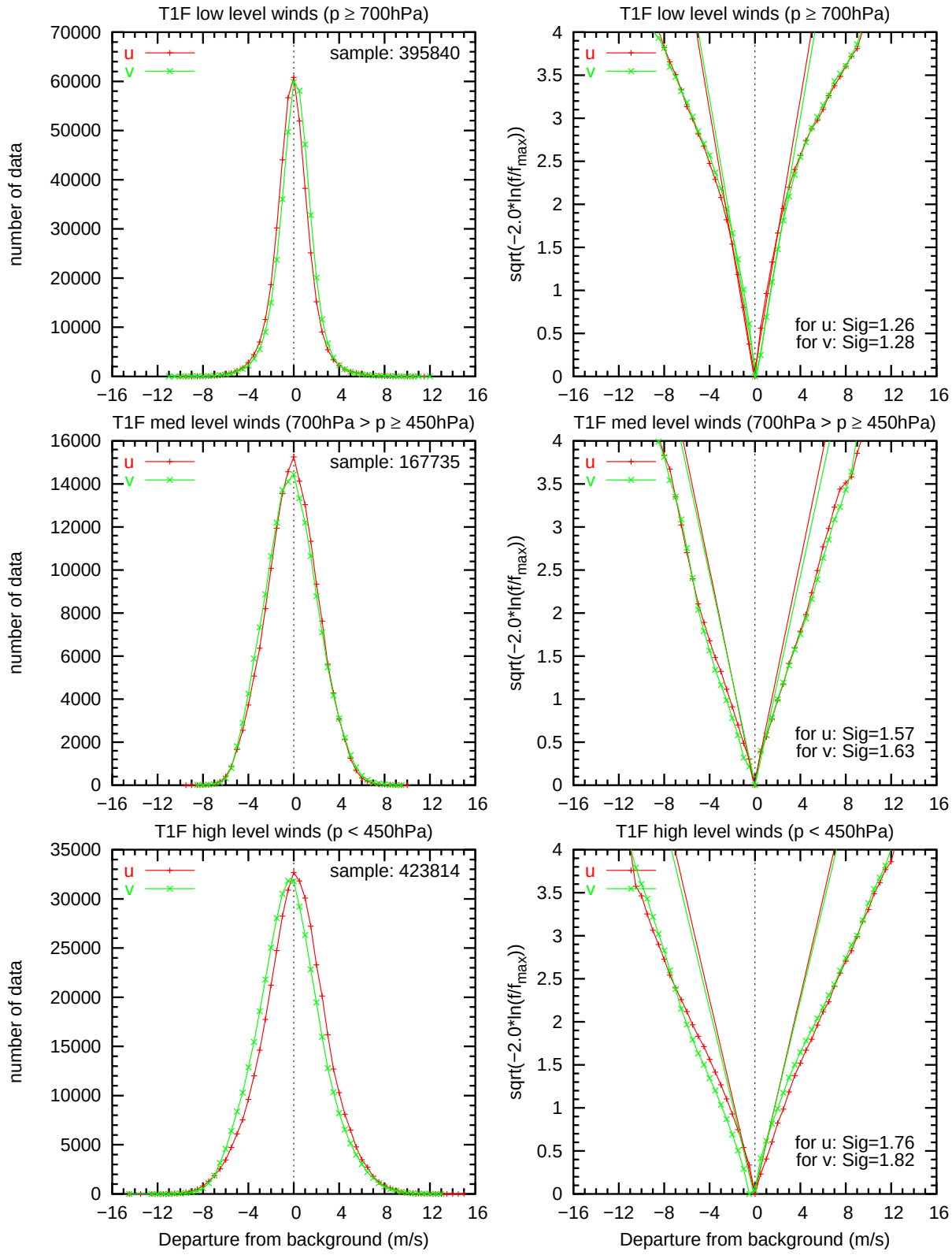

Figure 39: Distribution (in bins of 0.5 m/s) of Meteosat-8 AMV wind speed innovations (differences between the model first guess wind speeds and observed wind speeds) for the control run (T1F). The transformation $\sqrt{-2\ln(f/f_{\max})}$ make a Gaussian distribution linear on each side of 0.

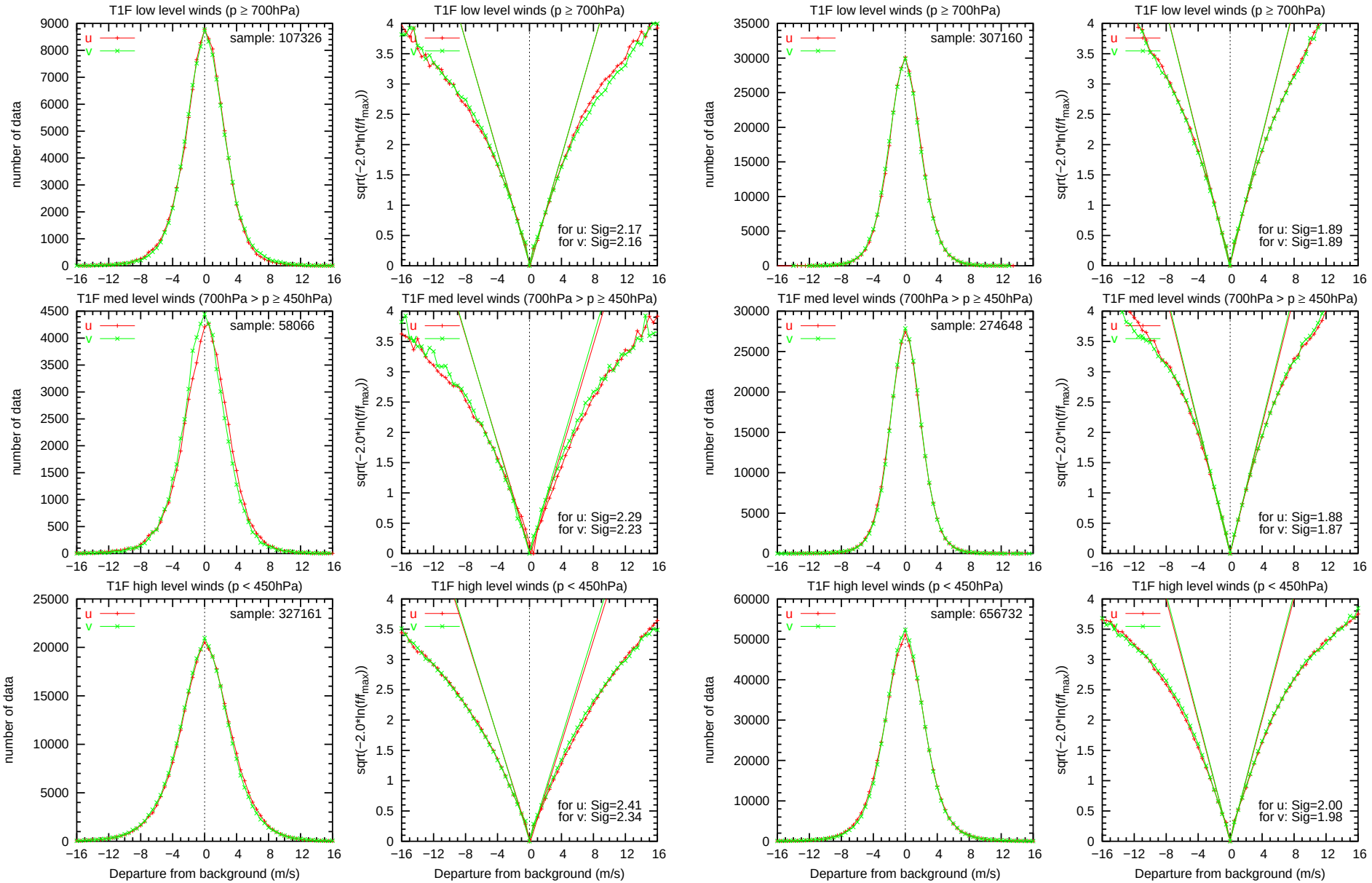

Figure 40: Distribution (in bins of 0.5 m/s) of radiosonde wind speed innovations (differences between the model first guess wind speeds and observed wind speeds) (left) and aircraft wind innovations (right) for the control run (T1F). The transformation $\sqrt{-2\ln(f/f_{\max})}$ make a Gaussian distribution linear on each side of 0.

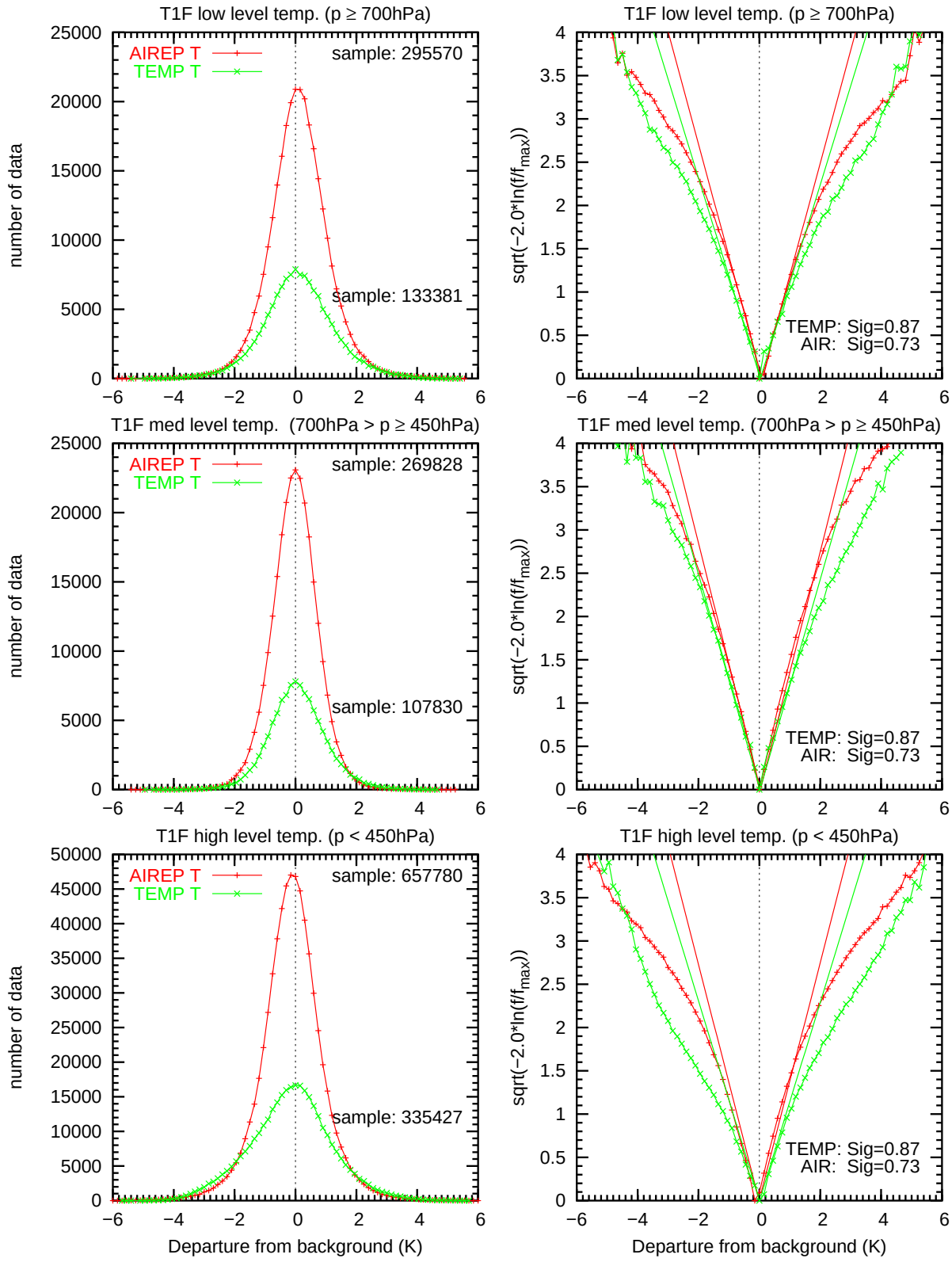

Figure 41: Distribution (in bins of 0.15 K) of aircraft and radiosonde temperature innovations (differences between the model first guess temperatures and observed temperatures) for the control run (T1F). The transformation $\sqrt{-2\ln(f/f_{\max})}$ make a Gaussian distribution linear on each side of 0.

Previous Reports

Previous reports from the Danish Meteorological Institute can be found at:
`http://www.dmi.dk/dmi/dmi-publikationer.htm`